

REMTECH INC.
2603 Artie Street, Suite 21
Huntsville, AL 35805
(205) 536-8581

RTR 014-9

A COMPUTER PROGRAM FOR THERMAL
RADIATION FROM GASEOUS ROCKET
EXHAUST PLUMES (GASRAD)

Prepared by

John E. Reardon

Young C. Lee

December 1979

Prepared Under Contract NAS8-29270

for

National Aeronautics and Space Administration
George C. Marshall Space Flight Center
Marshall Space Flight Center, Alabama 35812

ABSTRACT

A computer code for predicting incident thermal radiation from defined plume gas properties in either axisymmetric or cylindrical coordinate systems. The radiation model is a statistical band model for exponential line strength distribution with Lorentz/Doppler line shapes for 5 gaseous species (H_2O , CO_2 , CO , HCl and HF) and an approximate (non-scattering) treatment of carbon particles. The Curtis-Godson approximation is used for inhomogeneous gases, but a subroutine is available for using Young's Intuitive Derivative method for H_2O with Lorentz line shape and exp.-tailed-inverse line strength distribution. The geometry model provides integration over a hemisphere with up to 6 individually oriented identical axisymmetric plumes, a single 3-D plume, or a combined 3-D/axisymmetric plume for approximating clusters at high altitudes. Shading surfaces may be used in any of 7 shapes, and a conical limit may be defined for the plume to set individual line-of-sight limits. Intermediate coordinate systems may be specified to simplify input of plumes and shading surfaces.

TABLE OF CONTENTS

Section	Page
Abstract	i
1 Introduction	1
2 General Organization	3
3 Radiation Model	9
3.1 Band Models	9
3.2 Band Model Data	23
3.3 Spectral Averaging	28
3.4 Spatial Integration	32
4 Geometry Model	35
4.1 Component Descriptions	35
4.2 Line-of-Sight Operations	42
4.3 Plume Descriptions	45
5 References	57
Appendix	
A1 Input Guide	A1
A1.1 Program Set-up and Mapping	
A1.2 Card Input	
A1.3 Unformatted Binary Input	
A2 Output	A15
A2.1 Printed Output	
A2.2 Diagnostic Messages	
A2.3 Binary Files	
A3 Sample Problems	A31
A3.1 Case 1 - Typical Base Heating Problem	
A3.2 Case 2 - Evaluation of Band Model	
A4 Program Element Descriptions	A87
ACDATA	
BLOCKM	
BLOKIN	
COMMLT	
FFPREP	
FLOUT	
FLOW	
FLOWAX	
FLOWIN	

FLOW3D
MAIN
NOGO
PLANCK
PLUMPT
RAD
SKIP
SLGMLT
SLIMIT
SPCOUT
VIEW
YAPPRX
YF
YNGH20

A5 Details of the Plot Program A121

1 INTRODUCTION

The GASRAD code is the latest in a long series of evolutionary developments by NASA/MSFC to provide improved prediction of radiation transfer from rocket exhaust plumes. Some of the coding is unchanged from that for the earliest version of the program* (Ref. 1) for single constituent axisymmetric plumes. This initial code was followed by a modification to include four radiating species (H_2O , CO_2 , CO and carbon) (Ref. 2), a three-dimensional geometry for a single species (Ref. 3), and a combined code for four species using either axisymmetric or three-dimensional plume property formats (Refs. 4 and 5). This final version was expanded to include HCl and HF with provisions for adding a sixth gaseous species if desired (Ref. 6).

The current code uses a statistical band model with an exponential line strength distribution for combined Lorentz and Doppler line shapes. It uses the Curtis-Godson approximation for inhomogeneous gases, so it can be easily modified for approximating an exponentially-tailed-inverse line strength distribution. A subroutine is included incorporating Young's Intuitive Derivative method (Ref. 7) for H_2O , but the subroutine available in earlier versions for modeling radiation using multiple line groups to represent several energy levels has been omitted. Other changes in the radiation portion of the program include the ability to input band model data rather than using it in data statements to allow comparisons and use of the most recent data.

Significant changes have been made in the geometry procedures, but the code is still designed for heat transfer applications using lines-of-sight representing

* Original coding by A. L. McGarrity at the MSFC Computation Laboratory.

a hemisphere over a point rather than detection applications using parallel lines-of-sight through the plume. Shading surfaces can be described using seven geometric shapes, and plumes can have conical boundaries specified which automatically adjust line-of-sight limits to the region inside the cone. Several identical, independently oriented, axisymmetric plumes can be specified if it is assumed they do not interfere, and a three-dimensional plume description is available for describing flowfields which are not axisymmetric.

The following sections describe the general organization of the GASRAD code, the radiation modeling procedures, and the geometry modeling procedures. The Appendix includes operating information such as input and output formats, sample problems, and descriptions of the program elements. The operating descriptions are intended specifically for the MSFC UNIVAC 1108. But the program is coded entirely in FORTRAN, so it may be adapted to other systems with minor changes.

2 GENERAL ORGANIZATION

This section introduces the overall problem geometry which will be referred to in following sections. In addition, the general arrangements of the program design will be outlined to both orient the reader and define the goal of the overalay structure with the limitations inherent in the approach chosen.

All geometry is related to a central (or reference) coordinate system (CCS) which may be conveniently located to suit the problem. For example, Space Shuttle predictions were made with the orbiter coordinate system, so surface points could be easily located from vehicle drawings. However, if a single engine on a test stand is analyzed, it is usually most convenient to choose the central system at the engine gimbal point or the center of the exit plane (if no gimbaling is planned). Intermediate coordinate systems (ICS) may be located in the CCS by specifying a location and three axis rotations. Then the point-of-interest (POI), plumes, and shading surfaces can be located in either the CCS or a designated ICS by specifying a location and three axis rotations.

A typical arrangement is illustrated in Fig. 2.1. In this illustration an intermediate system is used to facilitate location of the plume and the shading surface representing the nozzle. Use of a gimbal point ICS also provides a convenient means of locating surfaces on the nozzle and providing gimbaling of the entire arrangement by rotating the ICS. The UVW coordinate system at the point-of-interest is used to define a hemispherical system for locating lines-of-sight. Positions are specified by elevation and azimuth angles θ and ϕ relative

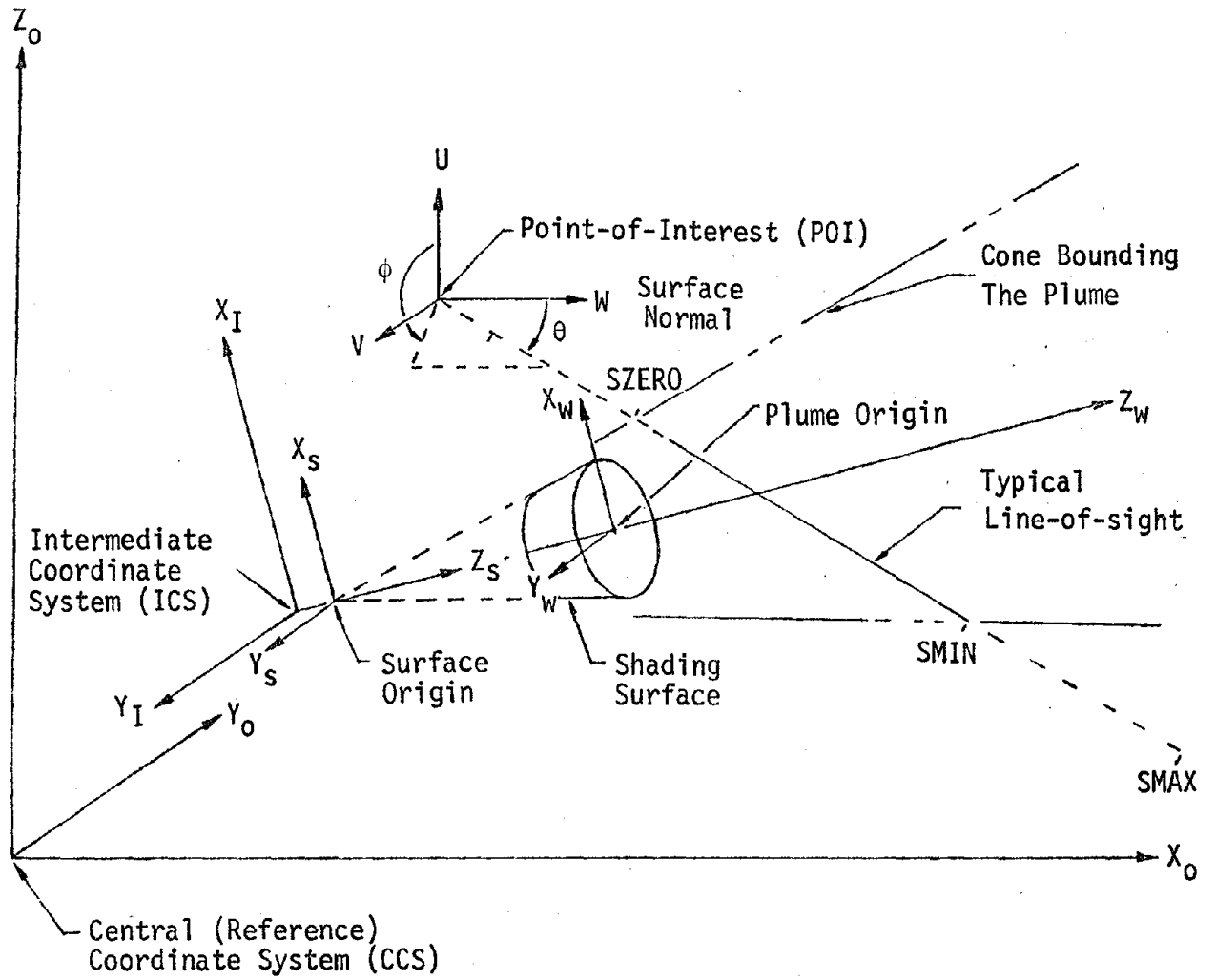


Figure 2.1 Overall Geometry Arrangement

to the surface normal W and the U axis. If a conical plume boundary is specified, the integration limits on each line-of-sight ($SZERO^*$ and $SMIN$) are defined by the program within the limits $SZERO$ and $SMAX$ specified as input.

In the general operation of the program, two large blocks of data representing the flowfield gas properties and the band model parameters must be stored for computation. Storing both data sets simultaneously would require a large memory, a limited flowfield description, or a relatively small spectral range, so the program was separated. Flowfield data are loaded, and as gas property interpolations are completed for each line-of-sight, it is written on an external storage device. When the flowfield interpolations are complete, the band model data are loaded in place of the flowfield, and gas properties are read in one line-of-sight at a time for the band model radiation calculation. This procedure does not use excessive CPU time, but increasing costs associated with use of external stores combined with decreasing internal storage costs may make other procedures more attractive for future applications.

General features of the program organization and operation are illustrated by the schematic in Fig. 2.2 which omits details within the flowfield interpolation and band model prediction blocks. Program control and integration limits and intervals are input in a small MAIN subroutine which controls the top level of program overlay. MAIN passes control to FLOW which controls overlay of subroutines used in the flowfield input and interpolation. In these subroutines, the remaining geometric data are read and the problem limits and geometry are output. Flowfield properties may be read from cards or a

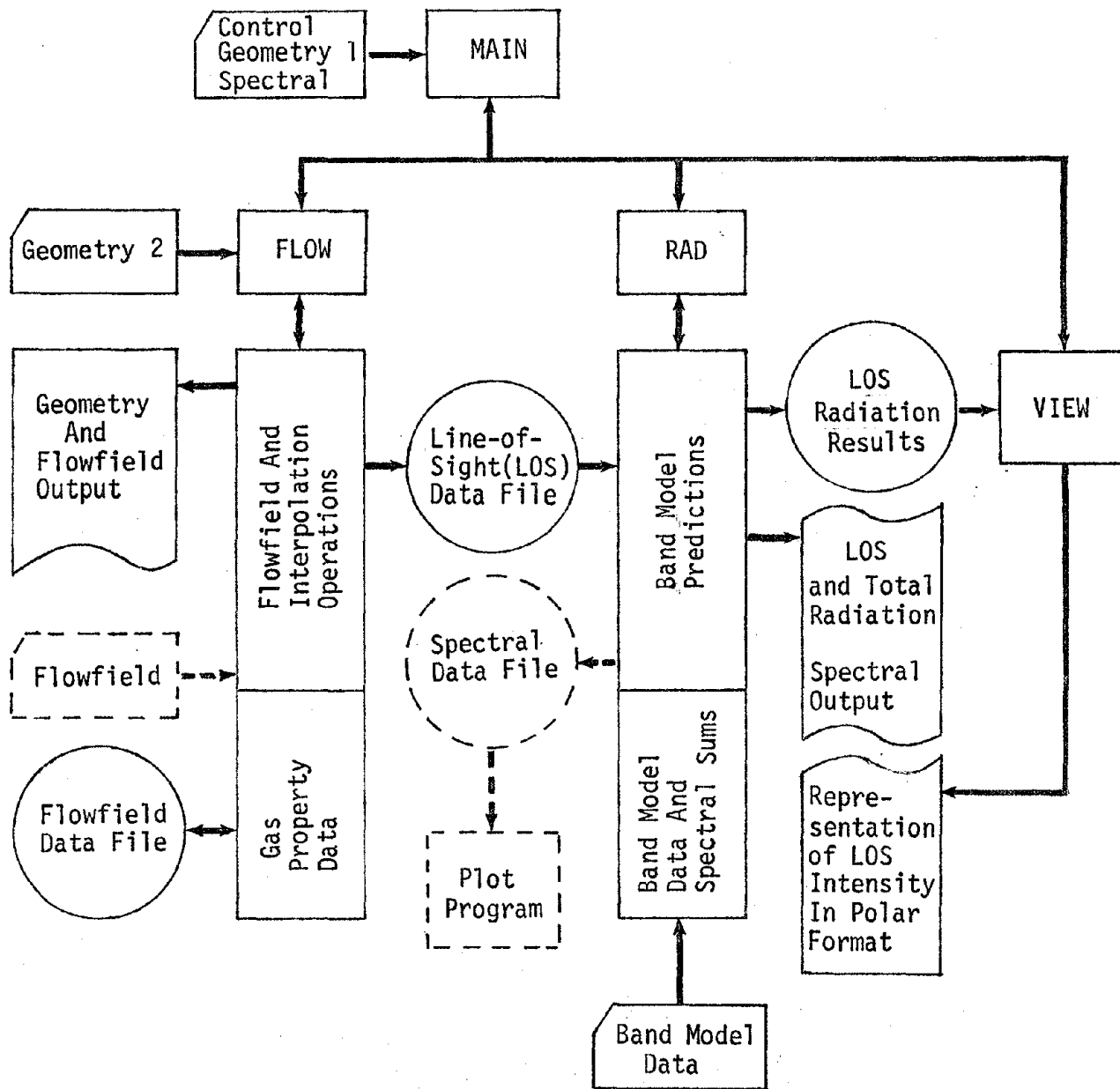


Figure 2.2 GASRAD General Arrangement

binary data file. But if they are input via cards, a binary data file is prepared before the interpolation process begins. As the flowfield properties are input, they are printed in either a long or short form to verify and record input.

After gas property data along each line-of-sight has been transferred to the external data file, MAIN transfers control to RAD which controls overlay of subroutines in the band model prediction. Band model data are input in card format to simplify additions or changes to the data, but in normal operation the card formatted data are stored on tape with the program and added to the runstream by control system command. The band model parameters are printed using either a short or long form to verify and record input. As radiation on each line-of-sight is calculated, details of the results and integration limits are printed, and the position (θ, ϕ) and radiance are transferred to an external store for later use by VIEW. Upon completion of all lines-of-sight, the total flux for the integration is printed followed by the spectral distribution. Spectral data also may be transferred to an external file, if requested, for use by the spectral plot program. Control returns to MAIN which calls the VIEW subroutine.

VIEW prepares a printer-plot representing the intensity in a polar format. The radius in the plot represents the elevation angle θ , and the angle represents the azimuth angle ϕ . The digits 0-9 are used to represent truncated values of radiance/peak-radiance. If lines are blocked before entering the plume they are represented by B, while if they miss the plume, the position is blank. Some detail discrepancies occur in averaging the results into the rectangular grid required for printing, but the larger scale characteristics shown help to verify the point orientation and integration limits and illustrate the major radiation sources.

3 RADIATION MODEL

Although the problem geometry is handled before the radiation calculation in the computer code, the radiation model will be discussed first to establish the gas properties necessary and the options used for spatial integration which both affect the geometry procedures. This section will describe the band model formulations used, the available band model data, and considerations in selecting spectral and spatial intervals for integration.

3.1 BAND MODELS

Band models have been developed as a simplification to monochromatic (line-by-line) calculation methods which become difficult and expensive in computing time as the number of spectral lines to be included becomes large. The objective of a band model is to provide an approximate mean value of transmission over a small spectral interval (usually 5 to 25 cm^{-1}) using a few parameters to describe the behavior of lines in the interval. The following discussion will: briefly introduce concepts used in describing gaseous radiation, introduce the homogeneous gas band models used in the GASRAD program, describe inhomogeneous gas approximations, and summarize the radiation prediction models available in the GASRAD program.

Gaseous Radiation Fundamentals

A basic parameter in gaseous radiation is the monochromatic absorption coefficient, $k(\omega, s)$ defined by

$$dN(\omega, s)/ds = -k(\omega, s) \rho(s) N(\omega, s) \quad (1)$$

where $N(\omega, s)$ is the spectral radiance at the wavenumber* ω and position s , and $\rho(s)$ is the concentration of the radiating species per unit path length. The functional dependence of k and ρ on s implies a dependence on gas property variations for a general case. For a homogeneous gas, these two parameters are not a function of s , but are determined by the gas temperature, pressure, and species concentration. Integration of Eq. 1 over a path length s defines the transmissivity

$$\begin{aligned}\tau(\omega, s) &= N(\omega, s)/N(\omega, 0) \\ &= \exp\left[-\int_0^s k(\omega, s)\rho(s)ds\right]\end{aligned}\quad (2)$$

which, for a homogeneous gas, is

$$\tau(\omega, u) = \exp[-k(\omega)u] \quad (3)$$

where u represents the concentration, ρs , in units inverse to those of k .

Spectral lines representing energy transitions in a molecule are broadened by collision and Doppler effects. The collision broadening is adequately described by the Lorentz line shape while the broadening due to thermal motion of the molecules is represented by the Doppler line shape. The line-strength or intensity describes the integrated absorption coefficient over the broadened line

$$S = \int_0^{\infty} k(\omega)d\omega \quad (4)$$

while the integrated absorptance is a function of both k and u

$$\begin{aligned}W &= \int_0^{\infty} \alpha(\omega, u)d\omega = \int_0^{\infty} [1-\tau(\omega, u)]d\omega \\ &= \int_0^{\infty} [1-\exp(-k(\omega)u)]d\omega\end{aligned}\quad (5)$$

This is usually termed the equivalent-width since it represents the spectral width of an equivalent black ($\alpha=1$) line. The variation of W with u is the curve-of-growth for the line.

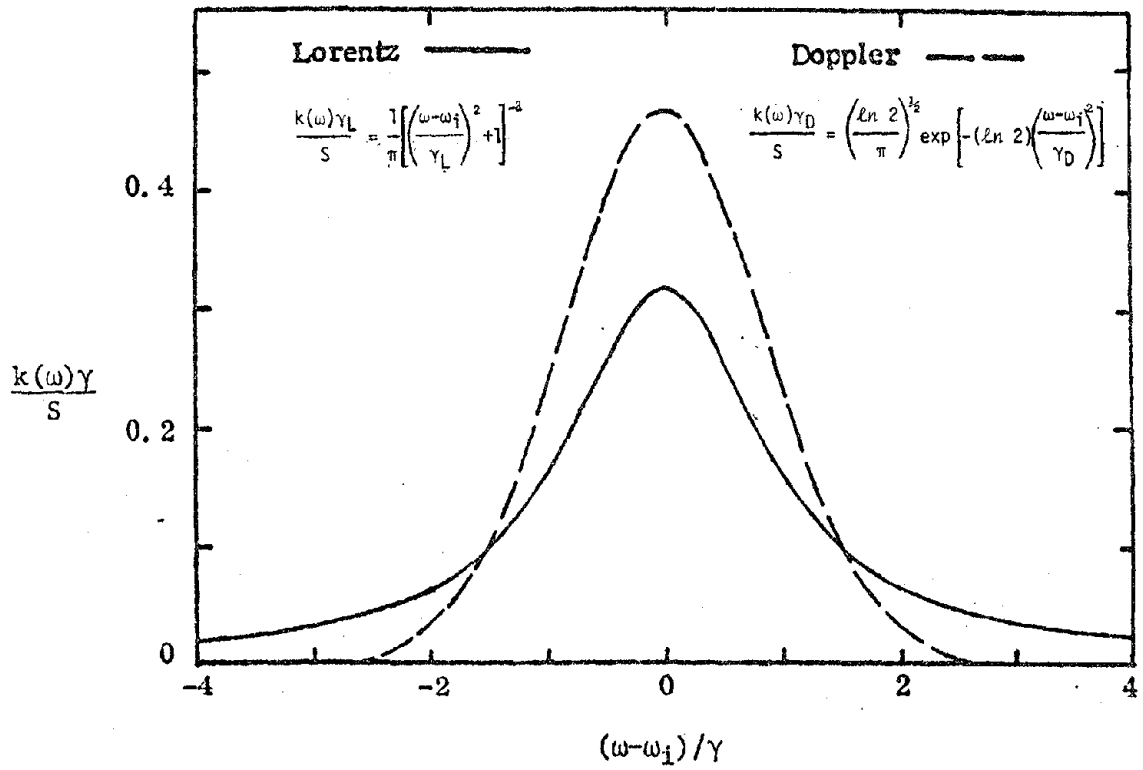
* Wavenumber (cm^{-1}) is the inverse of wavelength (μm), so $\omega = 10^4/\lambda$.

Representative line shapes and curves-of-growth are illustrated in Fig. 3.1 for a single line. In the weak-line limit ($Su/\gamma \ll 1$) the curves-of-growth approach a linear limit. As the absorption increases, the two line shapes produce different results. The Lorentz shape, which has significant absorption in the wings of the line, approaches a square-root limit, while the narrower Doppler line produces a much lower equivalent width which increases as $[\ln(Su/\gamma)]^{1/2}$.

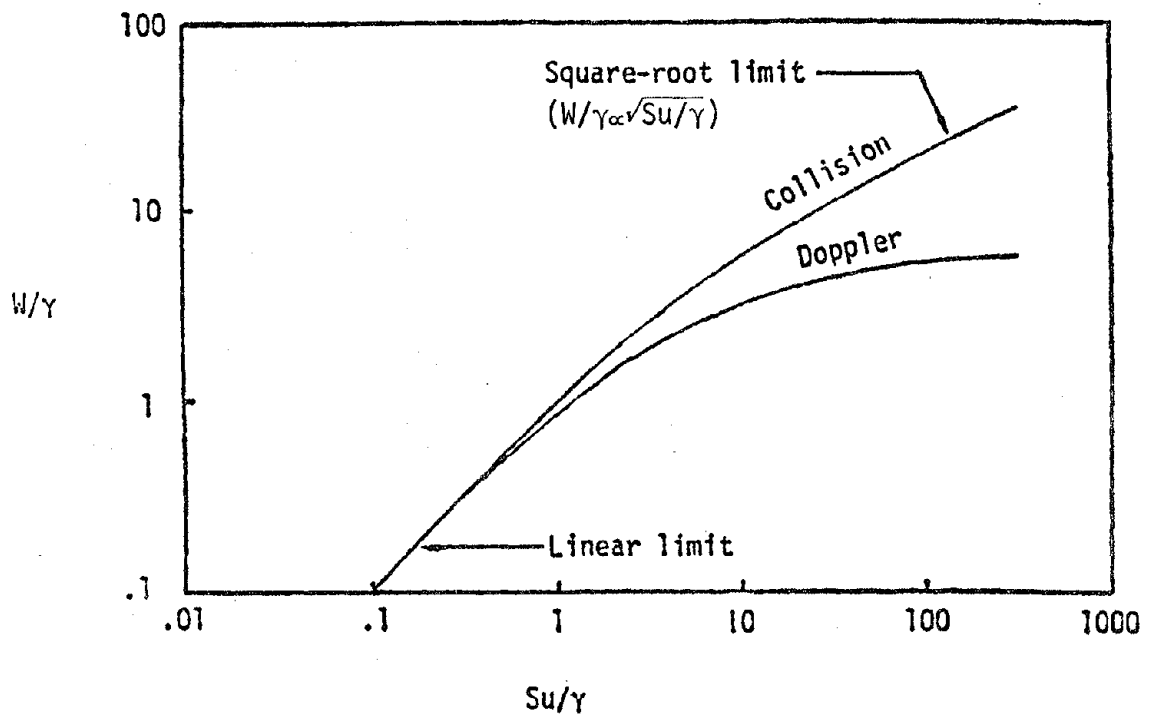
Band Models for Homogeneous Gases

Band models are generally characterized by assumptions made for the line strength (or intensity) distribution. They are commonly divided into three classes: the regular model, the statistical (or random) models, and the mixed models. The regular model considers absorption by identical, equally spaced lines. This approximates the spectra of many diatomic molecules such as HF or NO. Statistical models assume that lines are randomly distributed with a specified intensity distribution. With proper choices of intensity distribution functions, random models approximate features of polyatomic molecules, such as H₂O and CO₂. Mixed models interpolate between the limits of regularity and randomness of the other two models. For example, a mixed model may use a random superposition of regular models.

Three parameters are used in band models to characterize the line structure and the resulting variation of mean transmissivity with path length in a small spectral interval. Representative line half-widths and spacing, γ and d , are used to characterize the spectral structure varying from isolated lines ($\gamma \ll d$) to strongly overlapping lines ($\gamma \gg d$), and the mean line strength is represented by the absorption coefficient \bar{k} which is proportional to the line-strength-to-spacing ratio, S/d .



(a) Line Shape (γ = line half-width at half height)



(b) Curve-of-Growth

Figure 3.1 Line Shape and Curve-of-Growth for Lorentz and Doppler Lines.

The GASRAD program uses statistical band models to best describe H₂O and CO₂ which are the gases of primary interest in heat transfer, but this model is not usually expected to provide the best representation of diatomic gases. Statistical band models have been developed based on four assumptions concerning the probability of occurrence, P(S), of a line strength, S:

- A) Equal strength, $P(S) \propto \delta(S-\bar{S})$,
- B) Exponential distribution, $P(S) \propto \exp(-S)$,
- C) Inverse distribution, $P(S) \propto 1/S$,
- D) Exponentially-tailed inverse, $P(S) \propto S^{-1}\exp(-S)$,

where δ in (A) refers to the Dirac delta function*. These distributions have been studied for both Lorentz and Doppler line shapes. For the Lorentz shape, the results can be represented by

$$(-\ln \tau) = \beta_L f(x) \quad (6)$$

where $\beta_L = 2\pi\gamma_L/d$, $x = \bar{k}u/\beta_L$, and $f(x)$ is determined by the probability function used. Because of variations in constants, a similar generalized Doppler relation must be stated in proportional form

$$(-\ln \tau) \propto \beta_D g(y) \quad (7)$$

where $\beta_D \propto \pi\gamma_D/d$, $y \propto \bar{k}u/\beta_D$, and $g(y)$ is determined by the intensity distribution.

The parameters \bar{k} and $1/d$ are usually tabulated as functions of wave-number (ω) and temperature (T), while algebraic expressions are available for γ_L and γ_D . The expression normally used for γ_L (Ref. 10) is

$$\gamma_{Li} = [c_i \gamma_{ii}(273/T)^{\eta_{ii}} + \sum_j c_j \gamma_{ij}(273/T)^{\eta_{ij}}] \quad (8)$$

where γ_{ii} represents resonant self broadening of the *i*th species and γ_{ij} represents broadening by foreign gases and nonresonant self broadening. The pressure, temperature, and mole fraction are indicated by *p*, *T*, and *c*, and estimates for the coefficients (γ) and exponents (η) are given in Table 3.1. An expression for Doppler broadening can be derived from the Boltzman distribu-

* $\delta(S-S)=0$ when $S \neq \bar{S}$ and $\int \delta(S-S)dS=1$ when the integration limits include \bar{S} .

Table 3.1

VALUES FOR THE COLLISION LINE WIDTH PARAMETERS (Ref. 10)

Molecule (i)	Broadener (j)	$(\gamma_{i,j})_{273}$ cm ⁻¹ atm ⁻¹	$\eta_{i,j}$	$(\gamma_{i,j})_{273}$ cm ⁻¹ atm ⁻¹	$\eta_{i,j}$
H ₂ O	H ₂ O	(0.09)	0.5	0.44	1.0
	N ₂	0.09	0.5		
	O ₂	0.04	0.5		
	H ₂	(0.05)	0.5		
	CO ₂	0.12	0.5		
	CO	(0.10)	0.5		
CO ₂	CO ₂	0.09	0.5	0.01	1.0
	H ₂ O	(0.07)	0.5		
	N ₂	0.07	0.5		
	O ₂	0.055	0.5		
	H ₂	0.08	0.5		
	CO	(0.06)	0.5		
CO	CO	0.06	0.5	0.0	1.0
	H ₂ O	(0.06)	0.5		
	CO ₂	(0.07)	0.5		
	H ₂	0.06	0.5		
	N ₂	0.06	0.5		
	O ₂	0.05	0.5		
NO	NO	0.05	0.5	0.0	1.0
	N ₂	(0.05)	0.5		
	O ₂	(0.04)	0.5		
	Other	(0.05)	0.5		
CN	CN	(0.05)	0.5	0.0	1.0
	Other	(0.05)	0.5		
OH	OH	(0.05)	0.5	0.45	1.0
	Other	(0.05)	0.5		
HCl	HCl	(0.05)	0.5	0.15	1.0
	Other	(0.05)	0.5		
HF	HF	(0.05)	0.5	0.45	1.0
	Other	(0.05)	0.5		

Note: Values in parenthesis are estimated.

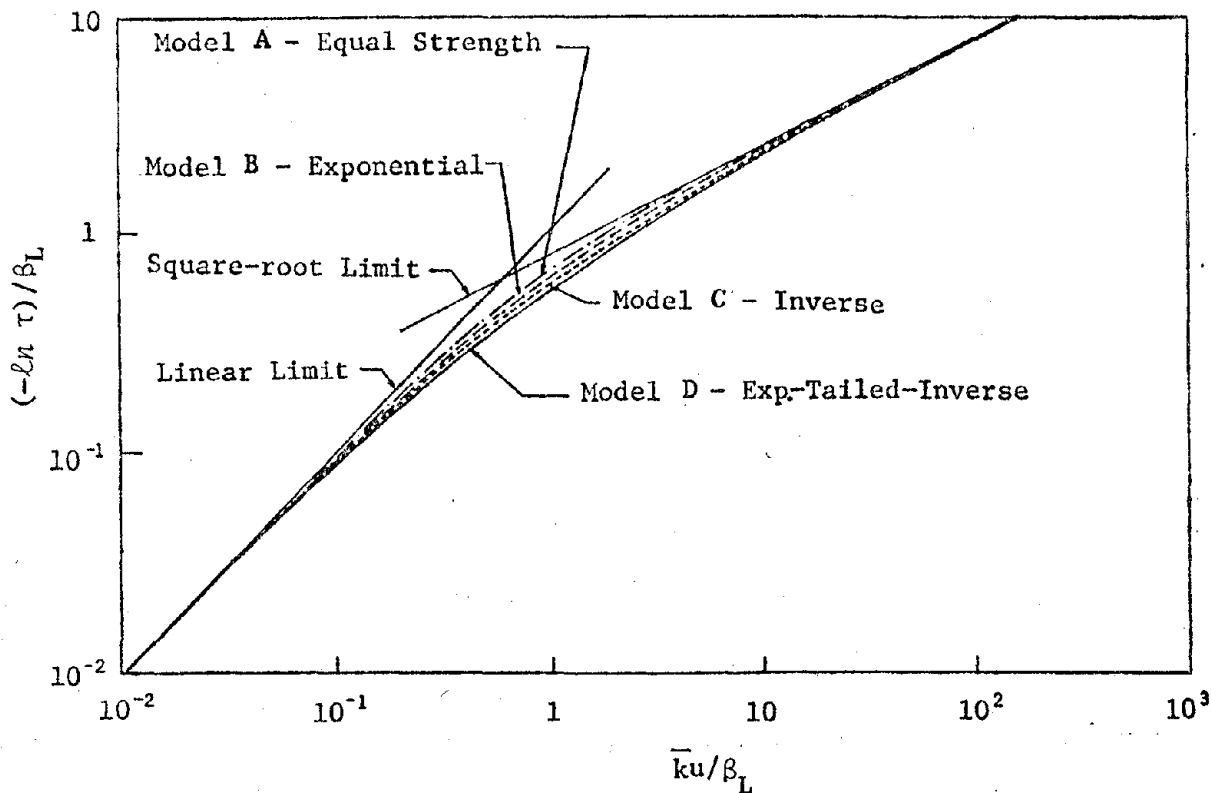
tion for molecular velocities. With the constants evaluated, it is

$$\gamma_{Dj} = 0.3581 \times 10^{-6} \omega(T/M_j)^{1/2} \quad (9)$$

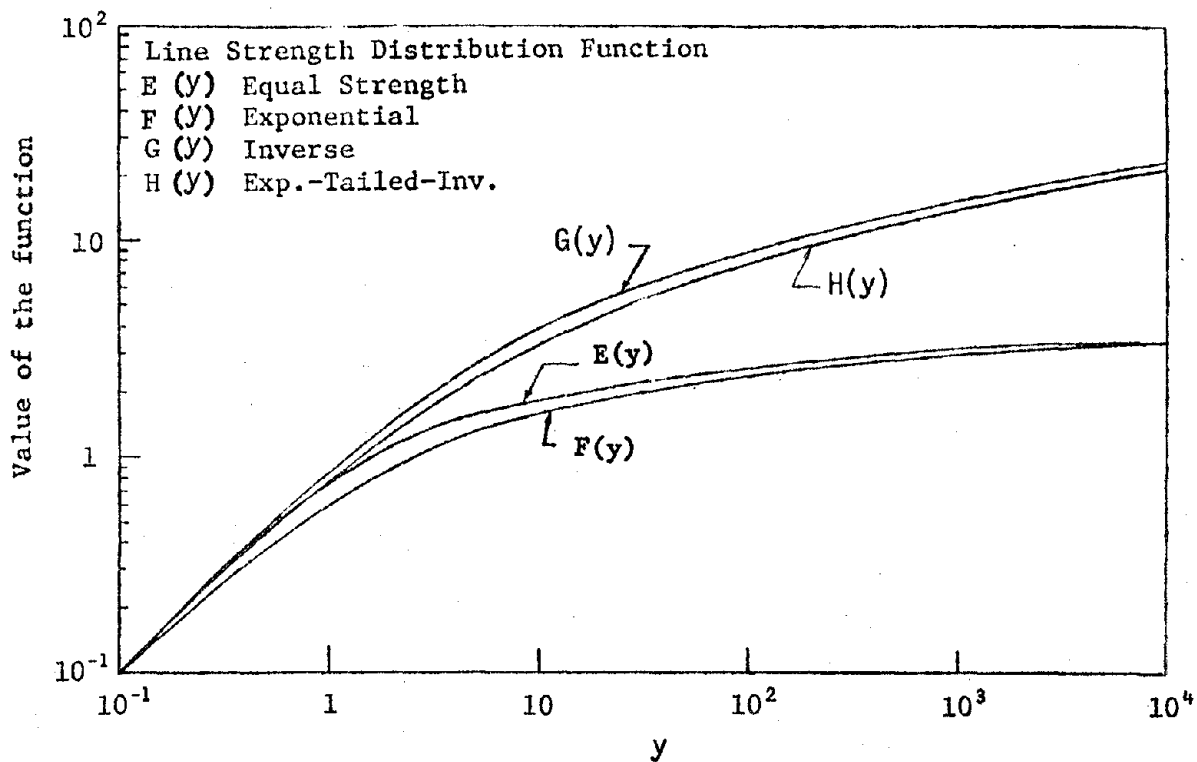
where M_j represents the molecular mass in unified atomic mass units (e.g. gm/gm-mole).

For given values of \bar{k} , γ , and d (determined by species concentrations, pressure, and temperature), the functions $f(x)$ or $g(y)$ can be viewed as representing the relative variation of $(-\ln \tau)$ with u . This variation is termed the "curve-of-growth" for the band model which is illustrated for the various statistical distributions in Fig. 3.1. These curves-of-growth are similar to those for a single line, and for statistical band models, $-\ln \tau$ represent a mean equivalent-width (\bar{W}) multiplied by the number of lines in the interval $(1/d)$, \bar{W}/d . Although the curves are similar to those for a single line, there are differences in implications caused by modeling a group of lines. For band models, the linear limit can be approached by strongly overlapping lines or weak lines, so that the net result is $\bar{k}u \ll \beta_L$. Conversely, the square root limit requires a relatively small line-width to spacing ratio, $\beta_L \ll \bar{k}u$. As a result, the linear limit is approached for high pressures (which produce large γ_L) or high line densities (such as in the $4.4\mu\text{m}$ band of CO_2). The Doppler line curves-of-growth also approach the linear limit for small y , but approach two different limits for large y .

The differences between the Lorentz curves-of-growth are not large, so Models B and D which have simple algebraic solutions are often used as approximations of Models A and C. Which have more complex solutions. All of the Doppler line models require lengthy series solutions, so two algebraic approximations have been used: one for solutions $E(y)$ and $F(y)$, and one for solutions $G(y)$ and $H(y)$. In the Doppler case, the model chosen could make a significant difference for large y in cases of relatively hot low-pressure gases where Doppler broadening is significant.



(a) Lorentz Line Shape (Ref. 8)



(b) Doppler Line Shape (Ref. 9)

Figure 3.2 Curves-of-Growth for Statistical Band Models

The band models considered for use in the GASRAD program are represented by the following approximations from Ref. 10 with $a_L = \gamma_L/d$ and $a_D = \gamma_D/d$:

Exponential Line Strength

$$\text{Lorentz } (\bar{W}/d)_L = X_L = \bar{k}u/\sqrt{1+\bar{k}u/(4a_L)} \quad (10a)$$

$$\text{Doppler } (\bar{W}/d)_D = X_D = 1.70 a_D \{ \ln[1+(\bar{k}u/(1.70a_D))^2] \}^{1/2} \quad (10b)$$

Exponentially-Tailed-Inverse Line Strength

$$\text{Lorentz } (\bar{W}/d)_L = X_L = 2a_L [(1+\bar{k}u/a_L)^{1/2}-1] \quad (11a)$$

$$\text{Doppler } (\bar{W}/d)_D = X_D = 0.937a_D \{ \ln[1+(\bar{k}u/(0.937))^{2/3}] \}^{3/2} \quad (11b)$$

Either of these equation sets are applied to the i radiating species in the gas. Then the Lorentz and Doppler components are combined to compute to transmissivity using the form

$$\ln \bar{\tau} = -\sum_i \bar{k}_i u_i (1 - y_i^{-1/2})^{1/2} \quad (12a)$$

$$y_i = [1 - (X_L/\bar{k}u)^2]^{-2} + [1 - (X_D/\bar{k}u)^2]^{-2} - 1 \quad (12b)$$

For a single species, these equations will reduce to $\ln \tau \approx -X_L$ if $X_L \geq 3X_D$ or $\ln \tau \approx -X_D$ if $X_D \geq 3X_L$, and will give the linear limit, $\ln \tau = -\bar{k}u$, if $X_L \approx \bar{k}u$ or $X_D \approx \bar{k}u$. Representative values of optical depth for H₂O are illustrated in Fig. 3.3 showing the effect of pressure on the curve-of-growth and the relative importance of the Doppler broadened optical depth.

Radiance along a line-of-sight \vec{L} to a point at $s=0$ is given by

$$\bar{N}(\omega, L) = -\int_0^L N^\circ(\omega, s) [d\bar{\tau}(\omega, s)/ds] ds \quad (13)$$

where $N^\circ(\omega, s)$ is the Planck function evaluated at ω and $T(s)$. The heat transfer to a point is obtained by integrating Eq. 13 over a spectral interval adequate to include the radiating species and a spatial region which includes the radiating gas. The result is

$$\dot{q}/A = -\int_{\theta_i}^{\theta_f} \int_{\phi_i}^{\phi_f} \int_{\omega_i}^{\omega_f} \left\{ \int_0^L N^\circ(\omega, s) [d\bar{\tau}(\omega, s)/ds] ds \right\} \sin\theta \cos\theta d\omega d\phi d\theta \quad (14)$$

where θ and ϕ are the elevation and azimuth angles measured from the surface normal. In numerical evaluation of Eq. 14, $\Delta\omega$ would correspond to the

spectral interval used in the band model representation.

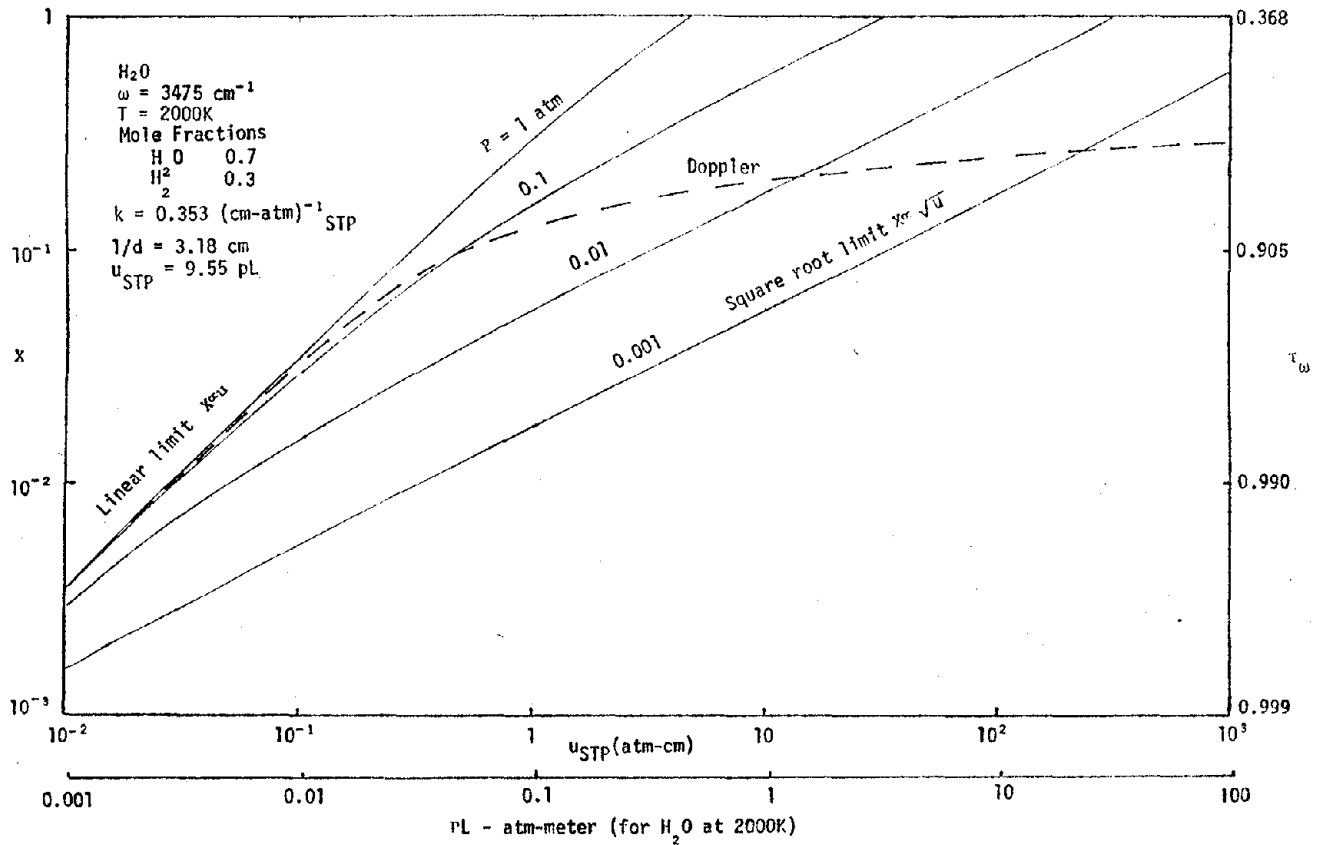


Figure 3.3 Representative Optical Depth Behavior of H_2O at $2.88 \mu m$.

Band Models for Inhomogeneous Gases

Application of homogeneous gas band models to inhomogeneous gases is made using one of three techniques: multiplying transmissivities, computing effective values of band model parameters using the modified Curtis-Godson approximation, or using derivative methods designed with the possibility of inhomogeneity included in the band model formulation. Multiplication of transmissivities, which is valid for gray media, is not valid in all cases for band models. The mean transmissivity representation of line structure by a band model is valid when applied to gray sources or sources with line structure which is uncorrelated, such as a different gas. But for trans-

mission through the same gas at a different temperature, some of the lines can be expected to correlate and produce more absorption than predicted by simple multiplication of homogeneous band model results.

The modified Curtis-Godson approximation uses the homogeneous band model formulation with effective parameters defined by

$$\bar{k}_e(\omega, i, s)u(i, s) = \int_0^s \bar{k}(\omega, i, s')c(i, s')p(s')ds' \quad (15a)$$

$$a_{Le}(\omega, i, s) = \left[\int_0^s \bar{k}(\omega, i, s')c(i, s')p(s')a_L(\omega, i, s')ds' \right] / [\bar{k}_e(\omega, i, s)u(i, s)] \quad (15b)$$

$$a_{De}(\omega, i, s) = \left[\int_0^s \bar{k}(\omega, i, s')c(i, s')p(s')a_D(\omega, i, s')ds' \right] / [\bar{k}_e(\omega, i, s)u(i, s)] \quad (15c)$$

where $c(i, s')$ is the mole fraction of the i th species and $p(s')$ is the pressure. The product $c \cdot p$ represents the ratio of density at s' to the density at one atmosphere and a temperature equal to that at s' . This requires absorption coefficients defined relative to density at the gas temperature. In some applications, \bar{k} is referenced to standard conditions ($p=1$ atm, $T_0=273K$), so the concentration must be represented by $cp(T_0/T)$.

Derivative models were summarized by Young (Ref. 7), and the Intuitive Derivative method he recommended on the basis of H_2O predictions will be summarized here. The recommended formulation is a representation of the inverse or exponentially-tailed-inverse intensity distribution for Lorentz lines (equivalent to Eq. 11a for homogeneous gas). The procedure is compared with the Curtis-Godson approximation in Table 3.2 where the functional notation of wavenumber (ω) has been omitted, and the parameter $\beta=2\pi\gamma_L/d$ is used rather than $a_L=\gamma_L/d$ as in Eq. 11a. An efficient algorithm for approximating $y(s)$ is provided by Young (Ref. 7), so the additional parameters are not difficult to compute. But the computation time can be greatly increased because of the decrease in integration step size required in the Intuitive Derivative method.

Table 3.2

COMPARISON OF CURTIS-GODSON AND INTUITIVE DERIVATIVE METHODS*
FOR AN INHOMOGENEOUS GAS WITH A SINGLE RADIATING SPECIES

Same	(16a)	$u(s) = \int_0^s c(s')b(s')ds'$	(17a)
Same	(16b)	$\bar{k}_e(s) = \frac{1}{u(s)} \int_0^s c(s')p(s')\bar{k}(s')ds'$	(17b)
Same	(16c)	$\beta_e(s) = \frac{1}{u(s)\bar{k}_e(s)} \int_0^s [c(s')p(s')\bar{k}(s')\beta(s')ds']$	(17c)
Same	(16d)	$x_e(s) = u(s)\bar{k}_e(s)/\beta_e(s)$	(17d)
N/A		$\bar{d}_e(s) = \frac{1}{u(s)\bar{k}_e(s)} \int_0^s [c(s')p(s')k(s')\bar{d}(s')ds']$	(17e)
N/A		$r(s) = \beta(s)/\beta_e(s)$	(17f)
N/A		$q(s) = \bar{d}_e(s)/\bar{d}(s)$	(17g)
N/A		$y(s) = y(\pi x_e(s), r(s), q(s))$	(17h)
N/A		$y(x, r, q) = \frac{2}{\pi} \int_0^\infty \left[\int_0^\infty \exp \left\{ \frac{2x\eta^q}{1+r^2z^2} \right\} \frac{dz}{1+z^2} \right] d\eta$	(17i)
N/A		$\frac{1}{d} \frac{d\bar{W}(s)}{ds} = c(s)p(s)\bar{k}(s)y(s)$	(17j)
		$\frac{\bar{W}}{d} = \int_0^s \frac{1}{d} \frac{d\bar{W}(s')}{ds'} ds'$	(17k)
		$\frac{d\bar{\tau}}{ds} = -\bar{\tau}(s) \frac{1}{d} \frac{d\bar{W}(s)}{ds}$	(17l)
		$\bar{\tau} = \exp(-\bar{W}/d)$	(17m)
		$\bar{N} = -\int_0^s N^o(s') \frac{d\bar{\tau}}{ds'} ds'$	(17n)
		$\frac{\bar{W}}{d} \frac{\beta_e(s)}{\pi} = [\sqrt{1+2\pi x_e(s)} - 1]$	(16k)
		$\bar{N} = -\int_0^s N^o(s') d\bar{\tau}(s')$	(16n)

* The Intuitive Derivative model and Eq. 16k of the C-G method are approximations for an inverse or exponentially-tailed-inverse Lorentz line strength distribution.

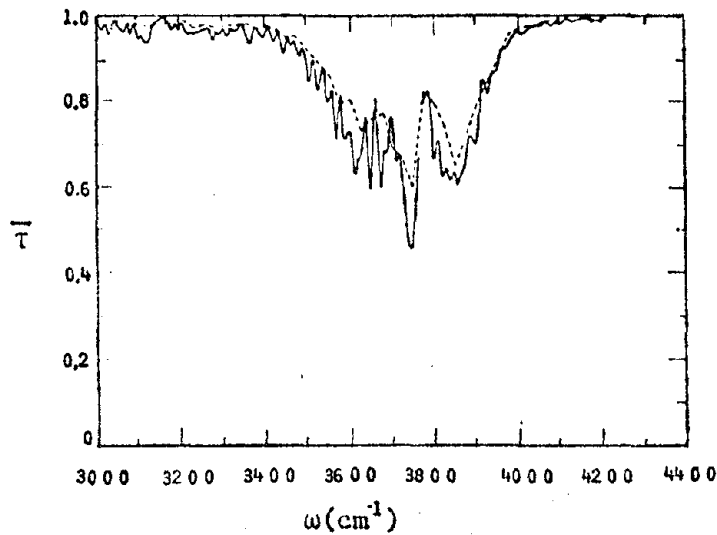
Numerical evaluation of radiance with the Curtis-Godson approximation takes the form

$$\bar{N}_m = \sum_{n=1}^m N_n^o (\tau_{n-1} - \tau_n) \quad (16)$$

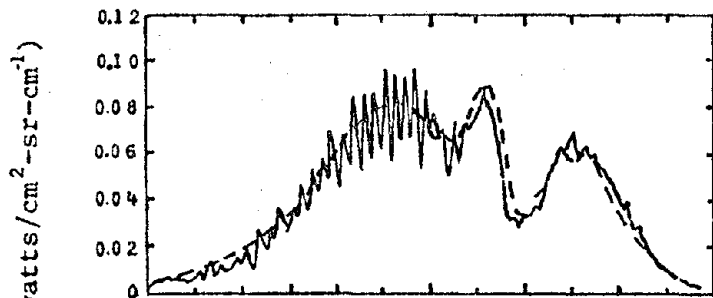
with $\tau_0=1$, and the size of the integration step can be arbitrarily large as long as the gas in the step can be assumed to be homogeneous. In contrast, the value of $y(s)$ changes continuously with x_e even in homogeneous sections, so small steps must be used to properly evaluate \bar{W}/d (Eq. 17k). In the GASRAD code for the Intuitive Derivative method, an input parameter is provided to vary the step size to give a specified value of $\Delta(\text{scpk})$ which then allows Δs to vary depending on the strength of the absorption at each spectral and spatial increment.

The Curtis-Godson approximation has proven satisfactory for inhomogenities in rocket exhaust plumes, and the long cold atmospheric transmission paths for which the Intuitive Derivative method was developed do not exist in the usual heat transfer problem. But the program user should be aware of the characteristics of the model he intends to use. An example of H_2O radiation through a long atmospheric path is illustrated in Fig. 3.4. Isothermal predictions of both cold and hot paths using Eq. 11a are compared with measurements in Fig. 3.4(a) and (b) showing good agreement with the measurements. The hot through cold measurement, Fig. 3.4(c), shows representative behavior of the two band models where the Curtis-Godson method typically overpredicts cold gas absorption. The solution obtained from the product of cold-gas transmissivity and hot-gas radiance underpredicts the absorption caused by line correlation effects as indicated in Fig. 3.4(d).

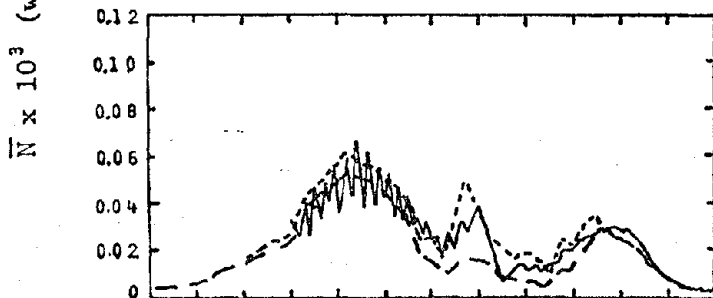
Cell	Gas Path (m)	Temperature (K)	Pressure (atm)	Mole Fraction	
				H ₂ O	N ₂
Cold	100	293	0.07	0.014	0.986
Hot	0.6	1202	0.1	0.5	0.5



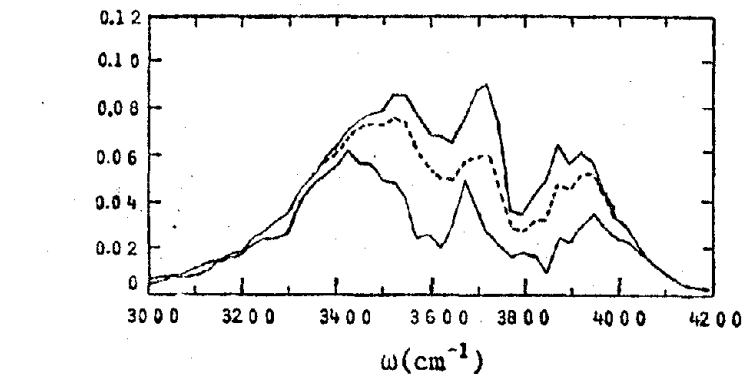
(a) Cold cell measurement and isothermal band model prediction.



(b) Hot cell measurement and isothermal band model prediction.



(c) Hot through cold measurement, Intuitive Derivative (----), and Curtis-Godson (- - - -).



(d) Hot cell prediction (upper), product of isothermal predictions of cold cell transmissivity and hot cell radiance (middle) and Intuitive Derivative prediction (lower).

Figure 3.4 Comparison of Measurements and Band Model Predictions for H₂O using an Exponential-Tailed-Inverse Intensity Distribution (Ref. 11).

Radiation Models in the GASRAD Program

The developments leading to the GASRAD program have used the exponential line strength band model represented by Eqs. 10 and 12 with the modified Curtis-Godson approximation for inhomogeneous gas effects. The code is easily modified to use the exponentially-tailed-inverse distribution (Eq. 11) if it is desired. A modified subroutine is available using the Intuitive Derivative method for an exponentially-tailed-inverse distribution so comparative studies of H₂O radiation results can be made.

Choice of the band model distribution is not significant in most heat transfer applications where Lorentz broadening is likely to dominate. However, the increasing emphasis on weak lines as the distribution function proceeds from Model A to D produces a significant change in the Doppler curve-of-growth as mentioned earlier (see Fig. 3.26).

The program is coded for five radiating species (H₂O, CO₂, CO, HCl, and HF), and provision exist in the code for adding a sixth species. There is also provision for including carbon particles (soot) with the assumption that there is negligible scattering so that they can be treated as a gas in the linear limit.

3.2 BAND MODEL DATA

Band model data are obtained by both analytical and empirical methods. Generally the line structure of diatomic molecules is simple and well defined, so analytical predictions are effective. As molecules become more complex, analytical descriptions become more difficult and empirical methods are more reliable. Much of the data available are in a processes of evaluation, so the most recent generally accepted tabulations are usually the best.

A reasonably complete set of data, compiled for NASA/MSFC, was summarized in Ref. 10. It included analytical predictions for many diatomic gases and CO₂, and empirical values for high temperature H₂O. Young (Refs. 11 and 12) made a significant improvement in the data by merging the high temperature H₂O data of Ref. 10 with the low temperature data developed for atmospheric transmission predictions (Ref. 13). He also proposed improvements in CO₂ data (Refs. 12 and 14), but comparison with measurements (Refs. 15 and 16) indicate the CO₂ data may be incorrect at low pressures. A similar result was found by Lindquist et al. (Ref. 17), but recent work by Bernstein (Ref. 18) appears to offer improvements in the CO₂ data. The new Standardized Infrared Radiation Model (SIRRM) Code (Ref. 19) will include a data bank of band model parameters which is expected to serve as a resource for the best current data.

The GASRAD code uses formatted card-image input for the band model parameters, so the parameters can easily be changed. It is planned to furnish the program with data sets corresponding to data in Ref. 10 extended by data from Refs. 20, 21, 22, and 23. Data sets for H₂O and CO₂ combining Young's data with the data developed for NASA/MSFC are also furnished, and these are recommended in preference to the other data sets. Much of the data filled in to give a more extensive spectral interval and temperature range is not considered high quality, but it is useful for heat transfer predictions. Sources used in preparing the data sets are summarized in Table 3.3.

Absorption coefficient data for carbon particles were taken from Ref. 24 (also available in Ref. 10) for 2500 to 10000 cm⁻¹ and extrapolated down to 1000 cm⁻¹ as indicated in Ref. 25. The data are approximated in the program as polynomials in wavenumber using the coefficients in Table 3.4.

Table 3.3

SOURCES OF BAND MODEL PARAMETER DATA SETS

Element Name	Parameter	Wavenumber Range (cm ⁻¹)	Temperature Range (k)	Source
H2OGDC	\bar{k}	50-9300	300-3000	Tabulation of Ref. 10 converted to gas temperature ref. rather than STP.
		9325-11000	300-3000	Tabulation of Ref. 20 converted to gas temperature ref. rather than STP.
	1/d	1150-7500	600-3000	Tabulation of Ref. 10
	50-11000 50-1125 7525-11000	300 600-3000 600-3000	Sinusoidal approximation of Ref. 21: $\ln(1/d) = 0.7941 \sin(0.0036\omega - 8.043) + D(T)$ $D(T) = -2.295 + 3.004 \times 10^{-3}T - 3.66 \times 10^{-7}T^2$	
H2OCMB	k & 1/d	2500-4500	300-3000	Tabulation of Ref. 11 interpolated to match temperatures of H2OGDC
		50-2475 4525-11000	300-3000 300-3000	Same as H2OGDC
CO2GDC	k & 1/d	500-875	300-3000	Tabulated \bar{k} of Ref. 10 at $\Delta\omega = 5\text{cm}^{-1}$ were used for $\Delta\omega = 25\text{cm}^{-1}$ without averaging, and referenced to gas temp. instead of STP. Value for 2400k used also at 3000 k. Values of 1/d approximated from values in Ref. 22.
		900-1875	300-3000	Filled with zeros for continuity.
		1900-2375	300-3000	Tabulated values of Ref. 10 at $\Delta\omega = 10\text{cm}^{-1}$ were interpolated for $\Delta\omega = 25\text{cm}^{-1}$ without averaging. All \bar{k} values converted to gas temperature ref.

Table 3.3 (cont)

SOURCES OF BAND MODEL PARAMETER DATA SETS

Element Name	Parameter	Wavenumber Range (cm ⁻¹)	Temperature Range (k)	Source
		2400-2975	300-3000	Filled with zeros for continuity
		3000-3750	3000-3000	Same source as 1900-2375 cm ⁻¹ .
CO2CMB	\bar{k} & 1/d	2000-2400 3100-3775	300-3000 300-3000	Tabulations of Refs. 12 and 14 at 5cm ⁻¹ intervals degraded to $\Delta\omega=25\text{cm}^{-1}$ as indicated in Ref. 12. Values interpolated to match temperatures in CO2GDC.
		500-1975 2425-3075	300-3000 300-3000	Same as CO2GDC.
COGDC	\bar{k} 1/d	1025-2350 ----	300-5000 ----	Tabulations of Ref. 20 changed to gas temp. ref. instead of STP Approximation from Ref. 23 and errata: $1/d = 0.29(\text{cm}) \frac{(1+F(T))}{(1-F(T)) (1+F(T))^{3/4}}$ $F(T) = \exp(-1561.5/T)$ (Tabulated values available in Ref. 10).
HCLGDC	\bar{k} & 1/d	1000-3225	300-3000	Tabulations from Ref. 10 changed to gas temp. ref. instead of STP and interpolated to give data at 25 cm ⁻¹ intervals.
HFGDC	\bar{k} & 1/d	1400-4450	300-3000	Tabulations from Ref. 10 changed to gas temp. ref. instead of STP and interpolated to give data at 25 cm ⁻¹ intervals.

Table 3.4

CARBON ABSORPTION COEFFICIENT PLOYNOMIALS

Temperature K	A $\times 10^4$	B $\times 10^1$	C $\times 10^{-3}$	D $\times 10^{-7}$	E $\times 10^{-12}$
300	-.13463853	.38710213	-.47055911	.35084341	-.79087507
600	-.19909966	.42759743	-.50848071	.37144485	-.83813311
1200	-.31886445	.48804827	-.52853813	.36589761	-.80385920
1700	-.38870225	.53648682	-.50955662	.33136839	-.69866129
2000	-.60273281	.86118469	-1.0340689	.64889548	-1.3474213
2300	-.89695742	1.3577194	-1.8257443	1.1016709	-2.2102493
2600	-.41368281	1.8460052	-2.9400371	1.9221795	-4.1482373

$$k_{\omega} = A + B\omega + C\omega^2 + D\omega^3 + E\omega^4$$

k_{ω} = Absorption coefficient, cm^2/gm

ω = Wavenumber, cm^{-1}

3.3 SPECTRAL AVERAGING

Increasing the spectral integration interval beyond the 5 to 25 cm^{-1} for which band model data are usually available cannot be recommended on any theoretical basis for inhomogeneous gases. However, experience in heat transfer prediction from rocket exhaust plumes has indicated that larger intervals can be used to give satisfactory results for spectrally integrated radiation with significant savings in computation time. Since most computing time in the radiation (as distinguished from flowfield interpolation) portion of the program is spent in the wavenumber integration loop, any factor increase in the wavenumber interval results in about the same factor decrease in the computation time. So increasing the wavenumber interval from 25 to 100 cm^{-1} will reduce the radiation integration time by a factor of about 4. Applications have been made of 400 cm^{-1} intervals on H_2O plumes and 100 cm^{-1} intervals on $\text{H}_2\text{O}/\text{CO}_2/\text{CO}$ plumes, but it is necessary to verify the procedures on each problem to assure reasonable results. This section briefly surveys methods of spectral averaging, and presents some of the results which have been achieved.

Selection of averaging methods is influenced by the conditions of the application. If the linear limit of the curve-of-growth predominates, an effective value of \bar{k} is appropriate, and the value of $1/d$ is only significant if it causes an incorrect indication of the location on the curve-of-growth. In the case where the square-root limit predominates, an effective value of $\sqrt{\bar{k}/d}$ is desired, so average based $\sqrt{\bar{k}}$ and $\sqrt{1/d}$ appear to be appropriate. Representative expressions for use in the linear (L) and square-root (S) limits will be used here with the Planck function included to weight the coefficients based on the blackbody distribution. The resulting expressions are

$$\bar{k}_L(\omega, \Delta\omega, T) = \frac{\sum_{n=1}^m N^\circ(\omega'_n, T) \bar{k}(\omega'_n, \Delta\omega', T)}{\sum_{n=1}^m N^\circ(\omega'_n, T)}, \quad (18)$$

$$\bar{k}_S(\omega, \Delta\omega, T) = \left[\frac{\sum_{n=1}^m N^\circ(\omega'_n, T) \sqrt{\bar{k}(\omega'_n, \Delta\omega', T)}}{\sum_{n=1}^m N^\circ(\omega'_n, T)} \right]^2, \quad (19)$$

$$1/d_S(\omega, \Delta\omega, T) = \left[\frac{\sum_{n=1}^m N^\circ(\omega'_n, T) \sqrt{\bar{k}(\omega'_n, \Delta\omega', T)/d(\omega'_n, \Delta\omega', T)}}{\sum_{n=1}^m N^\circ(\omega'_n, T) \sqrt{\bar{k}(\omega'_n, \Delta\omega', T)}} \right]^2 \quad (20)$$

where $m = \Delta\omega/\Delta\omega'$

and $\omega'_n = (\omega - \Delta\omega/2 + \Delta\omega'/2) + (n-1)\Delta\omega'$

If Eqs. 19 and 20 are used to represent the square root limit, the desired result is achieved, but if \bar{k}_L and $1/d_S$ are used, then \bar{k}/d becomes

$$(\bar{k}_L/d_S)^{1/2} = (\bar{k}_S/d_S)^{1/2} \left[\frac{\sum_{n=1}^m N^\circ k}{\sum_{n=1}^m N^\circ \sqrt{k}} \right] \quad (21)$$

with the two representations of the square root parameter differing by the factor in brackets. A similar deviation from the desired average occurs in using \bar{k}_S rather than \bar{k}_L for predictions in the linear limit. In either case, if \bar{k} does not change significantly in the interval, $\Delta\omega$, then either method of averaging \bar{k} will give essentially the same result. As the interval increases so that there is a significant difference between \bar{k}_L and \bar{k}_S , it is likely that wavenumber interval will be approaching the limit of acceptable accuracy. However, limited experience with heat transfer predictions for relatively large rocket plumes has indicated \bar{k}_S gives slightly better results than \bar{k}_L . Results for typical lines-of-sight using \bar{k}_S and $1/d_S$ are given in Table 3.5. These indicate that predictions for H₂O/CO₂ plumes become unreliable above 100 cm⁻¹ while the decrease in importance of the gaseous radiation when soot is present allows very large intervals. The two examples of water vapor plumes indicate $\Delta\omega$ up to 400 cm⁻¹ may be satisfactory. This has also been shown in results for the Space Shuttle Main Engine plumes (Ref. 26) listed in Table 3.6.

Table 3.5

RESULTS OF USING LARGE SPECTRAL
INTEGRATION INTERVALS IN TYPICAL APPLICATIONS (Ref. 10)

Line-of-sight (Engine type or stage)	Gas Constituent	Mole Fract.	$\Delta\omega$ cm^{-1}	Predicted Radiance watts/ $\text{cm}^2\text{-sr}$	Percent Change from $\Delta\omega = 25 \text{ cm}^{-1}$
Rocketdyne H-1 (No carbon) (With 1 per- cent mass fraction of carbon)	H ₂ O	0.359	25	4.978	0.6 16 20 12 5
	CO ₂	0.167	100	5.008	
	CO	0.335	400	5.760	
	H ₂	0.139	800	5.970	
			1600	5.926	
			8000	5.232	
	H ₂ O	0.359	25	18.612	0.1 1 2 3 3
	CO ₂	0.167	100	18.599	
	CO	0.335	400	18.837	
	Carbon*	0.020	800	19.013	
H ₂	0.119	1600	19.227		
		8000	19.172		
Saturn S-II Stage	H ₂ O	0.693	25	1.407	0.3 3 7 6 49
	H ₂	0.307	100	1.411	
			400	1.449	
			800	1.512	
			1600	1.495	
			8000	2.096	
Rocketdyne J-2	H ₂ O	0.693	25	0.1511	0.1 2 4 7 13
	H ₂	0.307	100	0.1513	
			400	0.1536	
			800	0.1509	
			1600	0.1622	
			8000	0.1701	

Note: All cases integrated from 1000 to 9000 cm^{-1}

* Carbon is treated as a gas with a molecular weight of 12.

Subroutine ACDATA of the GASRAD program is coded to produce a table of \bar{k}_S and $1/d_S$ (Eqs. 19 and 20) for a specified $\Delta\omega$ which is an integral multiple of the $\Delta\omega'$ used in the band model data input. Change of averaging to \bar{k}_L (Eq. 18) or other methods may be made by modifying a few lines of code.

Table 3.6

RESULTS OF LARGE SPECTRAL INTERVALS FOR A WATER VAPOR PLUME

$\Delta\omega$ cm ⁻¹	Predicted Incident Flux - Btu/ft ² -sec								
	ET Base Center			Nozzle Lip Normal to Eng. Centerline			Fin Trailing Edge Side		
	SL	20kft	40kft	SL	20kft	40kft	SL	20kft	40kft
25	2.80	1.84	1.04	10.5	3.16	1.41	1.60	0.90	0.53
400	2.84	1.88	1.06	10.7	3.26	1.45	1.63	0.93	0.54

The usual method of integration for band models is to evaluate radiance (for a single line-of-sight) over a spectral interval using

$$\bar{N}_m = \sum_{\omega_1}^{\omega_2} \sum_{n=1}^m N_{\omega,n}^{\circ} (\tau_{\omega,n-1} - \tau_{\omega,n}) \Delta\omega \tag{21a}$$

where $\Delta\omega$ is a small interval and N_{ω}° is evaluated at the center of each $\Delta\omega$ interval from ω_1 to ω_2 . When large values of $\Delta\omega$ are used, the radiance may not be represented well by the central value, so the radiation code uses a table of integrated values of the Planck function to evaluate Eq. 21a as

$$\bar{N}_m = \sum_{\omega_1}^{\omega_2} \sum_{n=1}^m \left\{ \int_0^{\omega+\Delta\omega} N_{\omega,n}^{\circ} d\omega - \int_0^{\omega} N_{\omega,n}^{\circ} d\omega \right\} (\tau_{\omega,n-1} - \tau_{\omega,n}) \tag{21b}$$

Since linear interpolation is used in the table of integrated values, a spectral plot by the program of a continuum spectra using small $\Delta\omega$ will show a stepwise appearance rather than a smooth curve. This can be avoided by replacing the call to the PLANCK subroutine (and the ENU1, ENU2 definitions) by the following code:

$$SE = 1./ENU$$

$$SEE = SE * EXP(0.47933 * ENU/TW)$$

$$EYE = (1.1905E - 12 / (SEE ** 3 - SE ** 3)) * DENU$$

The use of degraded band model parameters is recommended when a large number of predictions are required and spectral data are not necessary, but results should be checked periodically to assure the desired accuracy is being achieved. Where only a few predictions are required, it is unlikely that the checking overhead will be justified by the computation time saving.

3.4 SPATIAL INTEGRATION

The transfer equation (Eq. 14) is integrated numerically using the geometry and numerical procedure indicated below. The spectral interval is set at the band model parameter resolution or a larger interval with averaged parameters as described in Section 3.3. This section will discuss considerations in the selection and use of geometric intervals Δs , $\Delta\phi$, and $\Delta\theta$.

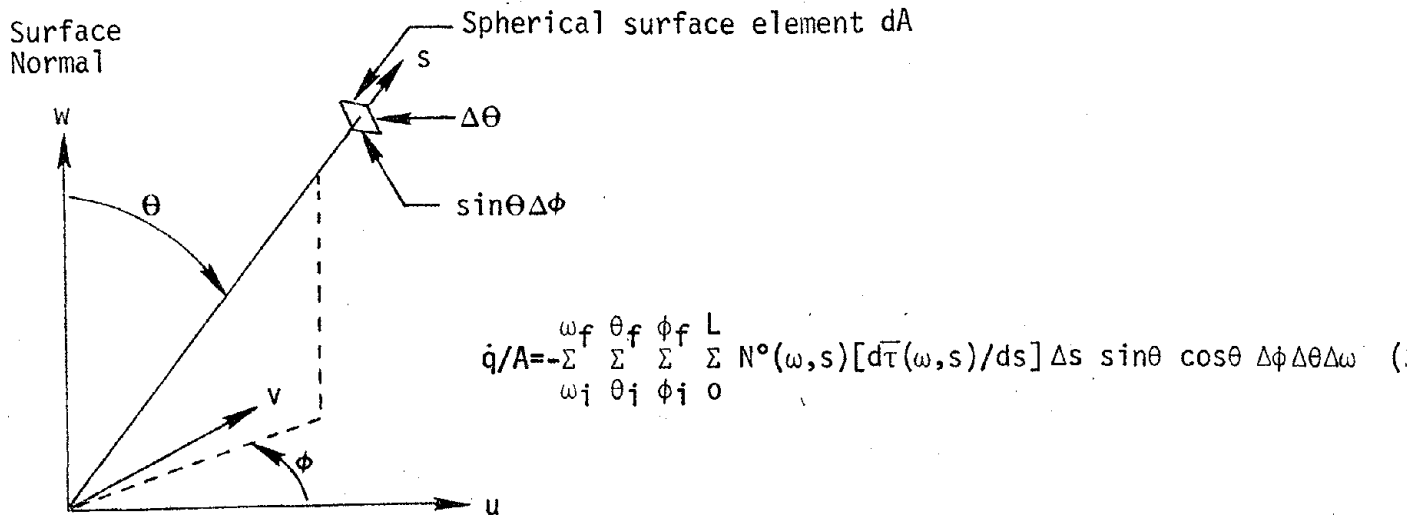


Fig. 3.5 Geometry for the Transfer Equation Integration

Selection of Δs should be made considering the features of the plume, the program run time limitations, and the memory size of the computer. The flowfield interpolation routines determine properties along each line-of-sight at input

specified Δs intervals. The value of Δs should be small enough to properly represent significant features in the plume, but large enough that the number of points on a line-of-sight will be less than the dimension parameter LPTMAX (which is normally set at 300). Once Δs is selected, values of $\Delta\theta$ and $\sin\theta\Delta\phi$ are normally assigned to be consistent with Δs . Equal spatial increments can be defined for a particular value of s by

$$\Delta s = s \sin\theta \Delta\phi = s \Delta\theta \quad (23)$$

and the program input provides specification of $\sin\theta\Delta\phi$ through the input variable TANGLE. TANGLE defines an upper limit $\Delta\phi'$ used in determining a $\Delta\phi$ which provides an integral number of increments in the range ϕ_j to ϕ_f . The procedure used is

$$\Delta\phi' = \text{TANGLE}/\sin\theta \quad (24)$$

$$\Delta\phi = (\phi_j - \phi_f) / \text{IFIX}((\phi_j - \phi_f) / \Delta\phi' + 1) \quad (25)$$

In a typical problem for the Space Shuttle Main Engine (SSME) plume radiation to the base, values of $\Delta s = 6$ inches and $\Delta\phi = \sin\theta\Delta\phi = 2^\circ$ have been used. These result in equal resolution in all three dimensions at $s = 172$ inches. As distance between the plume and the point-of-interest varies, Eq. 23 can be used to estimate consistent intervals. For example, to maintain the resolution on the SSME plume for a point 1000 inches from the base, $\Delta\theta$ and $\sin\theta\Delta\phi$ would have to be reduced to 0.34° .

After defining property variations along lines-of-sight using the resolution defined by Δs , $\Delta\theta$, and $\sin\theta\Delta\phi$ (or $\Delta\phi$), the radiation subroutines (SLGMLT and YNGH20) may increase the Δs integration interval based on temperature variations along each line-of-sight. The input variable TDIFF specifies the temperature change permitted in a line-of-sight segment which is to be

considered homogeneous. In the program operation, points are examined at the Δs intervals along a line-of-sight segment until a temperature, $T(L)$, exceeds the initial temperature on the segment, $T(1)$, by an amount greater than $TDIFF$, and if $|T(L)-T(1)| > 1.1 TDIFF$, the program retreats to $L=L-1$. Then the properties over the interval (points 1 thru L) are averaged, and it is considered to be a homogeneous region with a length of $L\Delta s$.

This allows an increase in integration speed while maintaining a small resolution to define plume features. In the usual plume problem any significant change in plume properties is accompanied by a change in temperature, so the procedure used is quite effective. However, caution should be exercised if the gas being analyzed has large changes in pressure or concentration which are not accompanied by a significant temperature change.

Because of the characteristics of the derivative band model procedure (Section 3.1) used in Subroutine YNGH20, the use of $TDIFF$ will not produce the time saving that will be realized for the Curtis-Godson method used in Subroutine SLGMLT. But time savings will be achieved since the program will select a $\Delta s'$ interval at each spectral position consistent with the absorption at that position. This procedure is controlled by the input variable IRAD which selects $\Delta s'$ by a procedure which gives

$$\Delta s'(\omega, s) \approx 1 / [IRAD * \bar{k}(\omega, s) c_i(s) p(s)] \quad (26)$$

for large values of the term in brackets and $\Delta s' \approx \Delta s$ for small values. So when the product $(\bar{k}cp)$ is small, a large spatial integration interval will be used. Very limited experience with the derivative method indicates values for $IRAD > 100$ should be considered, but each application should be evaluated based on the property variations and accuracy desired.

4 GEOMETRY MODEL

Discussion of the geometry model components will include: (1) the geometry of the receiving surface, shading surfaces, and plume; (2) the procedures used for defining line-of-sight limits as set by input limits, plume limits, and shading surfaces; and (3) the options available in describing the plume gas properties.

4.1 COMPONENT DESCRIPTIONS

The problem geometry is stated in terms of three components: the point-of-interest (POI), the plume, and the shading (or blocking) surfaces. These components are located in either the central coordinate system (CCS) or in an intermediate coordinate system (ICS) which is in a specified orientation in the CCS. All coordinate systems are right-hand as illustrated for a sample problem in Fig. 4.1. The CCS is defined in any orientation convenient for the problem, and the origin and orientation of the other systems are specified by location coordinates and three rotations. The sequence of rotations were selected to match the RAVFAC program (Ref. 27) so identical surface input could be used in both programs. The rotation sense and order are shown in Fig. 4.2 with some of the nomenclature used in defining the transformations.

The point-of interest (POI) is the first system input, and it is followed by the plume origin(s). In each case, a location and three rotations are specified along with an ICS number if applicable. The final position of the POI axes are represented by U , V , W with W representing the surface normal and the elevation and azimuth angles defined as indicated in Fig. 4.1. The final position of a plume system is typically X_W , Y_W , Z_W with Z_W representing

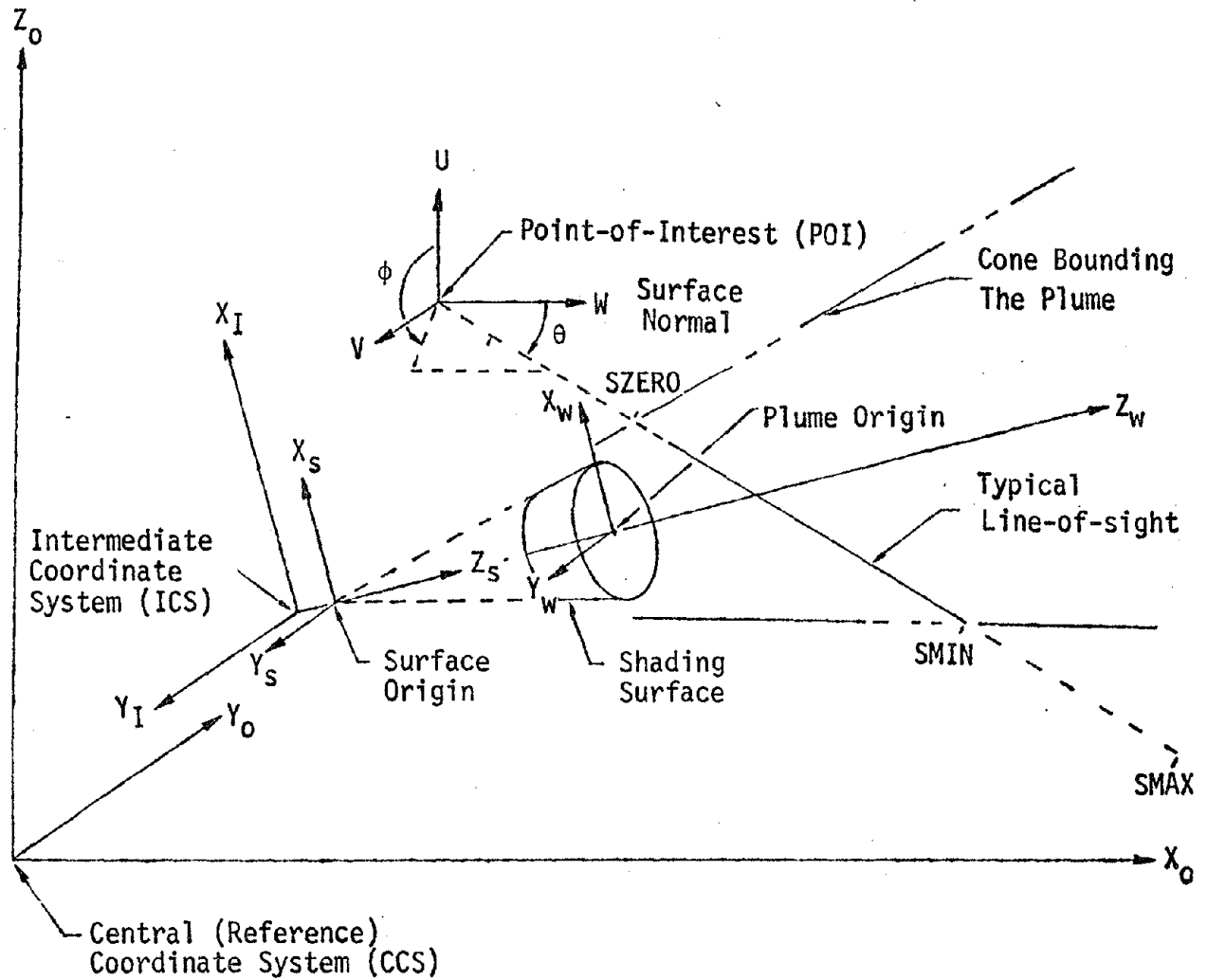
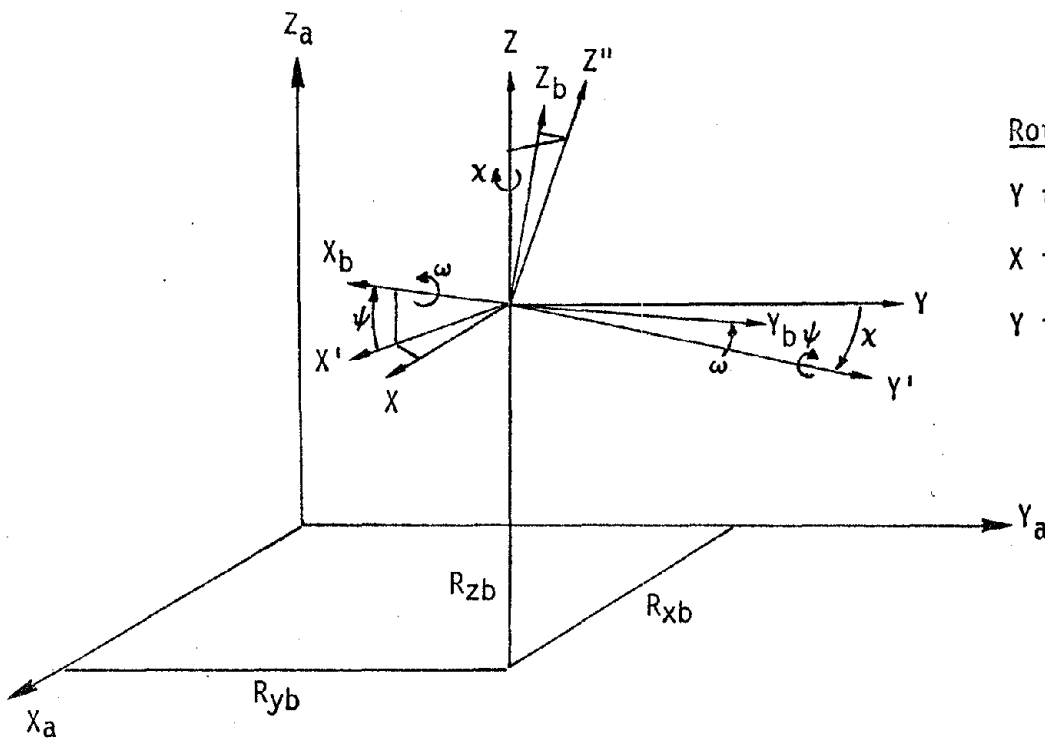


Figure 4.1 Overall Geometry Arrangement



Rotation Sense and Order

Y toward X	X
X toward Z	ψ
Y toward Z	ω

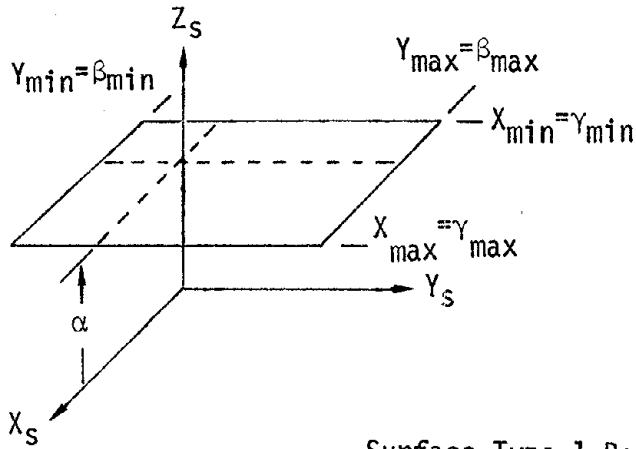
DIRECTION COSINES OF X_b, Y_b, Z_b RELATIVE TO X_a, Y_a, Z_a

X_b to X_a	$a_{11} = \cos\chi \cos\psi$
Y_a	$a_{12} = -\sin\chi \cos\psi$
Z_a	$a_{13} = \sin\chi$
Y_b to X_a	$a_{21} = \sin\psi \cos\omega - \cos\chi \sin\psi \sin\omega$
Y_a	$a_{22} = \cos\chi \cos\omega - \sin\chi \sin\psi \sin\omega$
Z_a	$a_{23} = \cos\psi \sin\omega$
Z_b to X_a	$a_{31} = -\sin\chi \sin\omega - \cos\chi \sin\psi \cos\omega$
Y_a	$a_{32} = -\cos\chi \sin\omega + \sin\chi \sin\psi \cos\omega$
Z_a	$a_{33} = \cos\psi \cos\omega$

TRANSFORMATION MATRIX AND ITS INVERSE

$$A_{ba} = \begin{bmatrix} a_{11} & a_{12} & a_{13} \\ a_{21} & a_{22} & a_{23} \\ a_{31} & a_{32} & a_{33} \end{bmatrix} \quad \text{and} \quad A_{ab} = A_{ba}^{-1} = \begin{bmatrix} a_{11} & a_{21} & a_{31} \\ a_{12} & a_{22} & a_{32} \\ a_{13} & a_{23} & a_{33} \end{bmatrix}$$

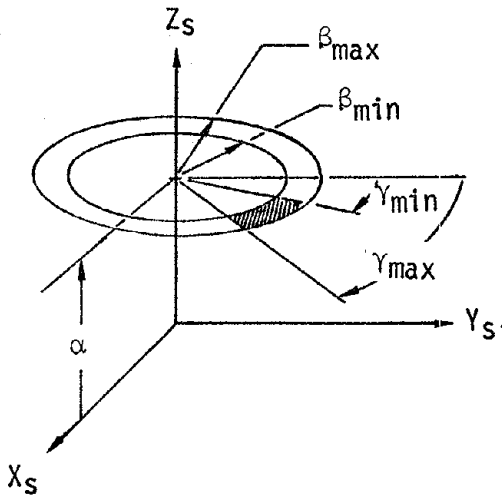
Fig. 4.2 Definition of Rotation Angles, Direction Cosines, and Rotation Matrices



Limitations:

- $\beta_{min} < \beta_{max}$,
- $\gamma_{min} < \gamma_{max}$

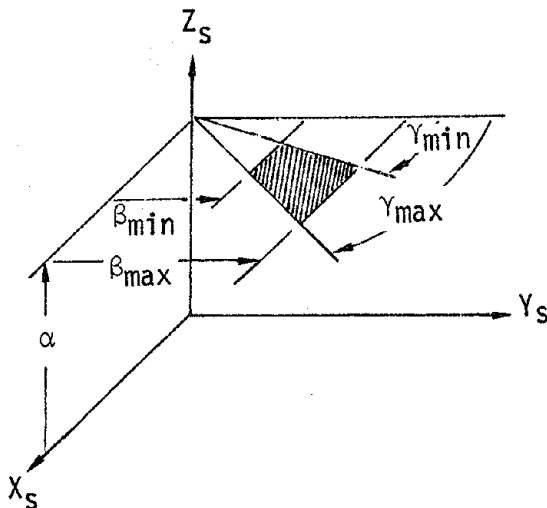
Surface Type 1 Rectangle



Limitations:

- $0 \leq \beta_{min} < \beta_{max}$,
- $-360^\circ < \gamma_{min} < \gamma_{max} \leq 360^\circ$,
- and $\gamma_{max} \leq (\gamma_{min} + 360^\circ)$

Surface Type 2 Disc

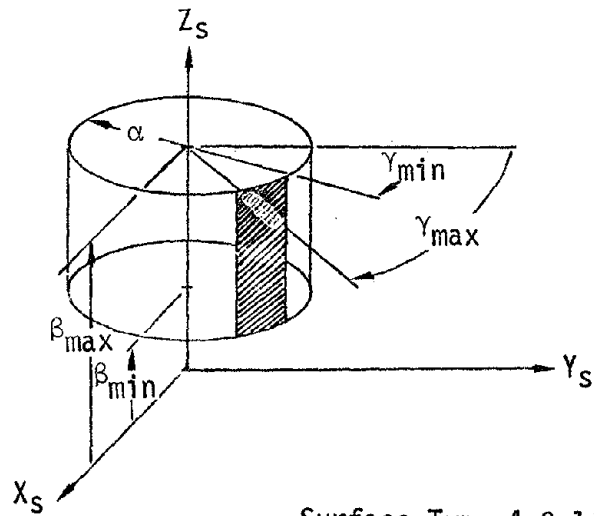


Limitations:

- a) $0 \leq \beta_{min} < \beta_{max}$
- $-90^\circ \leq \gamma_{min} < \gamma_{max} \leq 90^\circ$
- or
- b) $\beta_{min} < \beta_{max} \leq 0$
- $90^\circ \leq \gamma_{min} < \gamma_{max} \leq 270^\circ$

Surface Type 3 Trapezoid

Figure 4.3 Blocking Surface Geometry



Surface Type 4 Cylinder

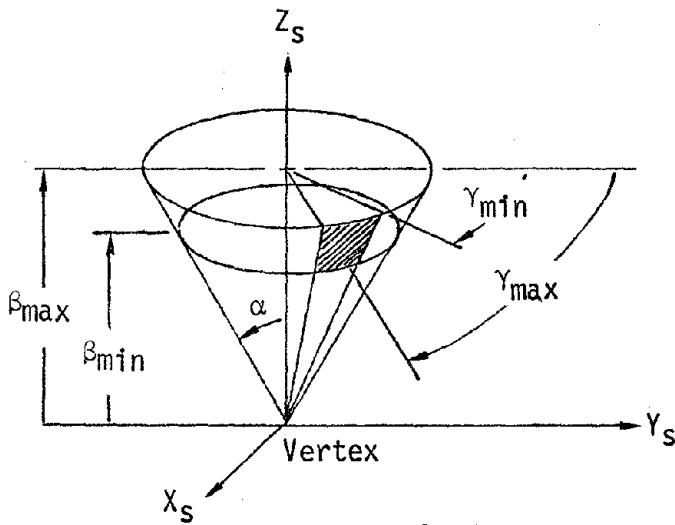
Limitations:

$$\alpha > 0,$$

$$\beta_{max} > \beta_{min},$$

$$-360^\circ \leq \gamma_{min} < \gamma_{max} \leq 360^\circ$$

$$\text{and } \gamma_{max} \leq (\gamma_{min} + 360^\circ)$$



Surface Type 5 Cone

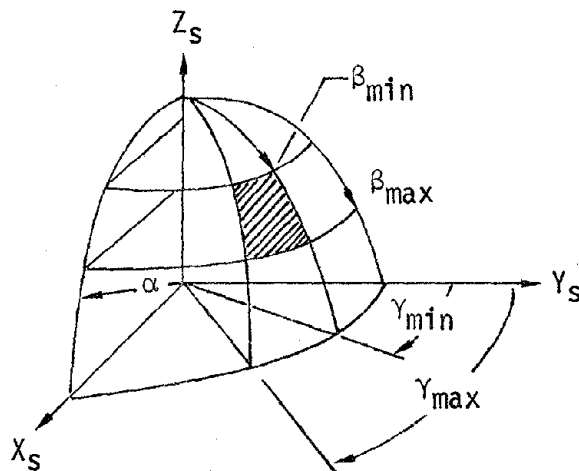
Limitations:

$$0 < \alpha < 90,$$

$$\beta_{max} > \beta_{min},$$

$$-360^\circ \leq \gamma_{min} < \gamma_{max} \leq 360^\circ$$

$$\text{and } \gamma_{max} \leq (\gamma_{min} + 360^\circ)$$



Surface Type 6 Sphere

Limitations:

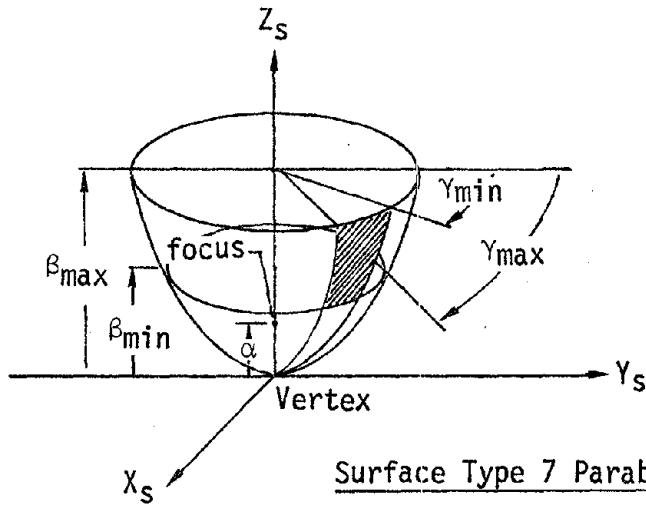
$$\alpha > 0,$$

$$0^\circ \leq \beta_{min} < \beta_{max} \leq 180^\circ,$$

$$-360^\circ \leq \gamma_{min} < \gamma_{max} \leq 360^\circ,$$

$$\text{and } \gamma_{max} \leq (\gamma_{min} + 360^\circ)$$

Figure 4.3 (continued) Blocking Surface Geometry



Limitations:

$$\alpha > 0$$

$$0 \leq \beta_{\min} < \beta_{\max}$$

$$-360^\circ \leq \gamma_{\min} < \gamma_{\max} \leq 360^\circ$$

$$\text{and } \gamma_{\max} \leq (\gamma_{\min} + 360^\circ)$$

Useful relations:

$$x^2 + y^2 = 4\alpha z$$

$$[dx/dz]_{y=0} = 2\alpha/x$$

Figure 4.3 (continued) Blocking Surface Geometry

A translation vector $R(I)$ is also prepared giving the location of the POI in all other systems ($I > 1$)

$$R(I) = \begin{bmatrix} R1(I) \\ R2(I) \\ R3(I) \end{bmatrix} = [T(I)] \begin{bmatrix} Rx(1) - Rx(I) \\ Ry(1) - Ry(I) \\ Rz(1) - Rz(I) \end{bmatrix} \quad (31)$$

4.2 LINE-OF-SIGHT OPERATIONS

Each line-of-sight (LOS) is defined based on the orientation of the point-of-interest (POI) as represented by the transformation matrix $T(1)$, defined earlier, and the direction in the POI system obtained by incrementing the hemispherical angles ϕ and θ (Fig. 4.1) between the input limits of integration ($\phi_i, \phi_f, \theta_i, \theta_f$). Operations to produce the LOS are performed in sequence at the center of each angular element beginning at $\theta = \theta_i + \Delta\theta/2$ and $\phi = \phi_f + \Delta\phi/2$. Integration limits for distance (s) along the LOS are adjusted as required to satisfy blocking surfaces and plume limits, then plume properties are obtained by interpolation at the center of Δs intervals beginning at $s=s_0+\Delta s/2$.

The direction of the LOS relative to the CCS is defined by the direction cosines $a, b,$ and g

$$\begin{bmatrix} a \\ b \\ g \end{bmatrix} = [T(1)] \begin{bmatrix} \sin\theta \cos\phi \\ \sin\theta \sin\phi \\ \cos\theta \end{bmatrix}, \quad (32)$$

and the components of the LOS vector in each surface coordinate system are defined by

$$\begin{bmatrix} C1 \\ C2 \\ C3 \end{bmatrix} = [T'(I)] \begin{bmatrix} S_m^a \\ S_m^b \\ S_m^g \end{bmatrix} \quad (33)$$

where $T'(I)$ is the inverse of the transformation matrix for surface I and S_m represents the upper limit of the LOS. Since the vector $\vec{R}(I)$ (Eq. 31) represents the position of the POI in the surface system, the equation of the LOS

in the surface system (X_S, Y_S, Z_S) is

$$\frac{X_S - R1}{C1} = \frac{Y_S - R2}{C2} = \frac{Z_S - R3}{C3} = \delta \tag{34}$$

where δ represents a fraction of the magnitude of the LOS upper integration limit S_m . So a solution is only applicable if δ lies in the range 0 to 1.

For the plane surfaces (Types 1, 2, and 3 in Fig. 4.3), the defining equation in the surface system is $Z_S = \alpha$ which combined with Eq. 34 yields

$$\delta = (\alpha - R3) / C3 \tag{35}$$

If $0 < \delta < 1$, the LOS may be blocked by the surface, so the position

$$X_S = R1 + \delta C1 \tag{36}$$

$$Y_S = R2 + \delta C2 \tag{37}$$

is computed and checked against the surface limits defined by β and γ (Fig. 4.3).

The conic shapes (Types 4, 5, 6, and 7 in Fig. 4.3) can be described by

$$X_S^2 + Y_S^2 = A + B Z_S + C Z_S^2 \tag{38}$$

where the coefficients for the surfaces represented are

	<u>A</u>	<u>B</u>	<u>C</u>
Cylinder	α^2	0	0
Cone	0	0	$\tan^2 \alpha$
Sphere	α^2	0	-1
Paraboloid	0	4α	0

Solution of Eqs. 34 and 38 yields

$$AA \delta^2 + BB \delta + CC = 0 \tag{39}$$

where

$$\begin{aligned} AA &= (C1^2 + C2^2 + C C3) \\ BB &= (2 R1 C1 + 2 R2 C2 - B C3 - 2 C R3 C3) \\ CC &= (R1^2 + R2^2 - A - B R3 - C R3^2) \end{aligned}$$

If either solution of Eq. 39 lies between 0 and 1, the position is computed (Eqs. 36 and 37) and tested against the surface limits defined by β and γ

(Fig. 4.3). If both solutions are between 0 and 1 and lie within the surface limits, then the smaller solution is chosen.

As each surface is tested in sequence, the upper limit of integration is reduced to correspond to the resulting δ if it is smaller than any previous solution. The final solution then represents the distance to the nearest blocking surface, and the LOS upper limit of integration is redefined by $S_m + \delta S_m$.

After checking for shading, the LOS is tested to determine if it intersects a conical boundary around the plume. The boundary is defined during surface input using the same parameters as a blocking surface, but the parameters are defined by the program using the plume origin and the intercept (AP) and slope (BP) of the boundary at $Z_W = 0$. Solution for the intercepts of the LOS and the plume boundaries is carried out in Subroutine SLIMIT using the same approach as for the blocking surfaces, but additional tests are required to set integration limits as a function of the LOS orientation. If the LOS lower limit computed in SLIMIT is greater than the input lower limit s_0 , the lower limit for the LOS is adjusted. Similarly, if the final intercept is less than the upper limit (set by either input or blocking), the upper limit for the LOS is reduced.

In all operations adjusting the LOS limits, the values used are multiples of Δs which fall just outside of the limit solutions. Once the limits are adjusted, the LOS distance is initialized at $s = s_0 + \Delta s/2$ and incremented in Δs intervals until $s > s_m$. At each value of s an interpolation is made in the plume property tables (described later) to define the temperature, pressure, and mole fractions of species identified by the input. Even though the portion of the LOS (s_0 to s_m) is within the cone bounding the plume, a point may not be within the plume property table since the cone does not usually fit the plume at all points. Points outside the plume are assigned a zero temperature, and after the LOS is complete, the temperatures are checked to determine if they

are non-zero and within the temperature range normally used in the band model parameter tables (300K to 3000K). If all temperatures are zero, the LOS is identified as having missed the gas, and if any points are found outside the 300K to 3000K range, a warning message is printed at the termination of all LOS processing.

The sequence used in line-of-sight testing was chosen to indicate first blocking and second missing the plume. This requires more computation than the reversed procedure since processing of each LOS missing the plume bounding cone could be immediately terminated. But the procedure used provides a more complete picture of the geometry to assure proper orientation of the POI and surrounding structure.

4.3 PLUME DESCRIPTIONS

Topics in the plume descriptions include the two basic forms, axisymmetric and three-dimensional, along with methods of interpolation and recognition of discontinuities caused by shocks. Dimensional considerations are also discussed including methods of stacking plume sections.

Forms of Gas Property Arrays

Plumes use a cylindrical coordinate system as illustrated below with properties specified as a function of Z , η , R in general. But for the axisymmetric

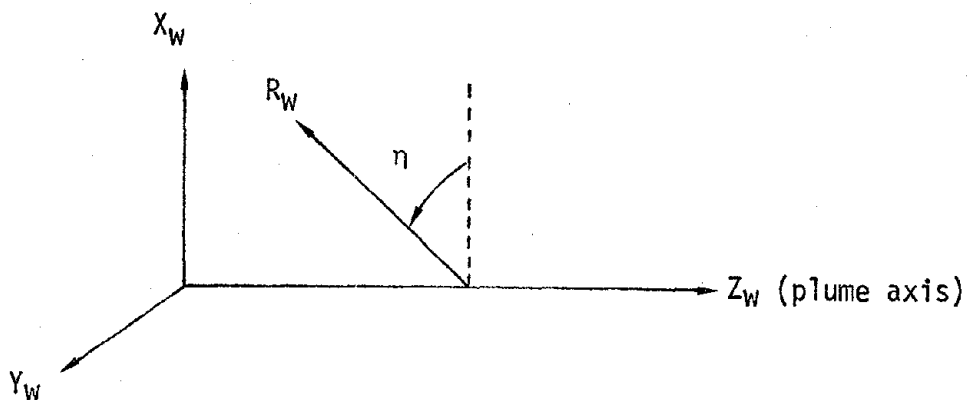


Fig. 4.4 Basic Plume Coordinates

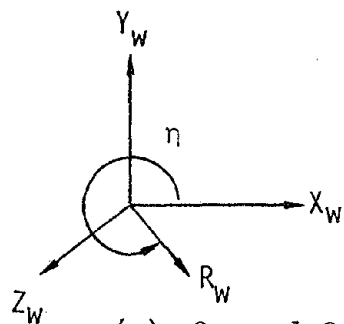
case, a single value of η is used and taken to apply for all η , and for 3-D plumes, optional parameters are available to modify the description to take advantage of engine cluster symmetry.

The axisymmetric plume description is used for plumes which are assumed to be non-interfering. Up to six separate plume origins and orientations can be specified for a single set of axisymmetric plume data to simulate multiengine arrangements. (The limit of 6 plumes was chosen to fit existing input control flag limits and could easily be expanded.) Descriptions of the Space Shuttle low-altitude plumes (Ref. 26) used this procedure with three plume origins located at the three main engine exits even though plume interference occurs between plumes in this arrangement because of the close engine spacing. Operation of the program chooses the closest plume for evaluation of gas properties, so adjacent plumes are effectively terminated at a surface equidistant from the plume axes.

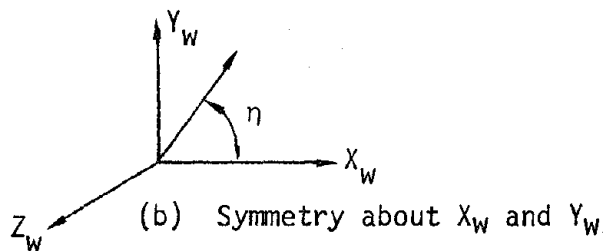
The form of 3-D flowfield input is governed by three parameters intended to facilitate the property description using symmetry in engine clusters. Brief descriptions of the parameters identified by the input names are:

CTCD	Represents the center-to-center distance between an engine and the axis of the engine cluster. Actually it is the distance between the plume cluster axis Z_w and an axis used for property input Z'_w which is displaced along the X_w axis.
HANG	Represents the half-angle of a symmetrical sector of a plume cluster. The sector is assumed to have symmetry about the X_w axis.
ISYMSC	A flag to specify assumptions of symmetry about a plane normal to the X_w axis at a distance of CTCD/2 from the Z_w axis. This is used if the center and outboard plumes in a cluster are assumed to be mirror images within the limits defined by HANG.

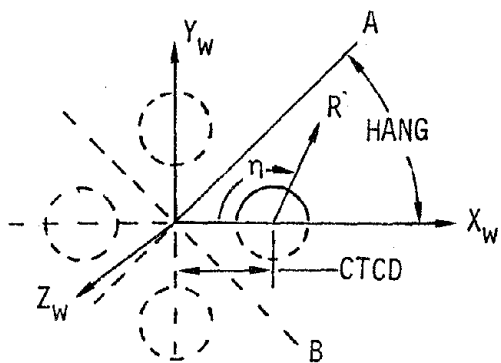
A few examples illustrating the use of these parameters are shown in Fig. 4.5. As noted in the descriptions above for cases of CTCD > 0, the axis used for property definition (Z'_w) is defined parallel to Z_w .



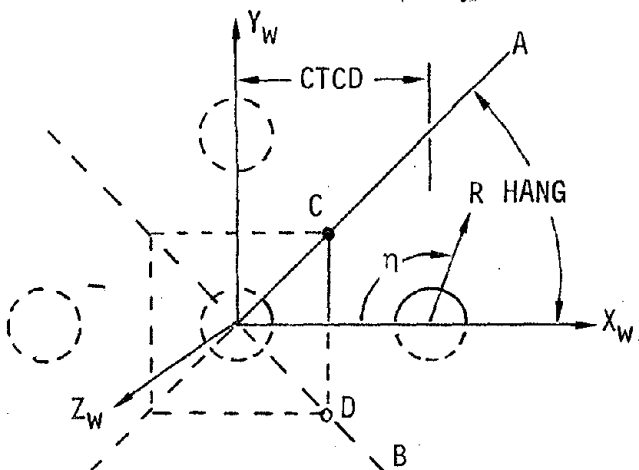
(a) General Case



(b) Symmetry about X_w and Y_w



(c) Symmetry about X_w , Y_w , A, and B. For a 4 engine cluster.



(d) Symmetric about X_w , Y_w , A, B, and CD. For a 5 engine cluster.

RANGE OF η	CTCD	HANG	ISYMSC
0-360°	0	360°	1

0-90°	0	90°	1
-------	---	-----	---

0-180	>0	45°	1
-------	----	-----	---

0-180°	>0	45°	0
--------	----	-----	---

Fig. 4.5 Illustration of optional plume descriptions using the parameter CTCD, HANG, and ISYMSC.

For engine clusters which are not symmetrical or in which the engines are canted, special consideration needs to be given to the 3-D plume description. Use of the general case (Fig. 4.5a) requires a relatively large internal storage capacity to obtain satisfactory detail in the plume, but the more effective descriptions represented by $CTCD > 0$ (Fig. 4.5c and d) may not fit well for non-symmetric clusters or canted nozzles. In applications for the Space Shuttle Main Engine (SSME) vacuum plume (Ref. 26), a symmetric 3-engine cluster was assumed which approximated the actual arrangement, and a flowfield transformation program (DTRANS, Ref. 28) was used to put the flowfield developed for canted nozzles into the form required with the flowfield property axis parallel to the cluster axis (Z_w). In the SSME vacuum plume some characteristics of this three-dimensional solution became unacceptable downstream, so the 3-D portion was terminated at $Z_w = 200$ inches. The remainder of the cluster flowfield was approximated by an extension of the axisymmetric central core of the flow which was expected to contribute most significantly to the plume radiation. To accommodate this circumstance, an option was included in the program to switch from a 3-D plume in the nearfield to an axisymmetric approximation in the farfield.

Due to the large internal memory requirement for the plume, dimensioning deserves special attention. Each location in the plume at which properties are specified requires three memory locations for radius, temperature, and pressure plus the number of species mole fractions dimensioned for the problem (parameter NK, data NKO) which is usually less than the allowable number of species in the input flowfield (parameter NKTP). The parameters specifying the maximum number of flowfield locations are outlined below:

	<u>Axisymmetric</u>	<u>3-D</u>	
Z_w positions	MZ2	MZ3	
η positions at each Z_w	1	MN3	(40)
Radius positions at each η	MR2	MR3	

Combining these parameters with the number of values stored at each point gives an approximation of the flowfield internal memory requirement:

$$\text{Axisymmetric } (3 + NK)(MR2)(MZ2) \quad (41a)$$

$$\text{3-D } (3 + NK)(MR3)(MN3)(MZ3) \quad (41b)$$

An early goal in the program was to maintain the flowfield memory requirement in the 11K to 12K word range so the program could be run within a 32K word memory limit. Values chosen for the multiconstituent program ($NK=6$) were $MR2=MR3=30$, $MN3=13$, $MZ2=40$, and $MZ3=3$. For the SSME predictions, NK was reduced to 2 (for H_2O and N_2) and the Z_w positions were increased to $MZ2=78$ and $MZ3=6$. Even with this increase, the severe limitation on $MZ3$ is apparent. Because of this limitation, the program was designed to handle the plume in sections to prevent a restriction in length by the internal memory size.

Procedures for stacking plume sections will be automatically applied by the program to either a single axisymmetric or 3-D plume. The flexibility allowed in positioning multiple axisymmetric plumes was not compatible with the stacking procedure. The procedure starts by reading in the allowed (dimensioned) Z_w positions, interpolating for properties on all lines-of-sight, and storing the partial solution on Unit 3. The last Z_w position in memory is moved to the initial location and additional Z_w positions are loaded. Partial lines-of-sight are read from Unit 3, extended, and written on Unit 4. This procedure is repeated with the partial lines-of-sight shifting between Unit 3 and 4 until the plume processing is complete. At that time the completed lines-of-sight are output on Unit 10 as they are when no piecing together is required. This process is relatively straightforward for lines-of-sight in the $+Z_w$ direction, but it requires some maneuvering when a line-of-sight is in the $-Z_w$ direction because the last section of the line-of-sight is completed first.

The large amount of input/output required when the plume sections must be stacked has become quite significant in the current computer cost assignment

system at MSFC. Therefore, it is recommended that the dimension parameter product (Eq. 41) be made as large as currently allowable and the relative parameter values be adjusted to the particular plume requirements so the plume does not have to be sectioned.

Interpolation Methods

The interpolation procedure used to define gas properties in the plume will be described first for axisymmetric plumes. Then the additional interpolation in η required by 3-D plumes will be discussed. Plume data are stored as an array at a set of Z_w values and arbitrary values of R_w . An illustration of a pair of adjacent Z-cuts in Fig. 4.6 indicates the physical arrangement including the optional shock location.

The property search begins with a location in the plume (Z_w, R_w) of the point desired on the line-of-sight. The selection of the plume (in multiple plumes) and transformation of the location to the plume coordinate system is performed in Subroutine PLUMPT. The values of Z in the plume property table are searched sequentially* to define the two values $Z(I1)$ and $Z(I2)$ containing the interval in which Z_w is located, and the ratio for linear interpolation is defined (refer to Fig. 4.6 for nomenclature)

$$ZRATIO = (Z_w - Z(I1)) / (Z(I2) - Z(I1)) \quad (42)$$

Next, the plume boundary is defined at Z_w by

$$R_{wMAX} = R_{MX1} + (R_{MX2} - R_{MX1}) * ZRATIO, \quad (43)$$

If $R_w > R_{wMAX}$ the interpolation is terminated, otherwise, values of $R_{wZ}(1)$ and $R_{wZ}(2)$ are defined to represent R_w in radial interpolation at $ZZ(I1)$ and $ZZ(I2)$.

* Test using a uniform binary search in Z and R did not indicate a measurable saving in overall computation time for a typical problem.

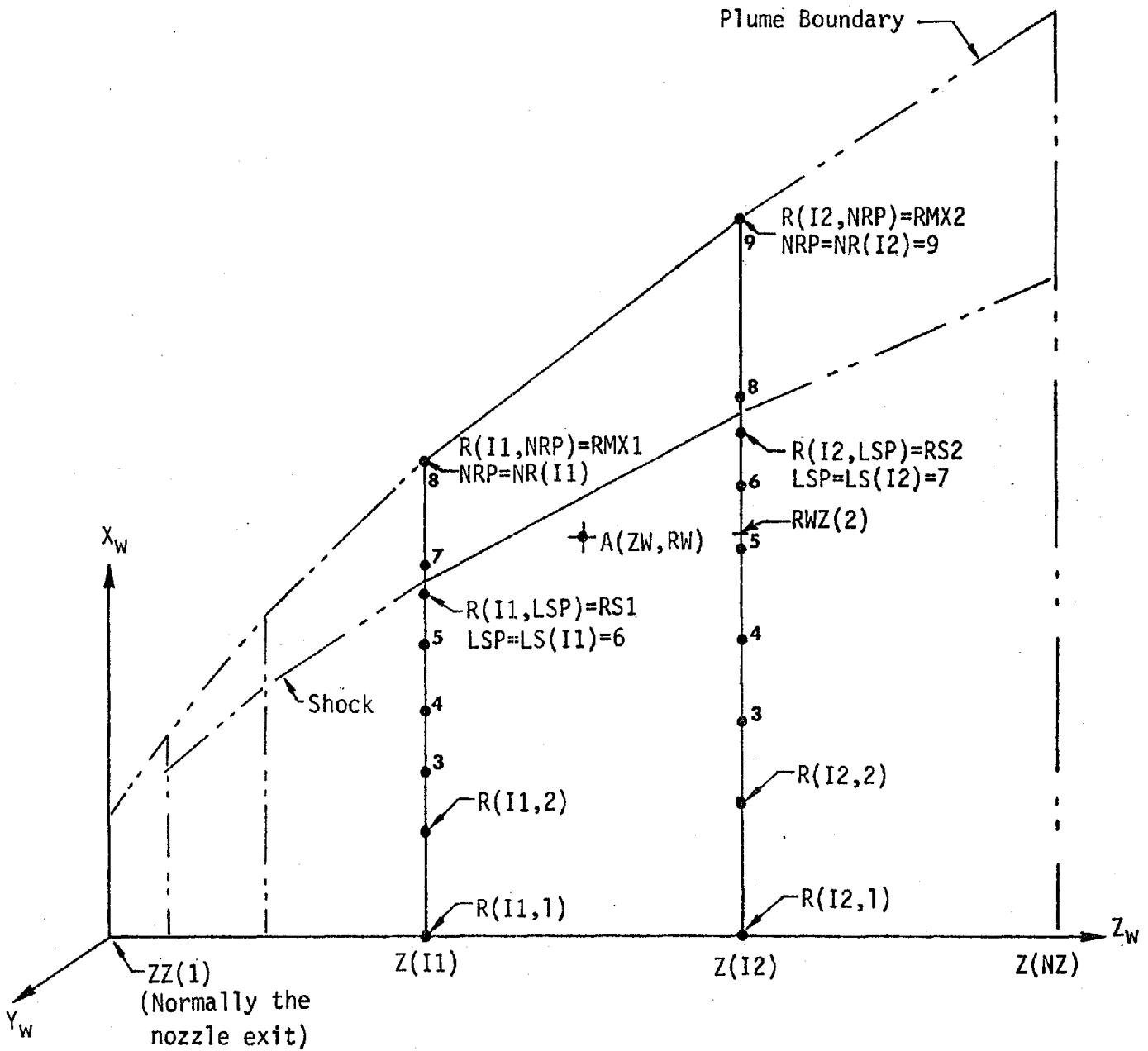


Fig. 4.6 Illustration of Axisymmetric Plume Data Arrangement

The code is currently written to interpolate parallel to the plume axis

$$RWZ(1) = RWZ(2) = RW, \quad (44)$$

but comment cards are included for code which can be used to vary the interpolation so that it becomes parallel to the plume boundary at the boundary. The revised procedure which was used in earlier versions of the code is

$$\begin{aligned} RDUB &= RW/RWMAX \\ RWZ(1) &= RMX1 *RDUB \\ RWZ(2) &= RMX2 *RDUB \end{aligned} \quad (45)$$

Although this procedure appears attractive, it produced unrealistic results for some portions of the SSME (3-D) vacuum plume due to large changes in the boundary and properties in the η -direction.

The radial values of Z(I1) (and Z(I2)) are searched sequentially for the intervals containing RWZ(1) (and RWZ(2)). Search limits are determined by the optional shock specification. If a significant shock is in the plume, two radial points very close together should be specified to define the properties on both sides of the shock. The radial index of the smaller radius point is indicated by LS(I) where I is the index of the Z-cut. The shock locations RS1 and RS2 are defined at consecutive Z-cuts as shown in Fig. 4.6. If both radii are >0 , the shock option is invoked, and the shock position at ZW is computed

$$RS = RS1 + (RS2-RS1) *ZRATIO \quad (46)$$

This radius is tested against RW to determine if the point is inside or outside the shock surface. The outcomes of the shock handling, and the resulting radial search limits for RWZ1 and RWZ2 are summarized below:

<u>Condition</u>	<u>Flag</u>	<u>Radial Search Index</u>
RS1 = 0 or RS2 = 0	LSHOCK = 0	N = 1, NR(I)
RW \geq RS	LSHOCK = 1	N = [LS(I)+1], NR(I)
RW < RS	LSHOCK = -1	N = 1, LS(I)

When the radial interval is located containing RWZ(II) (where II is 1 or 2), linear interpolation is performed to determine the corresponding properties

(temperature, pressure, and species mole fractions). If the upper limit of the radial search is reached before finding the interval containing $RWZ(II)$, the properties of the point at the end of the search are used for $RWZ(II)$. After properties are determined at $RWZ(1)$ and $RWZ(2)$, a linear interpolation in Z_w is performed for all properties (similar to the procedure in Eqs. 43 and 46).

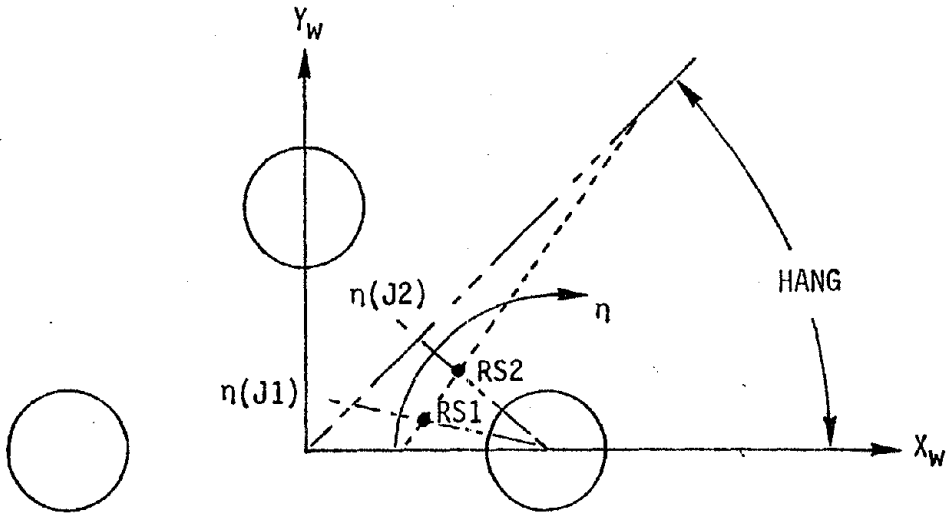
As an illustration, consider Point A in Fig. 4.6 as the line-of-sight point located at Z_w, RW . First, Z -values in the table are searched to identify $Z(I1)$ and $Z(I2)$ and the interpolation fraction $ZRATIO$ (Eq. 42) is computed. The plume boundary points at these Z -cuts are identified, the plume boundary is defined (Eq. 43), and the point is found to be inside the plume ($RW < RWMAX$). Shock radii at $Z(I1)$ and $Z(I2)$ are >0 , so the shock radius is computed at Z_w and the point is determined to be inside the shock ($RW < RS$) which sets $LSHOCK=-1$. The desired radial values for interpolation at each Z -cut are defined ($RWZ(1) = RWZ(2) = RW$), and a loop is entered to define properties at $RWZ(1)$ and $RWZ(2)$. Since the search is limited by the shock position, the search at $Z(I1)$ cannot reach RW , so the properties at $R(I1,6)$ are used for $RWZ(1)$. Properties for $RWZ(2)$ are determined by linear interpolation between $R(I2,5)$ and $R(I2,6)$. Finally properties at Point A are determined by linear interpolation in Z between $RWZ(1)$ and $RWZ(2)$.

Without shocks, 3-D interpolation is a relatively straightforward extension of the axisymmetric procedure, but with shocks, special procedures are added which complicate the description. The values XW, YW, ZW returned by Subroutine PLUMPT for the location of a point in the plume are converted to Z_w, SIG, RW , where SIG represents the angle η in the plume property description (refer to Fig. 4.4). All interpolation is linear and the sequence of interpolation is radial (RW in R_w), angular (SIG in η), and axial (Z_w in Z_w).

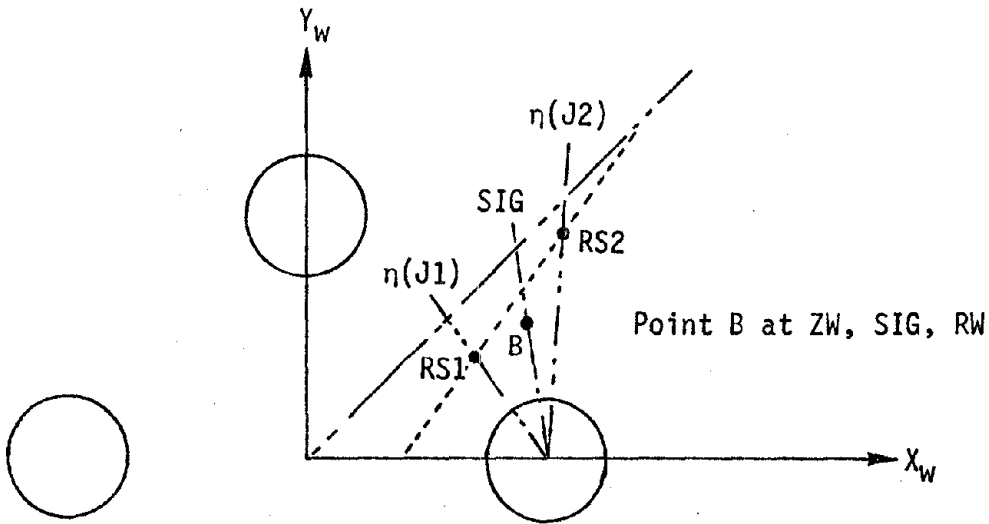
As in the axisymmetric case, Z_w is searched first to find $I1$ and $I2$ which satisfy $Z(I1) \leq Z_w < Z(I2)$. Then the values of η are searched at each of the two Z_w locations to define $\eta(J1) \leq SIG < \eta(J2)$, and the maximum radius ($RSIGMX(II)$) and shock radius ($RSHOK(II)$) are determined (at each Z) by linear interpolation in η between the values at $\eta(J1)$ and $\eta(J2)$. An interpolation in Z_w is then made to obtain the maximum radius ($RWMAX$) and shock radius (RS) at Z_w . If shocks are not defined for all four sets of radial data involved in this process, the interpolation for properties follows the same sequence as summarized above for $RWMAX$ with linear interpolation in radius to match RW at each of the four η -cuts (2 at each Z -cut).

Existence of shock data ($LS(I,J) > 1$) for all four η -cuts invokes the shock option which has a special procedure useful in flowfield descriptions for clustered engines. Typical examples of the two cases considered are shown in Fig. 4.7. In each case the procedure is designed to treat the properties as axisymmetric in the region between the nozzle centerline and the shock. This is accomplished by using radial interpolation on the η -cut with the largest shock radius. For the case in Fig. 4.7a the radial properties at $\eta(J1)$ would be used, while the case in Fig. 4.7b would use properties at $\eta(J2)$. For example, Point B in Fig. 4.7b lies between $\eta(J1)$ and $\eta(J2)$ and inside the shock surface, so its properties will be best represented by the properties on $\eta(J2)$ at the same radius. As a result the program determines properties at Point B as though it were in an axisymmetric plume described by $\eta(J2)$.

This feature can be disabled by setting control flag $ISHOCK = 1$. The result in Fig. 4.7b would be a linear interpolation in η between properties at $RS1$ (on the side of the shock closest to the nozzle) and those at a radius RW along $\eta(J2)$.



(a) Case for KETA(II)=1



(b) Case for KETA(II)=2

Fig. 4.7 Illustrations for the 3-D Flowfield Geometry With a Shock for a Typical 4-Engine Cluster.

The 3-D code is written to interpolate in Z_w parallel to the flowfield axis as described in Eq. 44 for axisymmetric plumes. However, code is included as comments which can be used to interpolate as in Eq. 45 for axisymmetric plumes.

5 REFERENCES

1. B. Alligood, B. Conway, and R. Yossa, "Analysis and Computer Program for Determining Gaseous Thermal Radiation," Brown Engineering Co., TN R210 (1966).
2. R. M. Huffaker and M. J. Dash, "A General Program for the Calculation of Radiation from an Inhomogeneous, Nonisobaric, Nonisothermal Rocket Exhaust Plume," NASA/MSFC TM X-53622 (1967).
3. M. Delwadia, J. E. Reardon, and S. A. White, "A Three-Dimensional Radiation Program for the Saturn S-II Stage," Hayes International Corp., ER 1470 (1967).
4. Multi-constituent radiation program - NASA/MSFC Computation Laboratory Job No. 353887 (1970).
5. J. E. Reardon, "Prediction of Radiation from Rocket Exhaust Gases," AIAA Paper 70-841, Fifth Thermophysics Conference (1970).
6. J. E. Reardon, "A Computer Program for the Prediction of Radiation from Rocket Exhaust Plumes (2 Volumes)," REMTECH, Inc. RTR 013-1, (1973).
7. S. J. Young, JQRST 18, 1 (1977).
8. W. Malkmus, J. Opt. Soc. Am. 57, 323 (1967).
9. W. Malkmus, J. Opt. Soc. Am. 58, 1214 (1968).
10. C. Ludwig, et al, "Handbook of Infrared Radiation from Combustion Gases," NASA SP 3080 (1973).
11. S. J. Young, JQRST 18, 29 (1977).
12. S. J. Young, "Band Model Parameters for the 2.7 μm Bands of H_2O and CO_2 in the 100 to 3000 K Temperature Range," Aerospace Corp. Report TR-0076(6970)-4 (1975).
13. R. A. McClatchey, et al., "AFCRL Atmospheric Absorption Line Parameters," Air Force Cambridge Research Laboratory Report AFCRL-TR-73-0096 (1973).
14. S. J. Young, "Band Model Parameters for the 4.3 μm Fundamental Band of CO_2 in the 100 to 3000 K Temperature Range," Aerospace Corp. Report TR-0076(6754-03)-1 (1975).
15. P. C. Sukanelis and L. P. Davis, "An Assessment of the NASA Band Model Formulation for Calculating the Radiance and Transmission of Hot and Cool Gases," AFRPL-TR-76-9 (1976).

16. P. C. Sukanek and L. P. Davis, "A Band Model for Calculating Radiance and Transmission of Water Vapor and Carbon Dioxide," AFAA Progress in Astronautics and Aeronautics 59, 204 (1977).
17. G. H. Lindquist, C. B. Arnold, and R. L. Spelling, "Atmospheric Absorption Applied to Plume Emission - Experimental and Analytical Investigations of Hot Gas Emission Attenuated by Cold Gas," Environmental Res. Inst. of Mich., AFRPL-TR-75-30 (1975).
18. L. Bernstein, JQRST publication expected in 1980.
19. "Development and Validation of Standardized Infrared Radiation Model (SIRRM) - Gas/Particle Radiative Transfer Model," Photon Research Associates report on AFRPL/PACP Contract F04611-78-C-0081 (1979).
20. "Study on Exhaust Plume Radiation Predictions - Interim Progress Report," General Dynamics Convair GD/C-DBE-66-001 (1966).
21. "Study on Exhaust Plume Radiation Predictions - Final Report," General Dynamics Convair NASA CR-61233 (1968).
22. C. B. Ludwig, C. C. Ferriso, and L. Acton, "High Temperature Spectra of the 15- μ Band of CO₂," General Dynamics Convair GD/C-DBE65-024 (1965).
23. "Study on Exhaust Plume Radiation Prediction - Interim Progress Report - Part II," General Dynamics Convair GD/C-DBE-66-001a (1966).
24. "Study on the Spectral Emissivity of Carbon Particles Produced by a Rocket Motor," General Dynamics Convair GD/C-DBE66-006 (1966).
25. J. E. Reardon, et.al., "Study of the Radiation and Convection Environment of the Saturn V," Hayes International Corp., Birmingham, Al., Report ER 1333 (1966).
26. J. E. Reardon and Y. C. Lee, "Space Shuttle Main Engine Plume Radiation Model," REMTECH, Inc. RTR 014-7 (1978).
27. J. K. Lorin and A. W. Lubkowitz, "User's Manual for 'RAVFAC', a Radiation View Factor Digital Computer Code," LMSC/HREC NASA CR-61321 (1969).
28. C. Engel, "Multi-Engine Plume Flowfield Transformation Program," REMTECH Inc. RTR 014-2 (1974).

A1 INPUT GUIDE

The input guide describes aspects of the program set-up and mapping, the card input formats and order, and the unformatted binary input. Nearly all of the binary files listed in Table A1.1 are used for both input and output, so they cannot be clearly assigned to either category. However, the program is usually run with the gas property data (flowfield) input so it will be described as an input file although it can also be generated as an output file from card input. The other binary files (problem data and line-of-sight properties, radiance data, and spectral data for plotting) will be described as output since they are normally generated by the program.

A1.1 PROGRAM SET-UP AND MAPPING

The job control cards currently used on the MSFC UNIVAC 1108 are illustrated with the Sample Problems (Appendix A3). A typical sequence involves: assignment of input tape(s) containing the program source code, object code, map element, band model data elements (card image), and flowfield property input (binary); increase in the default size of the temporary program file; and assignment of file units to be used by the program (3, 4, 8, 10, and occasionally 11). The code and band model data elements are copied into the temporary program file while the flowfield is copied to Unit 8 (or 11 if it is to be modified as noted on Input Card 2), and the object code is executed if no updates are required.

The normal program map element in Table A1.2 shows the segmentation and usual deck names. All deck and subroutine names are identical with the exception of Subroutine SLG. Here, the normal radiation deck using the statistical

Table A1.1

EXTERNAL FILE UNITS FOR THE GASRAD PROGRAM

UNIT NUMBER	SUBROUTINE	FUNCTION
3	FLOWAX FLOW3D	Used as temporary storage when it is necessary to load the plume in sections. If the dimension parameter is larger than the number of Z-cuts in the plumes, it is not required, but it is still referenced by rewind statements.
4	FLOWAX FLOW3D	Same as Unit 3
	SLG VIEW	Used to store and transfer line-of-sight radiance data from Subroutine SLG to Subroutine VIEW.
	SPCOUT PLOTIT	Used to transfer spectral data from Subroutine SPCOUT to the plot program PLOTIT.
8	FFPREP	Stores gas property data read from cards or Unit 11
	FLOWIN	Provides flowfield title and constituent input
	FLOWAX FLOW3D	Provides flowfield gas property data.
10	FLOWIN	Stores input data so it can be used for program restart with abbreviated input.
	FLOUT	Uses stored input data for problem output.
	FLOWAX FLOW2D	Used to store line-of-sight gas property data for transfer to Subroutine SLG. The property data are stored after the problem specifications used in Subroutine FLOUT.
	SLG	Used to input line-of-sight gas property data.
11	FFPREP	Input gas property data which is to be modified (scaled) and output on Unit 8 for use by the program.

Table A1.2
 NORMAL PROGRAM MAP ELEMENT

@MAP,S A,GASRAD		
MAP 29R1 SL73R1 01/03/80 19:59:22 (4,)		
1.	LIB SYS\$*MSFC\$.	
2.	SEG MAINS	
3.		IN MAIN
4.	SEG LOSGEN*,(MAINS)	
5.		IN FLOW,SLIMIT,PLUMPT,BLOCKM,NOGO
6.	SEG FLOWIS*,(LOSGEN)	
7.		IN FLOWIN,BLOKIN,FFPREP
8.	SEG FLOUTS*,(LOSGEN)	
9.		IN FLOUT,SKIP
10.	SEG FLOWAS*,(LOSGEN)	
11.		IN FLOWAX
12.	SEG FLOW3S*,(LOSGEN)	
13.		IN FLOW3D
14.	SEG RADS*,(MAINS)	
15.		IN RAD
16.	SEG ACDATS*,(RADS)	
17.		IN ACDATA
18.	SEG SLGS*,(RADS)	
19.		IN SLGMLT,PLANCK
20.	SEG SPCOTS*,(RADS)	
21.		IN SPCOUT
22.	SEG VIEWS*,(MAINS)	
23.		IN VIEW

band model with exponential line-strength distribution and the Curtis-Godson approximation for inhomogeneous gases has the deck name SLGMLT. If a prediction is desired for H₂O using the Intuitive Derivative Method (Section 3.1) to account for inhomogeneous gas effects, the program should be mapped with the deck name YNGH2O used in place of SLGMLT, and Subroutine PLANCK can be omitted.

All declarations are included in program subroutines through reference to procedure entries in the (UNIVAC 1100 Series EXEC 8) PDP (procedure definition processor) element COMMLT. Reference to the procedures in a subroutine causes them to be inserted in the source code. Use of the program on another computer system will require changes to this system and may require duplications of the declarations for insertions at appropriate locations.

A1.2 CARD INPUT

The card input formats are described in Table A1.3. Since the program was used primarily for the Space Shuttle Main Engine (SSME) plumes, the input is designed to utilize program data statements for SSME plume locations unless IFLOIN=1 (Card 2). However, if the program were to be used extensively for another engine arrangement, the data statements could be changed accordingly to simplify input.

Card input requirements for the flowfield were omitted from the normal sequence and inserted at the end of Table A1.3 to simplify the input card sequence listed to that normally used with the flowfield input as a binary file.

In earlier versions of the program, (Refs. 1-6) the band model parameters were included in data statements, which is convenient from an input standpoint, but it limits flexibility in evaluating performance with other input sets and

limits the ease with which the program dimensioning can be varied for applications requiring less data. The input data elements summarized in Table 3.3 are usually included in the program storage file in the proper input format specified by Cards 17 through 19 so they may be added to the runstream with system control statements (@ADD) as illustrated in the sample problems. The coding is set to read band model parameters data for the first NKA (parameter) constituents identified on the program constituent data list IDENTC(I) (where there are 2 six-character words per constituent). In normal form, NKA=6, so the program will attempt to read six data sets. If only one data set is to be loaded, as in a run for H₂O only, the H₂O data would be loaded followed by 5 blank cards to indicate no data are loaded for the other 5 gases.

A1.3 UNFORMATED BINARY INPUT

Plume property data input on Unit 8 or 11 (Table A1.1) are normally considered as input, so the format is described here in Table A1.4. Other binary files are described in Appendix Section A2.2. For further clarification of the number of Z-cuts (Group 2 Record 1) allowed by the program the reader should refer to Section 4.3.

Table A1.3

INPUT GUIDE

CARD 1	(12A6)	TITLE CARD	
1-72		Heading for the problem - Blank terminates input.	
CARD 2	(16,20I3)	CONTROL CARD	
1-6	KASE	=0 Repeat previous case with scaling - See Note C at end of Card 2.	
		>0 Case number identifying the flowfield on tape.	
		<0 Flowfield input on cards and transferred to unit 8 with scaling if desired. Case number on tape will be KASE .	
7	IFLOTP	=0 Flowfield not modified.	
		>0 Flowfield input on unit 11, modified as indicated by scale factors (Card 8) and output on unit 8 for use in this problem.	
8	IFLOIN	=0 Nozzles (flowfield origin) located using data statement in subroutine FLOWIN (SSME flight null).	
		=1 Nozzle location input on Card 10.	
9	IFLOW	<7 Number of identical axisymmetric plumes	
		=7 Use previously generated line-of-sight data. See Note B.	
		=8 Three-dimensional flowfield.	
		=9 Three-dimensional flowfield followed by an axisymmetric flow field after IZF Z-cuts. (See note for IZF Col. 50, 51)	
12	NOKON	Number of species to be identified on Card 6. (The program is normal dimensioned for a maximum of 6.)	
13-24		Not used.	
26	NSPEK	=0 Spectral output per unit wavelength.	
		=1 Spectral output per unit wavenumber.	
27		=0 No spectral output.	
		=1 Spectral radiance per steradian - short form	
		=2 Spectral radiance per steradian - long form	
		=3 Spectral radiance for region specified on Cards 3 and 4 - short.	
		=4 Spectral radiance for region specified on Cards 3 and 4 - long.	
NOTE:		All spectral parameters other than radiance are for the last line-of-sight processed.	
29,30	NPLOT	Number of spectral plots specified on Card 16* (Requires NSPEK > 0)	
33	NFLOW	=0 Short flowfield output with only centerline and boundary.	
		=1 Complete flowfield output.	
36	NABS	=0 Short form absorption coeff. output	
		=1 Complete absorption coeff. output	
39	ISHOCK	=0 Special 3-D shock procedure for clustered engines Refer to Section 4.3	
		=1 Disable special 3-D shock procedure	
42	IUNITS	=0 Flowfield and geometry in English units (inches, R, lbf/ft ²).	
		=1 Flowfield and geometry in Metric units (cm, k, atm)	
45	ISCALF	=0 No plume scaling.	
		=1 Plume scale factor if KASE ≠ 0. Entire geometry scaled if KASE = 0.	

* The program is currently configured so that the plotting is done by PLOTIT which is compiled and executed separately but has all input passed from the radiation program on unit 3.

47,48 IZI =0 Read first Z-cut in input flowfield.
 >0 Index of first Z-cut to be used.

50,51 IZF =0 Read entire flowfield.
 >0 Index of final Z-cut to be included, or last Z-cut in the
 three-dimensional flowfield if IFLOW = 9.

54 IRAD Spatial integration control for Deck YNGH20 only. See Eq. 26.

60 ISCALA =0 No scaling of band model parameters (k and 1/d).

NOTES FOR USING PREVIOUSLY GENERATED LINE-OF-SIGHT DATA

- A. Input line-of-sight data on unit 10.
- B. If a change is desired in problem limits:
1. Set IFLOW = 7 and KASE equal to the case number used in generating the line-of-sight data.
 2. Input Cards 3 thru 6 using geometric integration limits and intervals which will produce line-of-sight data available on Unit 10. For example $\Delta\theta$ can be doubled but not halved.
 3. Omit Cards 7 and 9-14. Use remaining cards as required by options chosen.
- C. If only scaling is desired with no change in limits:
1. Set KASE = 0
 2. Omit Cards 3-7 and 9-14. Remaining cards are used as required by options chosen.

CARD 3 (8E10.6) ELEVATION ANGLE INTERVAL - DEGREES
 1-10 THETAI Initial value (θ_i).
 11-20 THETAF Final value (θ_f).
 21-30 DTHETA Integration Interval ($\Delta\theta$).

CARD 4 (8E10.6) AZIMUTH ANGLE INTERVAL - DEGREES
 1-10 PHII Initial value (ϕ_i).
 11-20 PHIF Final value (ϕ_f).
 21-30 DPHI Integration interval ($\Delta\phi$).
 31-40 TANGLE Used to increase $\Delta\phi$ at small θ . $\Delta\phi = \text{TANGLE}/\sin\theta$ will be used if it is larger than DPHI.

CARD 5 (8E10.6) WAVENUMBER INTERVAL - CM^{-1}
 1-10 ENUI Lower spectral limit - ω_i .
 11-20 ENUF Upper spectral limit - ω_f .
 21-30 DENU Integration interval - $\Delta\omega$

CARD 6 (8E10.6) LINE-OF-SIGHT INTERVAL - UNITS PER COL 42 ON CARD 2
 1-10 SZERO Distance from point-of-interest to initial LOS point
 11-20 SMAX Upper limit of LOS from the point of interest.
 21-30 DS Integration increment on the LOS.
 31-40 TDIFF Temperature step size used to increase LOS integration increment. Assumes gas with a temperature change of less than TDIFF is isothermal.

41-50 AP These values for the plume limiting cone intercept (AP)
 51-60 BP and slope (BP) will override plume input value from binary or card input (Card 2F) if either AP or BP are >0 on this card.

CARD 7 (126A) CONSTITUENT IDENTIFICATION
 1-6 KON(1) First Constituent - first word
 7-12 KON(2) First constituent - second word
 13-18 KON(3) Second constituent - first word
 Continue with a list of NOKON (Card 2) two word names
 in the form specified in the IDENTC data list:
 H2O1(G), C1O2(G), C1O1(G), HCL, HF, C1(S), N2(G), H2(G), O1(G).

CARD 8 (9E8.5) FLOWFIELD/GEOMETRY SCALE FACTORS - USE ONLY IF ISCALF = 1
 1-8 RSCAL Length scale. Notes: 1.If KASE \neq 0 (Card 2) the flowfield will
 be scaled, but if KASE = 0, the entire
 problem will be scaled.
 9-16 TSCAL Temperature scale. 2.Zero entries will be set to 1.
 17-24 PSCAL Pressure scale.
 25-32 FSCAL(1) Mole fraction scale for first constituent on Card 7.
 33-40 FSCAL(2) Mole fraction scale for second constituent.
 ⋮
 65-72 FSCAL(6) Mole fraction scale for sixth constituent

IF KASE < 0 INSERT CARD FLOWFIELD DATA HERE.
 SEE INPUT REQUIREMENTS AFTER CARD 19.

CARD 9 (8X, I2, 10X, 6F10.3) POINT-OF-INTEREST LOCATION AND ROTATION
 9,10 ICS(1) Intermediate coordinate system number. 0 if none is used.
 21-30 RX (1) }
 31-40 RY (1) } Coordinates of the point in the ref. or inter. coord. sys.
 41-50 RZ (1) }
 51-60 CHS(1) X }
 61-70 PSS(1) ψ } Rotations of the axes relative to the ref. or inter. coord.
 71-80 OMS(1) ω } sys.

CARD(S) 10 (8X, I2, 10X, 6F10.3) PLUME ORIGIN(S) LOCATION AND ROTATION
 9,10 ISC(I) Inter. coord. system.
 21-30 RX (I) }
 31-40 RY (I) } Coordinates Notes: 1) USED ONLY IF IFLOIN = 1
 41-50 RZ (I) } 2) CARD(S) 10 = IFLOW IF IFLOW < 7
 51-60 CHS(I) X } 3) CARD(S) 10 = 1 IF IFLOW > 7
 61-70 PSS(I) ψ } Rotations
 71-80 OMS(I) ω }

CARD(S) 11 (I5, 45X, 5A6) BLOCKING SURFACE IDENTIFICATION
 1-5 NSF(I) Surface number USE -1 TO END SURFACE INPUT.
 51-80 COMMET(I,J) Surface identification.

CARD(S) 12 (9X, I1, 20X, 5F10.3) BLOCKING SURFACE SHAPE PARAMETERS
 10 ISF(I) Surface type
 31-40 ALF(I) α }
 41-50 BMIN(I) β_{min} } Geometric surface limits. Refer to Fig. 4.3
 51-60 BMAX(I) β_{max} }
 61-70 GMIN(I) γ_{min} }
 71-80 GMAX(I) γ_{max} }

CARD(S) 13 (8X, I2, 10X, 6F10.3) SURFACE COORDINATE SYSTEM ORIENTATION
 9,10 ICS(I) Intermediate coordinate system. (0 if none is used.)
 21-30 RX(I) }
 31-40 RY(I) } Surface system origin in reference or inter. coord. sys.
 41-50 RZ(I) }
 51-60 CHS(I) } χ y toward x }
 61-70 PSS(I) } ψ x toward z } Rotations relative to reference or
 71-80 OMS(I) } ω y toward z } inter. coord. sys.

REPEAT CARDS 11 THRU 13 IN SETS OF 3 CARDS FOR EACH SURFACE.

END SURFACE INPUT BY A CARD 11 WITH NSF(I) = -1.

CARD(S) 14 (8X, I2, 10X, 6F10.3) INTERMEDIATE COORDINATE SYSTEMS.
 9,10 NCS(J) Coordinate system number. USE -1 TO END ICS INPUT.
 21-30 RXI(J) }
 31-40 RYI(J) } Coordinates of intermediate coordinate system origin.
 41-50 RZI(J) }
 51-60 CHC(J) } χ y toward x }
 61-70 PSC(J) } ψ x toward z } Rotations relative to the reference system.
 71-80 OMC(J) } ω y toward z }

REPEAT CARDS 14 UNTIL ICS REQUIREMENTS ARE SATISFIED.

END ICS INPUT BY A CARD 14 WITH NCS(J) = -1.

CARD 15 (12E6.3) BAND MODEL PARAMETER SCALE FACTORS - USE ONLY IF ISCALA = 1
 1-6 ABSCL(1) Abs. coef. scale factor
 7-12 DINSCL(1) Line density scale factor
 13-18 ABSCL(2) Repeat up to 6 pairs depending on the number of radiating species
 19-24 DINSCL(2) which are being used. The order must follow the IDENTC(I)
 list with unscaled species left blank.

CARD 16 (16I5) PLOT CONTROL CARD. USE ONLY IF NPLOT > 0.
 3-5 JPLOT(1) A series of NPLOT three digit numbers coded to define the
 8-10 JPLOT(2) plots as follows:
 : First digit - abscissa control
 : = 1 wavenumber (cm^{-1})
 : = 2 wavelength (μm)
 :
 :
 : JPLOT(NPLOT)
 Second digit - ordinate control
 = 1 irradiance
 NSPEK
 1 or 2 watts/ cm^2 - μ -sr
 3 or 4 watts/ cm^2 - μ
 11 or 12 watts/ cm -sr
 13 or 14 watts/cm
 = 2 transmissivity
 = 3 linear optical depth, X^*
 = 4 collision fine structure parameter, a_c
 = 5 Doppler fine structure parameter, a_D } For the final
 line-of-sight
 only.

Third digit - constituent according to IDENTC(I) data
 = 0 used for second digit = 1 or 2
 = 1 first
 = 2 second Not applicable when second
 = 3 third digit = 1 or 2.
 etc.

NOTE: Loop to read six sets of band model parameters in the order specified by the identc list: H2O, CO2, CO, HCL, HF, undefined. Blank cards are used for omitted species.

CARD 17 (16I5) BAND MODEL DATA CONTROL PARAMETERS AND LIMITS
 IABSCO = 0 No data input for this constituent (blank card). Skip cards 18 and 19.
 > 0 Data input for \bar{k} .
 IFINST = 0 No line density (1/d) input. This assumes program will compute a value as in the case of CO.
 > 0 Data input for 1/d using the same table format as for \bar{k} .
 NACT(I) Number of temperatures in the tables
 NUL(I) Lower wavenumber in the table (cm^{-1})
 NUU(I) Upper wavenumber in the table (cm^{-1})
 IDNU(I) Wavenumber interval for the table (cm^{-1})

CARD 18 (7E10.5) TEMPERATURE VALUES IN THE TABLE
 TEMAC(I,1) Temperatures (K) in ascending order.
 TEMAC(I,2)
 ..
 ..
 TEMAC(I,NT) NT = NACT(I) If NACT(I) > 7, two cards will be required.

CARD 19 (7E10.5) BAND MODEL PARAMETERS FOR TEMAC(I,1)
 COEF(J,K) K = 1, Absorption coefficient at NUL(I), TEMAC(I,1)

NOTE: NT = NACT(I)

COEF(NT,K) K = 1, Absorption coefficient at NUL(I), TEMAC(I,NT)

REPEAT CARD 19 FOR K = 2 TO (NUU(I)-NUL(I)/IDNU(I)+1) TO READ THE ABSORPTION COEFFICIENTS. THEN IF IFINST > 0 REPEAT THE RANGE OF K FOR THE LINE DENSITY 1/d.

RETURN TO READ CARD 17 UNTIL IT HAS BEEN READ 6 TIMES.

PROGRAM EXECUTION COMMAND - Program begins execution on the first case and then reads data for subsequent causes starting at CARD 1. Execution terminates normally when CARD 1 is blank.

CARD FLOWFIELD INPUT BELOW TO BE INSERTED
BETWEEN CARDS 8 AND 9 IF KASE < 0 ON CARD 2

CARD 1F (12A6) FLOWFIELD HEATING
1-72 HDG Heading

CARD 2F (4A6, I2, 5X, 4E10.6) PROPELLANT OR GAS ID AND GEOMETRY (Refer to Fig. 4.5)
1-24 BETA Propellant or gas identifier for information only
25 ISYMSC = 0 Axisymmetric plume or a cluster with a center engine
(assuming symmetry between center and outboard engines about
the normal bisector of a line connecting the exit centerlines)
= 1 A 3-D plume with no symmetry assumptions about a center engine
31-40 HANG Included angle of a 3-D plume symmetrical sector.
41-50 CTCD Distance from the plume property input axis to the Z-axis of a
3-D plume system.
51-60 AP = 0 No limiting cone used around the plume.
> 0 X intercept of a limiting cone about the plume Z-axis. Used
to speed interpolation by eliminating property searches for
points outside the plume.
61-70 BP Slope of the cone bounding the plume (dR/dZ). Must be > 0.

CARD 3F (12A6) FLOWFIELD CONSTITUENT IDENTIFICATION
1-6 CON(1) First constituent - first word.
7-12 CON(2) First constituent - second word.
13-18 CON(3) Second constituent - first word.
19-24 CON(4) Second constituent - second word.
Repeat up to a maximum of 6 constituents.

REPEAT CARDS 4F THRU 6F AS REQUIRED WITH ZZ, ETA, AND R IN NUMERICAL SEQUENCE

Card 4F (E10.6, I10) AXIAL POSITION - Units set by IUNITS on CARD 2.
1-10 ZZ(I) Z coordinate of the data to follow
20 NETA = 0 Terminates flowfield
> 0 Number of η values for this Z. Use 1 for axisymmetric

CARD 5F (E10.6, I10, I5) ANGULAR POSITION
1-10 ETA(I,J) η position (use 0 for axisymmetric flowfield) - degrees
20 NETA = 0 Terminates flowfield
> 0 Number of values for this Z. Use 1 for axisymmetric
24,25 LS(I,J) Index of the radial point adjacent to and at a smaller radius
than a shock discontinuity.

CARD 6F (9E8.5) RADIAL PROPERTY DATA - Units set by IUNITS on CARD 2.
1-8 R(I,J,L) Radius - the first value (L=1) will be set at 0
regardless of input.
9-16 T(I,J,L) = 0. Return to Card 5F for next ETA or Card 4F for next ZZ.
> 0. Temperature
17-24 P(I,J,L) Pressure
25-32 F(I,J,L,1) First constituent mole fraction.
33-40 F(I,J,L,2) Second constituent mole fraction.
Continue for constituents on Card 3F.

Use the same order
as on CARD 3F.

Table A1.4

FLOWFIELD GAS PROPERTY FILE

GROUP I GENERAL INFORMATION (3 RECORDS)

Record

1	(HDG(I),I=1,12)	Heading or title
	ICASE	Case number
2	(BETA(I),I=1,4)	Gas identification
	ISYMSC	} 3-D geometry parameters (Ref. Card 2F, Table A1.3)
	HANG	
	CTCD	
	AP	} Plume boundary cone parameters (Ref. Card 2F, Table A1.3)
	BP	
3	NOCON	Number of constituents defined
	(CON(2*I-1), CON(2*I), CONWT(I), I=1,NOCON)	Constituent name (2 words) and molecular weight (not used in program) for the NOCON constituents.

GROUP II GAS PROPERTY DATA (NZ(1+2*NETA(I)) RECORDS)

Record

1	ZZ(I)	Value of Z_w for data in records 2 and 3 in units specified by IUNITS (Card 2, Table A1.3)
	NETA(I)	Number of ETA values used at this Z. This is the upper limit of a loop on J for reading Records 2 and 3. For axisymmetric plumes NETA = 1, and the dimension limit is set by the parameter MN3.

Table A1.4
(concluded)

FLOWFIELD GAS PROPERTY FILE

Record

- 2 ETA(I,J) Value of η (degrees) for data in record 3.
- NR(I,J) Number of radial points in record 3. This is the upper limit (NOPS) for a loop on L for reading the radial points in Record 3. The dimension limit is set by parameter MR2 or MR3.
- LS(I,J) Index (L) of the radial point in Record 3 which is just smaller than the shock radius RS. If LS(I,J) = LL, then $R(I,J,LL) < RS < R(I,J,LL+1)$
- 3 (R(I,J,L) Radius Note: Units as specified by IUNITS
 T(I,J,L) Temperature (Card 2, Table A1.3)
 P(I,J,L) Pressure
 (F(L,N), N=1,NOCON), Mole fractions in the same order as specified in
 L=1, NOPS) Group I Record 3.

Records 2 and 3 are repeated NETA(I) times for each Record 1. The number of Records 1 (NZ) allowed for a single plume is unlimited, but for multiple axisymmetric plumes NZ is limited to MZ2.

A2 OUTPUT FORMATS

The output formats to be described include the normal printed output, diagnostic messages, and binary files used for data storage and transfer.

A2.1 PRINTED OUTPUT

Printed output is provided in up to seven sections in separate subroutines. Output of these subroutines will be summarized in the paragraphs below in sequence of output, and examples of the usual output forms are illustrated in the sample problems (Section A3).

FFPREP

This subroutine is used only for reading and flowfields or scaling. When it is used, a portion of the flowfield data are output to assure proper operation and indicate the point that operation ceased if a difficulty is encountered. The data output is described in Table A1.4 as Group I and Records 1 and 2 of Group II.

FLOUT

The output in this subroutine is normally the first printed output. It contains general problem identification, geometry, and input limits. The data are obtained from the initial group of records on Unit 10 (Table A2.1) which are prepared by Subroutine FLOWIN. The general output features in sequence are:

- Problem identification and data.
- Flowfield identification, plume orientation, relative to the central coordinate system, and plume conical limits (intercept and slope).

- Statement of the units used for input and output. The internal operation of the program is metric, and the radiation output is always metric as indicated by output formats.
- Tabulated limits and increments for integration.
- Location and direction cosines for the point-of-interest system (U,V,W) relative to the central coordinate system.
- List of constituents in the input order (Table A1.3, Card 7)
- Geometry input data for the point-of-interest and plumes.
- Input data for blocking (shading) surfaces.
- Input data for intermediate coordinate systems.
- Identification of flowfield scaling performed on the input.

FLOWAX/FLOW3D

Output of the flowfield properties is made in one of these subroutines depending on the flowfield geometry used. Normal output omits all interior points on each set of radial data to limit output while assuring proper flowfield operation, but the complete set of property data can be obtained by setting the control flag NFLOW = 1 (Table A1.3, Card 2). The output is labeled by headings of Z, R, T, P for axial position, radius, temperature, and pressure. The mole fractions of the constituents are listed from F1 to F6 (as required) according to the input order (Table A1.3, Card 7) printed in FLOUT (above). If the temperature range encountered in preparing the line-of-sight data is outside the range of 300K to 3000K, a message is printed at the end of the subroutine as a warning that the user should evaluate the temperature range of the band model data. If the gas temperature is above (or below) the table limits for the band model data, the upper (or lower) table value is used. A calculation time is printed for the flowfield interpolation, but because of a change in the MSFC UNIVAC 1108 system the number listed is currently SUP-seconds rather than actual time or CPU time.

ACDATA

Band model parameters are output in this subroutine. First, the broadening coefficients for unidentified species (G1 through G6) are listed for the first six species in the IDENTC data list order (IDENTC(I), I=1,12). These correspond to the coefficients γ_{ij} (Eq. 8) for the fraction of the plume gases which are not identified by the problem input. Following the broadening parameters, band model parameter scale factors are output if they are used. Next, the band model data being used are output after scaling or averaging over larger wavenumber intervals. Only the portion of the spectra to be integrated (ENUI to ENUF) is listed regardless of the range of data which may be input. The wavenumbers listed are at the center of the wavenumber interval represented by the parameters, and this is the interval specified for spectral integration (Table A1.3, Card 5, DENU). Normally only the first and last wavenumber entry in each parameter set are listed to verify operation while minimizing output, but a full listing can be obtained by setting the control flag NABS=1 (Table A1.3, Card 2).

SLG

If Deck YNGH20 is used, the optical depth integration step size set by IRAD (Table A1.3, Card 2) is output. The step size is equivalent to $1/IRAD$. The bulk of the normal output is a one-line summary of results for each line-of-sight. The values tabulated are defined below:

- THETA - Value of the hemispherical elevation angle θ .
- PHI - Value of the hemispherical azimuth angle ϕ .
- SHAPE FACTOR - This is not a true shape factor. It is defined by

$$\text{SHAPE FACTOR} = \sum_{\theta_j}^{\theta} \sum_{\phi_j}^{\phi} \sin\theta \cos\theta \Delta\theta \Delta\phi/\pi \quad (\text{A2-1})$$

where the summation is performed only for θ and ϕ defining lines-of-sight which intersect the plume.

- FLUX - Incident radiation for the line-of-sight (DELTA) and the cumulative value (SUM)

$$\text{FLUX-DELTA} = \sum_{\omega} \sum_{s} N^{\circ}(\omega, s) [\tau(\omega, s-\Delta s) - \tau(\omega, s)] \sin\theta \cos\phi \Delta\theta \Delta\phi \Delta\omega \quad (\text{A2-2})$$

$$\text{FLUX-SUM} = \sum_{\theta_i} \sum_{\phi_i} (\text{FLUX-DELTA}) \quad (\text{A2-3})$$

- RAD - Radiance for the line-of-sight (LOS) and the average for all lines-of-sight through this one (AVG).

$$\text{RAD-LOS} = \sum_s N^{\circ}(\omega, s) [\tau(\omega, s-\Delta s) - \tau(\omega, s)] \quad (\text{A2-4})$$

$$\text{RAD-AVG} = \text{FLUX-SUM} / (\Delta\omega \sum_{\theta_i} \sum_{\phi_i} \sin\theta \cos\theta \Delta\theta \Delta\phi) \quad (\text{A2-5})$$

The denominator in RAD-AVG is summed over all lines-of-sight rather than just those intersecting the plume as in Eq. A2-1, so RAD-AVG represents an average radiance for the space integrated.

- AVG TRANS - This is a straight spectral average of the transmissivity over all wavelengths for the line-of-sight defined by:

$$\text{AVG TRANS} = \sum_{\omega} \tau(\omega, s_m) \Delta\omega / \sum_{\omega} \Delta\omega \quad (\text{A2-6})$$

where s_m indicates the upper limit of integration along the line-of-sight.

- COMB OPT PATH - This is a summation of the optical paths in (cm-atm)_{STP} for all radiating species along the line-of-sight. It is defined by:

$$\text{COMB OPT PATH} = \sum_s \sum_i [p_i(s) c_i(s) 273/T_i(s)] \Delta s \quad (\text{A2-7})$$

where c represents the mole fraction and i represents the radiating species only. In Deck YNGH20 the title is changed to H₂O PATH since H₂O is the only radiating species.

- LBLOCK - This is the identifying number (NSF(I) on Card 11) for the shading surface blocking this line-of-sight. If no blocking occurs, zero is printed.
- SZERO - This is the lower limit for integration along the line-of-sight, s_0 . It is set either at the input value (SZERO on Card 6) or by Subroutine SLIMIT.

- SMIN - This is the upper limit for integration along the line-of-sight, s_m . It is set either at the input value (SMAX on Card 6) or by Subroutine SLIMIT.

After all lines-of-sight are processed, a summary of "shape-factor", radiance, and incident radiation flux is printed. The plume "shape-factor" was defined above in Eq. A2-1. The total "shape-factor" can also be expressed by Eq. A2-1 if all values of ϕ and θ are included rather than only values representing plume intersections. The exact total shape factor is the exact value of the integration which is

$$\begin{aligned} \text{EXACT TOTAL SHAPE FACTOR} &= \int_{\theta_i}^{\theta_f} \int_{\phi_i}^{\phi_f} \sin\theta \cos\theta \, d\phi d\theta / \pi & (A2-8) \\ &= \frac{0.5}{\pi} (\sin^2\theta_f - \sin^2\theta_i)(\phi_f - \phi_i) \end{aligned}$$

Overall radiance is defined by Eq. A2-5 using numerical-total-shape-factor in the denominator, while the plume radiance is defined similarly using the numerical-plume-shape-factor in the denominator. The calculation time output for the SLG subroutine is in SUP-seconds for the MSFC UNIVAC 1108.

SPCOUT

Spectral data can be output per unit wavenumber or wavelength in either long or short formats as specified by NSPEK (Card 2). In the short form, only the first 5 values described below are output, but even in this case, the fourth and fifth values are for the final line-of-sight processed. In the long form, additional band model values are listed for the final line-of-sight. These values are generally valid only for the Curtis-Godson approximation using the exponential line strength distribution. They are not generally valid if Deck SLGMLT is converted to the exponentially-tailed-inverse line strength distribution or if Deck YNGH20 is used for the Intuitive Derivative method. The values output are:

- WAVENUMBER - Wavenumber at the center of the interval.
- WAVELENGTH - Wavelength at the center of the interval.
- IRRADIANCE - Radiation per unit spectral interval as specified by NSPEK (Card 2). The units in the format indicate the option chosen. It should be noted that the conversion to radiation per unit wavelength is a function of the wavenumber interval used. For example,

$$N_{\lambda}(\text{watts/cm}^2\text{-}\mu\text{m-sr}) = (\omega^2 - (\Delta\omega/2)^2) 10^{-4} N_{\omega}(\text{watts/cm}^2\text{-cm}^{-1}\text{-sr}) \quad (\text{A2-9})$$

- G - Transmissivity (τ) over the final line-of-sight
- OPTICAL DEPTH - The value of optical depth defined as

$$X = \sum_i X_i = -\ln \tau \quad (\text{A2-10})$$

is printed on line with the wavenumber. If the long form output is selected, additional lines are printed for each radiating constituent with X_i for the species identified or each line.

- CONSTITUENT - Identifies the radiating species associated with each row of output.
- X^* - The value of the optical depth for the linear limit of the curve of growth for the species identified (Eq. 15)

$$X^* = \bar{k}_e(\omega, i, s_m) u(i, s_m) \quad (\text{A2-11})$$

- X/X^* - Ratio of the optical depth for combined collision (Lorentz) and Doppler broadening (X) to the linear limit optical depth.
- X_C/X^* - Ratio of the collision (Lorentz line) broadened optical depth (Eq. 10a) to X^* .
- X_D/X^* - Ratio of the Doppler broadened optical depth (Eq. 10b) to X^* .
- AC - Collision broadened fine structure parameter, a_{Le} (Eq. 15b).
- AD - Doppler broadened fine structure parameter, a_{De} (Eq. 15c).

VIEW

This subroutine produces a printer plot of the line-of-sight radiance (the result RAD-LOS in the line-of-sight output). The plot is in a polar format with the elevation angle (θ) used as the radius and the azimuth angle (ϕ) used as the

angle. The radiance is represented as tenths of the peak radiance by the digits 0 to 9. So if the line-of-sight radiance is N and the maximum radiance computer for a line-of-sight is N_p , then an integer D defines a radiance interval

$$DN_p/10 < N \leq (D+1)N_p/10 \quad (A2-12)$$

The value of $N_p/10$ is printed above the plot.

Lines-of-sight which are blocked and do not enter the gas are represented by the character B, but if radiating gas is encountered before blocking occurs a digit is printed and no indication of the blocking is given. Blanks in the plot generally indicate lines-of-sight missing the gas, but they also may occur locally due to the lack of precision in converting the polar plot format to a rectangular grid with one symbol/line resolution. If lines-of-sight are closer than the resolution of one symbol, the results are averaged. But if they are widely spaced, no interpolation is performed, so blanks will occur.

A2.2 DIAGNOSTIC MESSAGES

Diagnostic messages are provided in 7 subroutines of GASRAD and the plot program (PLOTIT). The messages and corrective actions usually implied are listed below for each subroutine in the usual sequence of subroutine use.

MAIN

NUMBER OF CONSTITUENTS REQUESTED (KKK) EXCEEDS THE NUMBER ALLOWABLE (LLL).

ACTION: Reduce input (NOKON, Card 2) or increase dimension parameter NK.

(ENUF-ENUI)/DENU+1 IS GREATER THAN THE MAXIMUM NUMBER OF SPECTRAL INTERVALS DIMENSIONED.

ACTION: Reduce input interval, increase DENU, or increase dimension parameter MNU.

*****SORRY, CASE LLLLLL IS NOT ON THIS TAPE. RUN TERMINATED.

ACTION: Input case LLLLLL (KASE, Card 2) could not be matched to any flowfield stored on Unit 8. Check card and tape input. This message will only be written if the final record on Unit 8 is a 72 character string of *. Otherwise an end-of-file will be indicated with no diagnostic.

*****CASE NUMBER LLLLLL DOES NOT CONTAIN THE CONSTITUENT 'AAAAAABBBBBB'

ACTION: Check input case numbers (KASE, Card 2) and spelling of input constituent names on both Card 7 (KON) and the flowfield (KONAME). Note that the names are all two words (2A6), and the flowfield tape (Table A1.4) has a list of 3 word items since the molecular weight was included (although it is not used in the program).

THE CONSTITUENT-AAAAAABBBBBB-IS NOT RECOGNIZED BY THE PROGRAM. CHECK AGAINST NAMES IN THE IDENTC LIST.

ACTION: Check as directed with the data list specifying the constituent names (IDENTC(I)) in Subroutine MAIN.

NO. OF CONSTITUENTS ON TAPE (IT) EXCEEDS STORAGE AVAILABLE (NKTP=K)

ACTION: Increase dimension parameter NKTP. The storage required by this parameter is only $(3+MR2[\text{or } MR3])*NKTP$.

FLOUT

All messages in this subroutine concern inconsistencies detected when using data on Unit 10 to restart or run a repeat case. The action in all cases is to check the input indicated.

LOS TAPE CASE NUMBER ICASE DOES NOT MATCH INPUT CASE NUMBER KASE. CASE TERMINATED.

INPUT SMAX XXXX.XX EXCEEDS LOS TAPE VALUE OF XXXX.XX

INPUT DTHETA XXXX.XX EXCEEDS LOS TAPE VALUE OF XXXX.XX

INPUT DPHI XXXX.XX EXCEEDS LOS TAPE VALUE OF XXXX.XX

THETA LIMITS DO NOT AGREE - INPUT VALUES ARE THETA I = XXXX.XX AND THETA F = XXXX.XX

PHI LIMITS DO NOT AGREE - INPUT VALUES ARE PHI I = XXXX.XX AND PHI F = XXXX.XX

FLOW3D

NUMBER OF ETA-CUTS EXCEEDS MN3. $NETA(I,J) = N$ $Z(I) = XXXX.XXXX$

ACTION: Correct input flowfield or increase dimension parameter MN3.

NUMBER OF RADIAL POINTS EXCEEDS LIMITS. NRMAX = MN3 NOPS = N

ACTION: Cosrect input flowfield or increase dimension MR3.

NO. OF LINE-OF-SIGHT POINTS EXCEEDS LV, NEED LARGER DELTA S.

ACTION: Increase DS(Card 6), reduce [SMAX-SZERO] (Card 6), or increase dimension parameter LV.

NEGATIVE PROPERTIES ON THE LINE-OF-SIGHT AT THETA = X.XXXE±XX RAD AND
PHI = X.XXXE ± XX RAD

ACTION: This message is followed by a labeled listing of line-of-sight properties. Examine it to determine the cause of negative properties and correct. Note that θ and ϕ are in radians and all parameters in the line-of-sight property list are in the cm/K/atm.

RADIUS POINTS NOT IN ORDER OR ARE EQUAL

ACTION: This is a warning message. No action is taken to correct the situation. The input should be examined to determine if the error will have a serious effect on linear interpolation.

***WARNING - GAS TEMP RANGE OF XXXX.X TO YYYY.Y IS OUTSIDE THE RANGE OF
COEFFICIENT TABLES

ACTION: This warning message is based on the usual table range of 300K to 3000K (actual ranges are not defined at this point in the program). No corrective action is taken and subroutine SLG does not extrapolate outside the band model parameter tables, so the nearest table value will be used for \bar{k} and $1/d$ if the gas temperature is outside the table limits.

FLOWAX

Messages are the same as FLOW3D except: there is no test on ETA, the parameter MR2 replaces the parameter MR3, and a test is made on the number of Z-cuts for multiple axisymmetric plumes.

*****Z-CUTS EXCEEDING MZ2 CANNOT BE LOADED WITH MULTIPLE PLUMES, INCREASE
PROGRAM DIMENSION MZ2 OR SET IZF = MZ2.

ACTION: Remove Z-cuts from the flowfield to reduce it to the MZ2 limit or follow the actions recommended in the message.

ACDATA

*****UPPER LIMIT HAS BEEN ADJUSTED TO GIVE AN INTEGRAL NO. OF INTERVALS
*****NEW ENUF = XXXXXX.

ACTION: Evaluate results based on altered spectral range. Since program is not designed to handle a fractional wavenumber interval, the limits of integration ($\omega_f - \omega_i$) must be an integral number of intervals ($\Delta\omega$).

NPLOT MUST NOT BE GREATER THAN 30.

ACTION: Correct input or increase the dimension of JPLOT.

NO. OF TEMPS EXCEED MAX. NACT(I) = L NTMAX = MT = K

ACTION: Reduce the number of temperature values in the input band model parameter table for constituent I (of the IDENTC list) from L to K; or increase the dimension parameter MT to L.

ABS COEF DATA BEING LOADED FOR IDENTC LIST SPECIE I EXCEEDED ALLOWABLE ARRAY.
INDXCO = J NCOMAX = K

ACTION: The dimensioned number of wavenumber/species combinations (MCO or NCOMAX) was exceeded by constituent I (of the IDENTC list) which would have required INDXCO positions to be loaded. Reduce the total wavenumber/species positions to less than the NCOMAX specified or increase the dimension parameter MCO.

WAVENO. INTERVAL IDNU(I) = J EXCEEDS DESIRED IDENU = K

ACTION: The input wavenumber interval J specified for constituent I (of the IDENTC list) is larger than the integration interval. Since the program is not designed for this condition, the integration interval must be increased to J or the input table of band model parameters needs to be corrected. See next note also.

WAVENUMBER INTERVAL MUST BE AN INTEGRAL NO. OF THE CONSTITUENT INTERVAL.
IDENU = J IDNU(I) = K

ACTION: If the wavenumber integration interval (DENU) is larger than the table interval (IDNU(I)), the procedure for averaging spectral parameters is invoked, but it requires that DENU be an integer multiple of IDNU(I). Modify either the input for constituent I (of the IDENTC list) or the integration interval.

SLG

The diagnostics are the same for either deck (SLGMLT or YNGH20).

*****THE SUM OF SPECTRAL INTERVALS FOR ALL CONSTITUENTS IS KKKKK. THE MAXIMUM ALLOWED IS LLLLL

ACTION: Reduce the spectral interval or number of species, or increase the dimension parameter MOD. Since all input has been read at this point, the program returns to MAIN to read the next case instead of stopping at the error message.

*****NEGATIVE DMO AT WAVENUMBER = JJJJJJ. DMO = -X.XXX±EXX

ACTION: This is a warning of a negative optical depth. It is treated as a transparent ($\Delta\tau=0$) interval and the program continues. The cause and importance of the negative value should be evaluated. It can be caused by a negative pressure or mole fraction, but this should have been detected causing an error message in FLOWAX or FLOW3D.

PLOTIT

Messages based on 3 digit value for JPLOT identified here as IJK.

ABSCISSA INDICATION MISSING

ACTION: Correct input. Either JPLOT < 0 or I = 0 for the missing plot.

ORDINATE INDICATION MISSING

ACTION: Correct input. Missing plot had J = 0.

FINE STRUCTURE PARAMETERS NOT USED FOR CARBON. PLOT LL DELETED.

ACTION: Correct input. Designed to notify deletion of plots of a_c and a_D if they are requested for carbon (I47 or I57), but this message will also be printed for any case with $K \geq 7$ and $J \geq 4$.

A2.3 BINARY FILES

Binary files are used on Units 3, 4, 8, 10 and 11 to specify flowfield properties (8 or 11), to store line-of-sight property data (3, 4, and 10), to transfer line-of-sight radiance from Subroutine SLG to Subroutine VIEW (4), and to transfer spectral data from Subroutine SPCOUT to the plot program (PLOTIT) (4). These functions are summarized in Table A1.1 and the format of the flowfield (Unit 8 or 11) was described in Section A1.3 as input. Formats for the line-of-sight data and the two other data transfers will be described here.

LINE-OF-SIGHT DATA

Unit 10 stores line-of-sight data for transfer from the flowfield Subroutines (FLOWAX and FLOW3D) to the radiation subroutine (SLG), but it also stores

input data to serve as a restart resource for input with IFLOW = 7 (CARD 2). Unit 3 and 4 may also be used in processing lines-of-sight when the flowfield must be processed in sections, but these units do not have the input data (Records 1 through 4) written on Unit 10 for output (in FLOW) and restart. Contents of the line-of-sight data file are described in Table A2.1.

RADIANCE DATA

At the end of the PHI loop in subroutine SLG, a record is written on Unit 4 for each line-of-sight. Each record contains the following values:

PTHETA - Elevation angle θ in degrees

PHI - Azimuth angle ϕ in radians

RADLOS - Radiance for the line-of-sight (Eq. A1.4)

MBLOCK - Missed/Block flag

= 0 Missed the gas

= 1 Blocked before reaching the gas

= 2 Radiation computed

The variable MLINE is incremented as each record is written, so that it can be used in Subroutine VIEW to read the correct number of records.

SPECTRAL DATA

At the end of Subroutine SPCOUT a single record is written on Unit 4 to provide spectral data to the plot program (PLOTIT). The arrangement of the record is described in Table A2.2.

Table A2.1

LINE-OF-SIGHT DATA FILE

GROUP I GENERAL PROBLEM SPECIFICATION (4 RECORDS)RECORD

- 1 DATE DATE OF TAPE GENERATION
- KASE, IFLOW, NOKON, ISHOCK, IUNITS, ISCALF, IZI, IZF, THETA1, THETA2, DTHETA, PH11, PH1F, DPHI, TANGLE, ENUI, ENUF, DENU, SZERO, SMAX, DS, TDIFF - Input data from cards 2 through 6 (Table A1.3)
- HDG(12), BETA(4), ISYMSC, HANG, CTCD, AP, BP - Input from flowfield (Table A1.4)
- NENG Number of plumes
- NEP1 NENG + 1
- (NUMCON(K), K=1,NOKON) - Order in IDENTC list of the K-th constituent in the input list (card 7).
- IBLOCK = 0 If no blocking surfaces input
 = Index of initial blocking surface in the surface input array (should be NENG + 2)
- (TX(N), TY(N), TZ(N), ((TCS(J,K,N),J=1,3), N=1, NEP1) - Coordinates and direction cosines of the point-of-interest (N=1) and the plumes in the central coordinate system. These are computed in BLOKIN.
- 2 RSCAL, TSCAL, PSCAL, FSCAL(NKTP) - Scale factor input from card 8 (Table A1.3)
- 3 (KON(I),J = 1, NOKON2) - Constituent identification input from card 7 (Table A1.3). Two word names are used, so NOKON2=2*NOKON.
- 4 NBLOCK Index of final surface.
- JBLOCK Index of final intermediate coordinate system.
- (NSF(I), (COMMET(I,K), K=1,5) ISF(I), ALF(I), BMIN(I), BMAX(I), GMIN(I), GMAX(I), NCS(I), RX(I), RY(I), RZ(I), CHS(I), PSS(I), OMS(I), I=1, NBLOCK) - Surface input from cards 9 through 13 (Table A1.3).
- (ICS(j), RXI(j), RYI(j), RZI(j), CUC(j), PSC(j), OMC(j), J=1, JBLOCK) - Intermediate coordinate system input from card 14 (Table A1.3)

Table A2.1
(Concluded)

LINE-OF-SIGHT DATA FILE

GROUP II LINE-OF-SIGHT DATA (See note below)

RECORD

ALL EXCEPT LAST	LSET	Line-of-sight sequence number is LSET . A negative value of LSET indicates the line-of-sight missed the gas.
	LPT	Number of points on the LOS.
	LBLOCK	Identification (NSF(I)) of blocking surface. If none, LBLOCK = 0.
	SINKO	(sin θ cos θ)
	THETA	Elevation angle θ .
	PHI	Azimuth angle ϕ .
	DSFACT	(sin θ cos θ $\Delta\theta$ $\Delta\phi/\pi$)
	DX, XY, DZ	- Dimension increments in the central coordinate system corresponding to DS.
	SMIN	Upper limit of the LOS length.
	(XT(L), YT(L), ZT(L), TWT(L), PWT(L), (FWT(L,K), K=1, NOKON), L=1, LPT)	- Location in the CCS and properties (Temperature, pressure, and mole fractions) for points on the LOS.
	DPHI	$\Delta\phi$ for this LOS. This may be different from the input DPHI because of the operation of the input value of TANGLE (Card 4 of Table A1.3)
	SZERO	Lower limit of the LOS length. This may be different from the input value of SZERO because of fitting the LOS length to the plumes boundaries in Subroutine SLIMIT.
LAST	LSET	= 0
	All other data identical to the previous LOS.	

NOTE: If TANGLE = 0, the number of lines-of-sight is

$$[(\text{THETA}_F - \text{THETA}_I) / \text{DTHETA}] [\text{PHI}_F - \text{PHI}_I] / \text{DPHI}.$$
 The number will be less for TANGLE > 0.

Table A2.2

SPECTRAL DATA FILE
(1 RECORD)

L	Number of wavenumber intervals = $(ENUT-ENUI)/DENU + 1$
I	Number of optical depth values.
NKC	Number of radiating species for which the program is set up. It is equivalent to the dimension parameter NKA.
NODC	Number of spectral intervals for carbon. It is equivalent to the dimension parameter MODC.
NPLOT	Number of plots from Card 2 (Table A1.3)
(ENUV(LL),	Spectral parameters - Wavenumber (cm^{-1})
ELAMV(LL),	- Wavelength (μm)
SFLXTO(LL),	- Spectral flux in units set in ACDATA for output. Determined by NSPEK (Card 2)
GNEW(LL,LL=1,L)	- Transmissivity of final line-of-sight
(FO(II),	Spectral parameters for each species - optical depth in weak line limit.
ACO(II),	- Lorentz line fine structure parameter, $\bar{\alpha}_{ce}$
ADO(II),II=1,I),	- Doppler line fine structure parameter, $\bar{\alpha}_{De}$
(JPLOT(N),N=1,NPLOT)	- Plot specifications from Card 16.
(TITLE(N1),N1=1,12)	- Title from Card 1.
(NUMCON(N2),N2=1,10)	- Position on the IDENTC list of constituent N2 in the input list (Card 7).
(NUL(N3),	Wavenumber interval of data for constituent N3 - lower limit
NUU(N3),N3=1,NKC)	- upper limit
(FOC(N4),N4=1,NODC)	- Optical depth for carbon.
NOKON	Number of constituents for this case from Card 2.

A3 SAMPLE PROBLEMS

ORIGINAL PAGE IS
OF POOR QUALITY

A31
PRECEDING PAGE BLANK NOT SHOWN

1.	@ASG,TJ GASRAD,U9S,17020	ASSIGN AND REWIND INPUT TAPE	
2.	@REWIND GASRAD		
3.	@FREE TPF5.		
4.	@ASG,T TPF5.,F/1/POS/5	INCREASE DEFAULT SIZE OF TEMP. PROG. FILE	
5.	@ASG,T 3,F///2500		
6.	@ASG,T 4,F///2500	ASSIGN EXTERNAL STORAGE DEVICES	
7.	@ASG,T 8,F///500		
8.	@ASG,T 10.,F///2500		
9.	@COPIN GASRAD		
10.	@FREE GASRAD	COPY IN AND FREE INPUT TAPE	
11.	@XGT GASRAD		
12.	SAMPLE PROBLEM 1. HEAT TRANSFER - SSME PLUME RADIATION TO ET BASE CTR.		
13.	-1 13 2 13 0 0 1 0 0 0 55 0		
14.	8. 74. 4.		
15.	0. 40. 4. 4.		
16.	1000. 9800. 400.		
17.	0. 1800. 6. 200.		
18.	H2O1(G) N2(G)	FLOWFIELD CARD IMAGE DATA ELEMENT FROM INPUT TAPE	
19.	@ADD SSMEST		
20.	0 1434.5 0. 63.5 180. 90. 0.	POINT-OF-INTEREST	
21.	5 0. 0. 157. 0. 0. 0.	PLUME ORIGINS	
22.	6 0. 0. 157. 0. 0. 0.		
23.	7 0. 0. 157. 0. 0. 0.		
24.	6201	ENG 2 BELL	
25.	7 4.2844 27.174 128.844 0. 360.	BLOCKING SURFACES	
26.	6 28.156		
27.	1200		ORBITER LOWER FUSELAGE
28.	3 0. 1240.7 -6. 6.		
29.	277. 0. 276.7 90. 0. 0.		
30.	3601	BODY FLAP	
31.	3 493.73 593.33 -12.56 12.56	INTERMEDIATE COORDINATE SYSTEMS	
32.	2103.78 0. 339.22 270. 0. -6.27		
33.	-1		
34.	5 1445. 0. 443. 180. 74. 0.		
35.	6 1468.17 53. 342.64 180. 80. 0.		
36.	7 1468.17 53. 342.64 180. 80. 0.		
37.	-1		
38.	@ADD H2OCMB	H ₂ O BAND MODEL PARAMETER CARD IMAGE DATA ELEMENT FROM INPUT TAPE	
39.			
40.			
41.		5 BLANK CARDS TO INDICATE NO DATA FOR OTHER GASES	
42.			
43.			
44.	SAMPLE PROBLEM 1A. HEAT TRANSFER FOR A 0.04 SCALE MODEL	REPEAT CASE BY SCALING DATA ON UNIT 10	
45.	0 1		
46.	0.04		
47.	@ADD H2OCMB		
48.			
49.		5 BLANK CARDS FOR BAND MODEL INPUT	
50.			
51.			
52.			
53.	@FIN	ONE BLANK CARD TO TERMINATE RUN	
54.			

RTR 014-9

SSME FLIGHT NOZZLE SEA LEVEL PLUME - TKE - 5/4/78 ICASE= 1
 BETA LH2/LO2/AIR ISYMSC= 0 HANG= .00 CTCD= .00 AP= 6.25E+01 BP= 1.25E-01
 NOCON= 4 H2O1(G) H2(G) O2(G) NZ(G) ← CONSTITUENT ORDER MUST MATCH MOLE
 FRACTION ORDER ON INPUT

.00	1		
5.00	1	20	1
10.00	1	23	1
15.00	1	21	1
20.00	1	19	1
30.00	1	20	1
35.00	1	19	1
40.00	1	20	1
45.00	1	17	1
51.00	1	17	1
52.00	1	18	1
52.10	1	20	1
60.00	1	14	1
70.00	1	12	1
80.00	1	13	1
90.00	1	10	1
100.00	1	13	1
105.00	1	15	1
115.00	1	15	1
120.00	1	15	1
130.00	1	15	1
140.00	1	13	1
150.00	1	13	1
160.00	1	14	1
180.00	1	13	1
190.00	1	14	1
	1	13	1

← ZZ(I), NETA(I)
 ← ETA (ETA(I,J), NR(I,J), LS(I,J), J=1, NETA(I)
 RADIAL POINTS AND PROPERTIES AT EACH ZZ(I)
 ARE OMITTED

PARTIAL ECHO PRINT OF FLOWFIELD
 INPUT IN SUBROUTINE FFPREP.
 ONLY OCCURS WITH CARD INPUT OR
 FLOWFIELD SCALING

210.00	.00	13	1
	1		
220.00	.00	13	1
	1		
230.00	.00	14	1
	1		
250.00	.00	14	1
	1		
280.00	.00	12	1
	1		
290.00	.00	14	1
	1		
300.00	.00	14	1
	1		
310.00	.00	14	1
	1		
320.00	.00	14	1
	1		
350.00	.00	14	1
	1		
360.00	.00	13	1
	1		
370.00	.00	12	1
	1		
380.00	.00	12	1
	1		
390.00	.00	12	1
	1		
400.00	.00	12	1
	1		
420.00	.00	12	1
	1		
440.00	.00	12	1
	1		
460.00	.00	13	1
	1		
480.00	.00	13	1
	1		
500.00	.00	14	1
	1		
520.00	.00	14	1
	1		
540.00	.00	14	1
	1		
560.00	.00	14	1
	1		
580.00	.00	14	1
	1		
600.00	.00	14	1
	1		
620.00	.00	15	1
	1		
640.00	.00	15	1
	1		
660.00	.00	15	1
	1		
680.00	.00	16	1
	1		

A33

SAMPLE PROBLEM 1

RTR 014-9

700.00	1		
.00	15	1	
720.00	1		
.00	16	1	
760.00	1		
.00	16	1	
800.00	1		
.00	15	1	
840.00	1		
.00	15	1	
860.00	1		
.00	15	1	
900.00	1		
.00	16	1	
920.00	1		
.00	16	1	
940.00	1		
.00	16	1	
1000.00	1		
.00	16	1	
1100.00	1		
.00	15	1	
1200.00	1		
.00	16	1	
.00	0		

124

RTR 014-9

3 AXISYMMETRIC PLUMES USING CASE 1 WITH EXIT CTRLINE LOCATIONS AND DIRECTIONS INDICATED RUN DATE 030680

RADIATION PROBLEM IDENTIFICATION - SAMPLE PROBLEM 1. HEAT TRANSFER - SSME PLUME RADIATION TO ET BASE CTR.

FLOW FIELD IDENTIFICATION - - - SSME FLIGHT NOZZLE SEA LEVEL PLUME - TKE - 5/4/78
 GAS IDENTIFICATION - LH2/LO2/AIR

ENG. NO.	LOCATION OF EXIT CENTER			DIRECTION X	COSINES OF AXIS		
	X	Y	Z		Y	Z	
1	1595.92	.00	486.28	.96126	.00000	.27564	
2	1622.78	-53.00	369.90	.98481	.00000	.17365	
3	1622.78	53.00	369.90	.98481	.00000	.17365	

FLOW FIELD CONICAL LIMITS - INTERCEPT= 6.250+01 SLOPE= 1.250-01

ENGLISH UNITS - LENGTH IN INCHES - TEMPERATURE IN DEGREES RANKINE - PRESSURE IN PSFA ← UNITS FOR INPUT

LIMITS OF INTEGRATION	VARIABLE	INITIAL VALUE	FINAL VALUE	INCREMENT
	Z-INDEX	1	55	
	THETA	8.00	74.00	4.0000
	PHI	.00	40.00	4.0000
	NU	1000.	9800.	400.
	S	.00	1800.00	6.0000
	TEMP STEP SIZE			200.0000
	TANGLE (DEG)			4.0000

POINT LOCATION X 1434.50 Y .00 Z 63.50 ← LOCATION IN CENTRAL COORDINATE SYSTEM

COSINES OF U	-.00000	-.00000	1.00000	} DIRECTION COSINES RELATIVE TO CENTRAL COORD. SYS.
V	.00000	-1.00000	.00000	
W	1.00000	.00000	.00000	

CONSTITUENTS H2O1(G) N2(G) ← NO PARTICULAR ORDER REQUIRED

COORDINATE DATA INPUT FOR THE POINT OF INTEREST AND PLUMES

POINT OF INTEREST	ICS NO.	X	Y	Z	CHI	PSI	OMEGA
	0	1434.50	.00	63.50	180.00	90.00	.00
PLUME NO. 1	5	.00	.00	157.00	.00	.00	.00
PLUME NO. 2	6	.00	.00	157.00	.00	.00	.00
PLUME NO. 3	7	.00	.00	157.00	.00	.00	.00

ORIGINAL PAGE IS OF POOR QUALITY

RTR 014-9

BLOCKING SURFACES

NO.	TITLE	TYPE ICS	ALF	BMIN	BMAX	GMIN	GMAX	OMS
			RX	RY	RZ	CHS	PSS	
6201	ENG 2 BELL	7	4.2844+00	2.7174+01	1.2884+02	.0	360.0	
		6	0.0000	0.0000	2.8156+01	.0	.0	.0
1200	ORBITER LOWER FUSELAGE	3	0.0000	0.0000	1.2407+03	-6.0	6.0	
		0	2.7700+02	0.0000	2.7670+02	90.0	.0	.0
3601	BODY FLAP	3	0.0000	4.9373+02	5.9333+02	-12.6	12.6	
		0	2.1038+03	0.0000	3.3922+02	270.0	.0	-6.3

INTERMEDIATE COORDINATE SYSTEM FOR BLOCKING SURFACES

ICS	RyI	RyI	RzI	CHC	PSC	QHC
5	1.4450+03	0.0000	4.4300+02	180.0	74.0	.0
6	1.4682+03	-5.3000+01	3.4264+02	180.0	80.0	.0
7	1.4682+03	5.3000+01	3.4264+02	180.0	80.0	.0

NO FLOW FIELD SCALE FACTORS WERE USED.

FLOW FIELD	Z	R	T	P	F1	F2	F3	F4	F5	F6
.000	.000	1406.4	39.6400	.7702	.0000					
5.000	45.390	558.0	2116.2200	.0010	.7900					
	.000	1366.0	34.8700	.7702	.0000					
10.000	64.570	558.1	2116.2200	.0000	.7900					
	.000	1326.9	30.6900	.7702	.0000					
15.000	62.580	558.7	2116.2200	.0002	.7898					
	.000	1866.1	118.5000	.7702	.0000					
20.000	61.160	562.4	2116.2200	.0014	.7885					
	.000	1866.2	129.0000	.7702	.0000					
30.000	60.180	574.3	2116.2200	.0050	.7849					
	.000	1810.9	118.0700	.7702	.0000					
35.000	73.760	558.1	2116.2200	.0000	.7900					
	.000	1843.9	128.8900	.7702	.0000					
40.000	72.200	558.3	2116.2200	.0001	.7899					
	.000	1776.4	110.0700	.7702	.0000					
45.000	72.630	558.9	2116.2200	.0003	.7897					
	.000	1801.1	117.6400	.7702	.0000					
50.000	71.870	559.9	2116.2200	.0006	.7894					
	.000	1767.5	178.7700	.7702	.0000					
52.000	70.610	561.7	2116.2200	.0011	.7890					
	.000	1765.7	108.3100	.7702	.0000					
52.100	70.610	561.7	2116.2200	.0011	.7890					
	.000	5600.0	4354.0000	.7700	.0000					
60.000	70.610	561.7	2116.2200	.0011	.7890					
	.000	5700.0	5400.0000	.7700	.0000					
70.000	67.920	566.1	2116.2200	.0023	.7880					
	.000	5600.0	4712.0000	.7700	.0000					
80.000	64.680	574.2	2116.2200	.0043	.7865					
	.000	5600.0	4602.0000	.7700	.0000					
90.000	62.380	587.1	2116.2200	.0072	.7844					
	.000	5600.0	4686.0000	.7700	.0000					
100.000	79.440	558.3	2116.2200	.0001	.7899					
	.000	5550.0	4033.0000	.7700	.0000					
105.000	80.700	558.8	2116.2200	.0003	.7898					
	.000	5530.0	3513.0000	.7700	.0000					
115.000	80.980	559.6	2116.2200	.0005	.7896					
	.000	5300.0	2386.0000	.7700	.0000					
120.000	81.540	561.1	2116.2200	.0010	.7893					
	.000	5170.0	1779.0000	.7700	.0000					
130.000	82.060	563.6	2116.2200	.0016	.7888					
	.000	4970.0	1099.0000	.7700	.0000					
140.000	82.300	567.3	2116.2200	.0026	.7881					
	.000	5070.0	1402.0000	.7700	.0000					
150.000	82.510	572.7	2116.2200	.0039	.7871					
	.000	5210.0	1958.0000	.7700	.0000					
160.000	98.750	558.1	2116.2200	.0001	.7900					
	.000	5210.0	1918.0000	.7700	.0000					
180.000	83.350	590.4	2116.2200	.0080	.7843					
	.000	5210.0	2035.0000	.7700	.0000					
190.000	98.860	558.9	2116.2200	.0003	.7898					
	.000	5190.0	1798.0000	.7700	.0000					

SHORT FORM OF FLOWFIELD
OUTPUT IN SUBROUTINE
FLOWAX. INTERIOR POINTS
ARE NOT PRINTED.

A37

RTR 014-9

FLOW FIELD (CONTINUED)

Z	R	T	P	F1	F2	F3	F4	F5	F6
190.000	97.570	559.6	2116.2200	.0005	.7896				
200.000	.000	5210.0	1932.0000	.7700	.0000				
	97.780	560.7	2116.2200	.0009	.7894				
210.000	.000	5480.0	3123.0000	.7700	.0000				
	98.470	562.2	2116.2200	.0013	.7891				
220.000	.000	5550.0	3760.0000	.7700	.0000				
	98.860	567.5	2116.2200	.0027	.7881				
230.000	.000	4920.0	2182.0000	.7700	.0000				
	99.040	571.7	2116.2200	.0038	.7873				
250.000	.000	4915.0	2184.0000	.7700	.0000				
	99.060	584.0	2116.2200	.0067	.7853				
280.000	.000	4920.0	2286.0000	.7700	.0000				
	123.220	558.8	2116.2200	.0003	.7898				
290.000	.000	4650.0	1332.0000	.7700	.0000				
	123.660	559.2	2116.2200	.0004	.7897				
300.000	.000	4550.0	1104.0000	.7700	.0000				
	123.870	559.8	2116.2200	.0006	.7896				
310.000	.000	4808.0	1802.0000	.7700	.0000				
	123.940	560.6	2116.2200	.0008	.7894				
320.000	.000	4901.0	2159.0000	.7700	.0000				
	124.130	561.6	2116.2200	.0011	.7892				
350.000	.000	4929.0	2218.0000	.7700	.0000				
	123.280	566.8	2116.2200	.0024	.7883				
360.000	.000	4860.0	1911.0000	.7700	.0000				
	122.920	569.5	2116.2200	.0030	.7879				
370.000	.000	5049.0	2798.0000	.7700	.0000				
	122.780	572.7	2116.2200	.0038	.7873				
380.000	.000	4755.0	3438.0000	.7700	.0000				
	122.870	576.7	2116.2200	.0047	.7867				
390.000	.000	4755.0	3483.0000	.7700	.0000				
	122.950	581.3	2116.2200	.0057	.7860				
400.000	.000	4532.0	2063.0000	.7700	.0000				
	123.260	586.9	2116.2200	.0068	.7852				
420.000	.000	4463.0	1807.0000	.7700	.0000				
	124.540	593.4	2116.2200	.0081	.7843				
440.000	.000	4540.0	2119.0000	.7700	.0000				
	170.720	558.5	2116.2200	.0002	.7899				
460.000	.000	4282.0	1210.0000	.7700	.0000				
	170.920	558.9	2116.2200	.0003	.7898				
480.000	.000	4540.0	2626.0000	.7700	.0000				
	171.140	559.8	2116.2200	.0005	.7897				
500.000	.000	4644.0	2637.0000	.7700	.0000				
	170.640	561.2	2116.2200	.0009	.7894				
520.000	.000	4532.0	2142.0000	.7700	.0000				
	170.380	563.0	2116.2200	.0013	.7891				
540.000	.000	4400.0	3276.0000	.7700	.0000				
	171.310	565.3	2116.2200	.0018	.7887				
560.000	.000	4152.0	1835.0000	.7700	.0000				
	172.700	568.5	2116.2200	.0025	.7883				
580.000	.000	4056.0	1563.0000	.7700	.0000				

0-2

A38

ORIGINAL PAGE IS
OF POOR QUALITY

RTR 014-9

FLOW FIELD (CONTINUED)

Z	R	T	P	F1	F2	F3	F4	F5	F6
580.000	174.030	572.7	2116.2200	.0033	.7877				
600.000	.000	4168.0	1932.0000	.7700	.0000				
	175.150	581.2	2116.2200	.0050	.7865				
620.000	.000	4024.0	1335.0000	.7700	.0000				
	174.310	588.6	2116.2200	.0063	.7856				
640.000	.000	4120.0	2355.0000	.7700	.0000				
	173.430	597.6	2116.2200	.0079	.7845				
680.000	.000	4020.0	2401.0000	.7700	.0000				
	217.180	559.1	2116.2200	.0003	.7898				

***WARNING - GAS TEMP RANGE OF 316.0 TO 3130.2 IS OUTSIDE THE RANGE OF COEFFICIENT TABLES

CALCULATION TIME 10.0000 SECONDS

BAND MODEL PARAMETERS

BROADENING COEFFICIENTS FOR UNIDENTIFIED SPECIES

g1	g2	g3	g4	g5	g6
.05	.08	.06	.05	.05	.01

639

H2O(16) ABSORPTION COEFFICIENTS

WAVE NO. (1/CM)	300.	600.	1000.	1500.	2000.	2500.	3000.
1200.	1.476-03	2.232-02	4.463-02	5.496-02	5.304-02	4.934-02	4.699-02
1600.	5.463-01	2.367-01	1.252-01	6.934-02	4.476-02	3.244-02	2.458-02
2000.	2.935-02	3.065-02	2.529-02	2.036-02	1.698-02	1.413-02	1.237-02
2400.	1.250-04	1.591-04	4.013-04	7.840-04	1.774-03	2.486-03	2.522-03
2800.	1.143-04	2.160-04	4.792-04	1.331-03	2.647-03	4.025-03	4.154-03
3200.	3.510-03	4.297-03	1.126-02	1.695-02	2.122-02	2.084-02	1.727-02
3600.	1.241-01	1.357-01	1.023-01	5.646-02	3.386-02	2.366-02	1.821-02
4000.	1.867-01	6.958-02	3.931-02	2.310-02	1.574-02	1.228-02	1.090-02
4400.	2.144-05	5.886-05	2.331-04	4.487-04	8.348-04	1.315-03	1.498-03
4800.	5.262-05	1.644-04	6.071-04	1.777-03	3.137-03	3.862-03	3.458-03
5200.	1.437-02	1.377-02	1.244-02	8.892-03	6.527-03	5.187-03	3.930-03
5600.	2.127-02	8.697-03	6.071-03	4.477-03	3.679-03	3.311-03	2.831-03
6000.	1.495-05	2.230-05	6.891-05	1.731-04	4.158-04	8.396-04	9.445-04
6400.	4.118-05	1.462-04	3.187-04	6.157-04	1.246-03	1.858-03	1.674-03
6800.	1.308-03	1.965-03	3.261-03	3.333-03	3.169-03	3.108-03	2.918-03
7200.	1.724-02	1.812-02	1.095-02	4.956-03	3.264-03	2.595-03	2.192-03
7600.	3.293-03	5.191-04	8.334-04	7.129-04	6.241-04	5.565-04	6.153-04
8000.	3.340-06	6.010-06	2.121-05	7.211-05	1.910-04	2.497-04	3.377-04
8400.	1.925-05	3.107-05	9.499-05	2.174-04	3.799-04	3.896-04	4.434-04
8800.	1.484-05	1.396-05	6.584-05	1.982-04	3.498-04	3.179-04	3.054-04
9200.	2.092-06	1.627-06	3.826-06	1.713-05	8.846-05	1.006-04	1.473-04
9600.	0.000	0.000	0.000	0.000	1.076-04	1.152-04	1.196-04

LONG FORM \bar{k} AND $1/\bar{d}$ OUTPUT
 (Parameters have been averaged over 400 cm^{-1} intervals and the output is for the center of the interval. Integration interval is 1000-9800 cm^{-1})

H2O(16) FINE STRUCTURE PARAMETERS

WAVE NO. (1/CM)	300.	600.	1000.	1500.	2000.	2500.	3000.
1200.	2.739-01	4.151-01	1.026-00	3.058-00	1.065-01	3.499-01	1.265-02

SAMPLE PROBLEM 1

RTR 014-9

WAVE NO. (1/CM)	TEMPERATURES (DEG K)						
	300.	600.	1000.	1500.	2000.	2500.	3000.
1600.	1.461-01	3.855-01	7.975-01	1.947+00	4.701+00	1.115+01	2.463+01
2000.	1.161-01	2.992-01	6.704-01	1.861+00	4.803+00	1.383+01	4.015+01
2400.	3.061-01	6.083-01	1.521+00	4.123+00	9.153+00	4.058+01	1.939+02
2800.	1.832+00	2.379+00	3.166+00	4.636+00	1.049+01	3.850+01	1.084+02
3200.	8.936-01	1.823+00	2.263+00	2.689+00	5.221+00	1.352+01	2.558+01
3600.	1.009+00	1.420+00	1.861+00	2.650+00	3.865+00	7.887+00	1.369+01
4000.	7.882-01	1.170+00	1.512+00	2.241+00	5.325+00	1.151+01	1.949+01
4400.	9.408-01	1.103+00	1.756+00	4.899+00	2.852+01	7.504+01	1.700+02
4800.	2.771-01	1.051-01	3.131-01	1.230+00	5.808+00	2.222+01	8.313+01
5200.	1.163-01	8.919-02	2.616-01	1.139+00	4.662+00	1.978+01	1.082+02
5600.	1.288-01	2.239-01	3.879-01	1.557+00	8.065+00	3.636+01	2.794+02
6000.	3.897-01	1.239-01	8.185-01	5.961+00	7.212+01	2.787+02	1.396+03
6400.	3.930-01	8.677-02	5.201-01	3.382+00	4.519+01	1.704+02	9.368+02
6800.	1.529-01	5.907-02	3.075-01	1.917+00	1.517+01	6.210+01	2.731+02
7200.	1.257-01	3.229-02	1.952-01	1.465+00	7.937+00	3.556+01	1.300+02
7600.	2.339-01	1.997-01	1.082+00	6.028+00	2.892+01	1.230+02	4.115+02
8000.	4.942-01	1.065+00	2.760+00	7.888+00	1.878+01	3.704+01	6.068+01
8400.	2.292-01	4.850-01	1.274+00	3.510+00	8.296+00	1.643+01	2.727+01
8800.	1.161-01	2.585-01	6.794-01	1.931+00	4.577+00	9.026+00	1.483+01
9200.	1.803-01	4.208-01	1.034+00	3.108+00	8.686+00	1.765+01	2.913+01
9600.	0.000	0.000	0.000	0.000	1.945+01	3.826+01	6.273+01

AM

CM-SR	AVG	COMB	OPT	PATH	LBLOCK	SZERO	S MIN
VG	TRANS	CM-ATH	(STP)				
	DY = -4.595+01CM,	DZ = 2.606+00CM				0.	0.
	DY = -1.323+00CM,	DZ = 2.292+00CM				0.	0.
	DY = -4.280+01CM,	DZ = 3.662+00CM				0.	0.
	DY = -1.261+00CM,	DZ = 3.465+00CM				0.	0.
	DY = -2.026+00CM,	DZ = 3.080+00CM				0.	0.
175-03	.964	1.309+00	0			912.	930.
	DY = -1.219+00CM,	DZ = 4.549+00CM				0.	0.
	DY = -1.990+00CM,	DZ = 4.268+00CM				0.	0.
	DY = -2.701+00CM,	DZ = 3.858+00CM				0.	0.
118-01	.753	2.079+01	0			726.	942.
106-01	.805	1.797+01	0			744.	942.
165-01	.944	2.649+00	0			912.	948.
	DY = -3.275+00CM,	DZ = 4.677+00CM				0.	0.
101+00	.477	4.309+01	0			612.	960.
194+00	.488	4.222+01	0			612.	960.
185+00	.754	2.890+01	0			666.	966.
	DY = -3.136+00CM,	DZ = 5.899+00CM				0.	0.
	DY = -3.927+00CM,	DZ = 5.405+00CM				0.	0.
27+00	.393	6.126+01	0			528.	984.
41+00	.370	6.917+01	0			522.	984.
28+00	.567	4.938+01	0			546.	984.
53+00	.834	2.924+01	0			630.	990.
	DY = -3.810+00CM,	DZ = 6.599+00CM				0.	0.
	DY = -4.550+00CM,	DZ = 6.112+00CM				0.	0.
22+00	.403	6.837+01	0			468.	1008.
53+00	.385	7.866+01	0			462.	1008.
51+00	.596	5.183+01	0			480.	966.
65+00	.874	1.600+01	0			564.	786.
	DY = -4.261+00CM,	DZ = 7.380+00CM				0.	0.
	DY = -5.089+00CM,	DZ = 6.836+00CM				0.	0.
43+00	.356	8.140+01	0			426.	1032.
49+00	.400	8.206+01	0			414.	1032.
47+00	.498	4.787+01	0			420.	822.
99+00	.812	2.582+01	0			456.	738.
	DY = -4.071+00CM,	DZ = 8.454+00CM				0.	0.
	DY = -4.892+00CM,	DZ = 8.006+00CM				0.	0.
	DY = -5.665+00CM,	DZ = 7.479+00CM				0.	0.
16+00	.355	8.932+01	0			390.	1062.
13+00	.404	8.760+01	0			378.	1062.
31+00	.527	3.895+01	0			384.	702.
78+00	.859	1.789+01	0			414.	630.
	DY = -4.425+00CM,	DZ = 9.188+00CM				0.	0.
	DY = -5.317+00CM,	DZ = 8.701+00CM				0.	0.
	DY = -6.157+00CM,	DZ = 8.129+00CM				0.	0.
19+00	.395	8.163+01	0			360.	990.
15+00	.475	7.150+01	0			348.	924.
12+00	.536	4.180+01	0			348.	624.

THESE HAVE BEEN MODIFIED FROM
INPUT LIMITS OF SZERO AND SMAX
BY SUBROUTINE SLIMIT. UNITS ARE
THE SAME AS INPUT

THETA DEGREES	PHI	SHAPE FACTOR	FLUX=WATTS/SQ=CM		RAD=WATTS/SQ=CM=SR		AVG TRANS	COMB CM-ATM(STP)	OPT PATH	LPLOCK	SZERO	SMIN
			DELTA	SUM	LOS	AVG						
46.00	17.500	3.071-02	2.16-03	1.15+00	7.096-01	6.597+00	.784	2.098+01		0	366.	588.
46.00	22.500	3.168-02	1.83-06	1.15+00	6.025-04	6.484+00	.969	1.444+00		0	432.	486.
46.00	27.500	LINE OF SIGHT MISSED THE GAS. DX= 1.059+01CM; DY= -5.062+00CM; DZ= 9.724+00CM										
46.00	32.500	LINE OF SIGHT MISSED THE GAS. DX= 1.059+01CM; DY= -5.890+00CM; DZ= 9.246+00CM										
46.00	37.500	LINE OF SIGHT MISSED THE GAS. DX= 1.059+01CM; DY= -6.674+00CM; DZ= 8.697+00CM										
50.00	2.500	3.263-02	4.67-02	1.19+00	1.558+01	6.315+00	.445	6.960+01		0	336.	852.
50.00	7.500	3.359-02	9.66-02	1.29+00	3.222+01	6.719+00	.400	7.477+01		0	324.	798.
50.00	12.500	3.454-02	6.23-02	1.35+00	2.077+01	6.935+00	.452	4.891+01		0	324.	558.
50.00	17.500	3.550-02	5.93-04	1.35+00	1.977-01	6.833+00	.832	1.747+01		0	342.	522.
50.00	22.500	LINE OF SIGHT MISSED THE GAS. DX= 9.796+00CM; DY= -4.468+00CM; DZ= 1.079+01CM										
50.00	27.500	LINE OF SIGHT MISSED THE GAS. DX= 9.796+00CM; DY= -5.391+00CM; DZ= 1.036+01CM										
50.00	32.500	LINE OF SIGHT MISSED THE GAS. DX= 9.796+00CM; DY= -6.273+00CM; DZ= 9.846+00CM										
50.00	37.500	LINE OF SIGHT MISSED THE GAS. DX= 9.796+00CM; DY= -7.107+00CM; DZ= 9.262+00CM										
54.00	2.222	LOS BLOCKED BY BODY FLAP										
54.00	6.667	LOS BLOCKED BY BODY FLAP										
54.00	11.111	LOS BLOCKED BY BODY FLAP										
54.00	15.556	LOS BLOCKED BY BODY FLAP										
54.00	20.000	LOS BLOCKED BY BODY FLAP										
54.00	24.444	LOS BLOCKED BY BODY FLAP										
54.00	28.889	LINE OF SIGHT MISSED THE GAS. DX= 8.958+00CM; DY= -5.957+00CM; DZ= 1.080+01CM										
54.00	33.333	LINE OF SIGHT MISSED THE GAS. DX= 8.958+00CM; DY= -6.775+00CM; DZ= 1.030+01CM										
54.00	37.778	LINE OF SIGHT MISSED THE GAS. DX= 8.958+00CM; DY= -7.553+00CM; DZ= 9.745+00CM										
58.00	2.222	LOS BLOCKED BY BODY FLAP										
58.00	6.667	LOS BLOCKED BY BODY FLAP										
58.00	11.111	LOS BLOCKED BY BODY FLAP										
58.00	15.556	LOS BLOCKED BY BODY FLAP										
58.00	20.000	LOS BLOCKED BY BODY FLAP										
58.00	24.444	LOS BLOCKED BY BODY FLAP										
58.00	28.889	LINE OF SIGHT MISSED THE GAS. DX= 8.076+00CM; DY= -6.244+00CM; DZ= 1.132+01CM										
58.00	33.333	LINE OF SIGHT MISSED THE GAS. DX= 8.076+00CM; DY= -7.102+00CM; DZ= 1.080+01CM										
58.00	37.778	LINE OF SIGHT MISSED THE GAS. DX= 8.076+00CM; DY= -7.917+00CM; DZ= 1.022+01CM										
62.00	2.222	LOS BLOCKED BY BODY FLAP										
62.00	6.667	LOS BLOCKED BY BODY FLAP										
62.00	11.111	LOS BLOCKED BY BODY FLAP										
62.00	15.556	LOS BLOCKED BY BODY FLAP										
62.00	20.000	LOS BLOCKED BY BODY FLAP										
62.00	24.444	LOS BLOCKED BY BODY FLAP										
62.00	28.889	LOS BLOCKED BY BODY FLAP										
62.00	33.333	LINE OF SIGHT MISSED THE GAS. DX= 7.155+00CM; DY= -7.394+00CM; DZ= 1.124+01CM										
62.00	37.778	LINE OF SIGHT MISSED THE GAS. DX= 7.155+00CM; DY= -8.243+00CM; DZ= 1.064+01CM										
66.00	2.000	LOS BLOCKED BY BODY FLAP										
66.00	6.000	LOS BLOCKED BY BODY FLAP										
66.00	10.000	LOS BLOCKED BY BODY FLAP										
66.00	14.000	LOS BLOCKED BY BODY FLAP										
66.00	18.000	LOS BLOCKED BY BODY FLAP										
66.00	22.000	LOS BLOCKED BY BODY FLAP										
66.00	26.000	LOS BLOCKED BY BODY FLAP										
66.00	30.000	LOS BLOCKED BY BODY FLAP										
66.00	34.000	LINE OF SIGHT MISSED THE GAS. DX= 6.199+00CM; DY= -7.785+00CM; DZ= 1.154+01CM										
66.00	38.000	LINE OF SIGHT MISSED THE GAS. DX= 6.199+00CM; DY= -8.572+00CM; DZ= 1.097+01CM										

A42

RTR 014-9

THETA DEGREES	PHI	SHAPE FACTOR	FLUX=WATTS/SQ=CM DELTA SUM	RAD=WATTS/SQ=CM=SR LOS AVG	AVG COMB OPT PATH TRANS CM-ATM(STP)	LBLOCK	SZERO	S MIN
70.00	2.000	LOS BLOCKED BY ORBITER LOWER FUSELAGE				1200	0.	0.
70.00	6.000	LOS BLOCKED BY ORBITER LOWER FUSELAGE				1200	0.	0.
70.00	10.000	LOS BLOCKED BY ORBITER LOWER FUSELAGE				1200	0.	0.
70.00	14.000	LOS BLOCKED BY ORBITER LOWER FUSELAGE				1200	0.	0.
70.00	18.000	LOS BLOCKED BY BODY FLAP				3601	0.	0.
70.00	22.000	LOS BLOCKED BY BODY FLAP				3601	0.	0.
70.00	26.000	LOS BLOCKED BY BODY FLAP				3601	0.	0.
70.00	30.000	LOS BLOCKED BY BODY FLAP				3601	0.	0.
70.00	34.000	LINE OF SIGHT MISSED THE GAS. DX= 5.212+00CM, DY= -8.008+00CM, DZ= 1.187+01CM					0.	0.
70.00	38.000	LINE OF SIGHT MISSED THE GAS. DX= 5.212+00CM, DY= -8.817+00CM, DZ= 1.129+01CM					0.	0.

NUMERICAL PLUME SHAPE FACTOR= .03550 PLUME RADIANCE = 1.2143+01 WATTS/SQ-CM-STER
 NUMERICAL TOTAL SHAPE FACTOR= .09843 OVERALL RADIANCE= 4.3791+00 WATTS/SQ-CM-STER
 EXACT TOTAL SHAPE FACTOR = .10052 TOTAL FLUX = 1.3541+00 WATTS/SQ-CM

CALCULATION TIME 12 SECONDS

NOT ACTUAL TIME

A43

SAMPLE PROBLEM 1

RTR 014-9

TRANSMISSIVITY

WAVE NUMBER 1/CM	WAVE LENGTH MICRON	IRRADIANCE WATTS/ CM	G	OPTICAL DEPTH
1200.	8.333	8.191-05	1.0000	0.000
1600.	6.250	9.102-05	1.0000	0.000
2000.	5.000	1.787-04	1.0000	0.000
2400.	4.167	1.675-04	1.0000	0.000
2800.	3.571	2.504-04	1.0000	0.000
3200.	3.125	2.992-04	1.0000	0.000
3600.	2.778	1.534-04	1.0000	0.000
4000.	2.500	2.198-04	1.0000	0.000
4400.	2.273	1.676-04	1.0000	0.000
4800.	2.083	3.142-04	1.0000	0.000
5200.	1.923	3.000-04	1.0000	0.000
5600.	1.786	2.636-04	1.0000	0.000
6000.	1.667	1.090-04	1.0000	0.000
6400.	1.563	1.908-04	1.0000	0.000
6800.	1.471	2.352-04	1.0000	0.000
7200.	1.389	1.826-04	1.0000	0.000
7600.	1.316	6.436-05	1.0000	0.000
8000.	1.250	2.901-05	1.0000	0.000
8400.	1.190	3.943-05	1.0000	0.000
8800.	1.136	2.890-05	1.0000	0.000
9200.	1.087	9.605-06	1.0000	0.000
9600.	1.042	9.030-06	1.0000	0.000

FOR LAST LINE-OF-SIGHT WHICH MISSED
THE GAS ON THIS PROBLEM.

SPECTRAL OUTPUT TIME .00000 SECONDS

A44

EACH SYMBOL REPRESENTS A RADIATION STEP OF 3.221670 WATTS/SQ. CM.
 THETA SCALE GOES TO 90.000 DEGREES

(0 DEG)

MAX RADIANCE IS 10 TIMES THIS (32.2 w/cm²-sr)

*

*

B B B B
 B B B B B B
 B B B B B B B B
 B B B B B B B B
 B B B B B B B B
 4 6 B B B
 6 5 0
 7 8 3 0
 8 4 0
 7 5 0
 7 7 1 0
 7 7 1 0
 5 5 0
 0 0 0
 0

PEAK RADIANCE

(9x3.22 < N ≤ 10xNMAX)

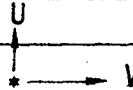
B INDICATES BLOCKING

*

*

A45

(270 DEG) *



W INTO PAPER

* (90 DEG)

OUTPUT POLAR PLOT OF
 RADIANCE IN SUBROUTINE
 VIEW

*

*

*

*

(180 DEG)

SAMPLE PROBLEM 1

NOTE

LINE OF SIGHT TAPE PRODUCED FOR CASE 1 ON 030680 DATE OF RUN 030680

RADIATION PROBLEM IDENTIFICATION - SAMPLE PROBLEM 1A. HEAT TRANSFER FOR A 0.04 SCALE MODEL

FLOW FIELD IDENTIFICATION - - - - SSME FLIGHT NOZZLE SEA LEVEL PLUME - TKE - 5/4/78
GAS IDENTIFICATION - LH2/L02/AIR

ENG. NO.	LOCATION OF EXIT CENTER			DIRECTION COSINES OF AXIS		
	X	Y	Z	X	Y	Z
1	63.84	.00	19.45	.96126	.00000	.27564
2	64.91	-2.12	14.80	.98481	.00000	.17365
3	64.91	2.12	14.80	.98481	.00000	.17365

FLOW FIELD CONICAL LIMITS - INTERCEPT= 2.500+00 SLOPE= 1.250-01

ENGLISH UNITS - LENGTH IN INCHES - TEMPERATURE IN DEGREES RANKINE - PRESSURE IN PSFA

LIMITS OF INTEGRATION	VARIABLES	INITIAL VALUE	FINAL VALUE	INCREMENT
	Z-INDEX	1	55	
	THETA	8.00	74.00	4.0000
	PHI	.00	40.00	4.0000
	NU	1000.	9800.	400.
	S	.00	72.00	.2400
	TEMP STEP SIZE			200.0000
	TANGLE (DEG)			4.0000

A46

POINT LOCATION	X	Y	Z
	57.38	.00	2.54
COSINES OF U	-.00000	-.00000	1.00000
V	.00000	-1.00000	.00000
W	1.00000	.00000	.00000

ALL GEOMETRY IS SCALED BY 0.04
FROM SAMPLE PROBLEM 1

CONSTITUENTS H2O(G) N2(G) 1

COORDINATE DATA INPUT FOR THE POINT OF INTEREST AND PLUMES

	ICS NO.	X	Y	Z	CHI	PSI	OMEGA
POINT OF INTEREST	0	57.38	.00	2.54	180.00	90.00	.00
PLUME NO. 1	5	.00	.00	6.28	.00	.00	.00
PLUME NO. 2	6	.00	.00	6.28	.00	.00	.00
PLUME NO. 3	7	.00	.00	6.28	.00	.00	.00

BLOCKING SURFACES
NO.

TITLE

TYP
ICS

ALF
RX

BMIN
RY

BMAX
RZ

GMIN
CHS

GMAX
PSS

OMS

6271 ENG 2 BELL

7 1.7138-01 1.0070+00 5.1538+00 .0 360.0
6 0.0000 0.0000 1.1262+00 .0 .0 .0

1200 ORBITER LOWER FLUSFLAGE

3 0.0000 0.0000 4.9628+01 -6.0 6.0
0 1.1080+01 0.0000 1.1068+01 90.0 .0 .0

3671 BODY FLAP

3 0.0000 1.9749+01 2.3733+01 -12.6 12.6
0 8.4151+01 0.0000 1.3569+01 270.0 .0 -6.3

INTERMEDIATE COORDINATE SYSTEM FOR BLOCKING SURFACES

ICS	RxI	RyI	RzI	CHC	PSC	OMC
5	5.7800+01	0.0000	1.7720+01	180.0	74.0	.0
6	5.8727+01	-2.1200+00	1.3706+01	180.0	80.0	.0
7	5.8727+01	2.1200+00	1.3706+01	180.0	80.0	.0

NO FLOWFIELD OUTPUT

SCALE FACTORS

RSAL	TSCAL	PSCAL	F1	F2	F3	F4	F5	F6
.04000	1.00000	1.00000	1.00000	1.00000				

BAND MODEL PARAMETERS

BROADENING COEFFICIENTS FOR UNIDENTIFIED SPECIES

G1	G2	G3	G4	G5	G6
.05	.08	.06	.05	.05	.01

H201(G) ABSORPTION COEFFICIENTS

WAVE NO. (1/CM)	TEMPERATURES (DEG K)	300.	600.	1000.	1500.	2000.	2500.	3000.
1200.	1.476-03	2.232-02	4.463-02	5.496-02	5.304-02	4.934-02	4.699-02	
9600.	0.000	0.000	0.000	0.000	1.076-04	1.152-04	1.196-04	

SHORT FORM OF PARAMETER OUTPUT

H201(G) FINE STRUCTURE PARAMETERS

WAVE NO. (1/CM)	TEMPERATURES (DEG K)	300.	600.	1000.	1500.	2000.	2500.	3000.
1200.	2.739-01	4.151-01	1.026+00	3.058+00	1.065+01	3.499+01	1.265+02	
9600.	0.000	0.000	0.000	0.000	1.945+01	3.826+01	6.273+01	

ORIGINAL PAGE NO
OF THIS QUALITY

A47

S/SQ=CM-SR	AVG	COMB	OPT	PATH	LELOCK	SZERO	SMIN
AVG	TRANS	CM-ATM(STP)					
11CM, DY= -1.838-02CM, DZ= 1.042-01CM						0.	0.
11CM, DY= -5.293-02CM, DZ= 9.167-02CM						0.	0.
11CM, DY= -1.712-02CM, DZ= 1.465-01CM						0.	0.
11CM, DY= -5.044-02CM, DZ= 1.386-01CM						0.	0.
11CM, DY= -8.104-02CM, DZ= 1.232-01CM						0.	0.
1 1.447-04 .997 5.235-02 0						36.	37.
11CM, DY= -4.876-02CM, DZ= 1.820-01CM						0.	0.
11CM, DY= -7.961-02CM, DZ= 1.707-01CM						0.	0.
11CM, DY= -1.080-01CM, DZ= 1.543-01CM						0.	0.
1 2.752-02 .961 8.318-01 0						29.	38.
1 3.418-02 .969 7.187-01 0						30.	38.
1 3.125-02 .995 1.060-01 0						36.	38.
11CM, DY= -1.310-01CM, DZ= 1.871-01CM						0.	0.
1 2.461-01 .975 1.723+00 0						24.	38.
1 4.181-01 .908 1.689+00 0						24.	38.
1 4.029-01 .953 1.156+00 0						27.	39.
11CM, DY= -1.255-01CM, DZ= 2.360-01CM						0.	0.
11CM, DY= -1.571-01CM, DZ= 2.162-01CM						0.	0.
1 5.815-01 .871 2.451+00 0						21.	39.
1 8.073-01 .858 2.767+00 0						21.	39.
1 8.332-01 .910 1.975+00 0						22.	39.
2 7.990-01 .966 1.170+00 0						25.	40.
11CM, DY= -1.524-01CM, DZ= 2.640-01CM						0.	0.
11CM, DY= -1.820-01CM, DZ= 2.445-01CM						0.	0.
1 8.851-01 .866 2.735+00 0						19.	40.
1 1.034+00 .853 3.146+00 0						18.	40.
1 1.036+00 .915 2.073+00 0						19.	39.
3 9.997-01 .979 6.402-01 0						23.	31.
11CM, DY= -1.704-01CM, DZ= 2.952-01CM						0.	0.
11CM, DY= -2.036-01CM, DZ= 2.734-01CM						0.	0.
1 1.070+00 .845 3.256+00 0						17.	41.
1 1.161+00 .854 3.283+00 0						17.	41.
1 1.201+00 .904 1.915+00 0						17.	33.
2 1.170+00 .964 1.033+00 0						18.	30.
11CM, DY= -1.628-01CM, DZ= 3.381-01CM						0.	0.
11CM, DY= -1.957-01CM, DZ= 3.202-01CM						0.	0.
11CM, DY= -2.266-01CM, DZ= 2.992-01CM						0.	0.
1 1.192+00 .838 3.573+00 0						16.	42.
1 1.267+00 .853 3.504+00 0						15.	42.
1 1.291+00 .917 1.558+00 0						15.	28.
3 1.262+00 .975 7.156-01 0						17.	25.
11CM, DY= -1.770-01CM, DZ= 3.675-01CM						0.	0.
11CM, DY= -2.127-01CM, DZ= 3.481-01CM						0.	0.
11CM, DY= -2.463-01CM, DZ= 3.252-01CM						0.	0.
1 1.238+00 .855 3.265+00 0						14.	40.
1 1.263+00 .881 2.860+00 0						14.	37.
1 1.275+00 .914 1.672+00 0						14.	25.

THETA	PHI	SHAPE	FLUX-WATTS/SQ=CM	RAD-WATTS/SQ=CM=SR	AVG COMB OPT PATH	LRLOCK	SZERO	SMIN	
DEGREES		FACTOR	DELTA	SUM	LOS	AVG	TRANS	CM-ATH(STP)	
46.00	17.500	3.071-02	4.20-04	2.18-01	1.378+01	1.255+00	.964	8.393-01	
46.00	22.500	3.168-02	2.44-07	2.18-01	8.005-05	1.234+00	.997	5.776-02	
46.00	27.500	LINE OF SIGHT MISSED THE GAS. DX= 4.235-01CM; DY= -2.025-01CM; DZ= 3.890-01CM							0.
46.00	32.500	LINE OF SIGHT MISSED THE GAS. DX= 4.235-01CM; DY= -2.356-01CM; DZ= 3.698-01CM							0.
46.00	37.500	LINE OF SIGHT MISSED THE GAS. DX= 4.235-01CM; DY= -2.669-01CM; DZ= 3.479-01CM							0.
50.00	2.500	3.263-02	9.35-03	2.28-01	3.117+00	1.204+00	.874	2.784+00	
50.00	7.500	3.359-02	1.54-02	2.43-01	5.124+00	1.265+00	.858	2.991+00	
50.00	12.500	3.454-02	1.07-02	2.54-01	3.550+00	1.300+00	.892	1.956+00	
50.00	17.500	3.550-02	1.17-04	2.54-01	3.905-02	1.281+00	.972	6.988-01	
50.00	22.500	LINE OF SIGHT MISSED THE GAS. DX= 3.918-01CM; DY= -1.787-01CM; DZ= 4.314-01CM							0.
50.00	27.500	LINE OF SIGHT MISSED THE GAS. DX= 3.918-01CM; DY= -2.156-01CM; DZ= 4.142-01CM							0.
50.00	32.500	LINE OF SIGHT MISSED THE GAS. DX= 3.918-01CM; DY= -2.509-01CM; DZ= 3.938-01CM							0.
50.00	37.500	LINE OF SIGHT MISSED THE GAS. DX= 3.918-01CM; DY= -2.843-01CM; DZ= 3.705-01CM							0.
54.00	2.222	LOS BLOCKED BY BODY FLAP							3601
54.00	6.667	LOS BLOCKED BY BODY FLAP							3601
54.00	11.111	LOS BLOCKED BY BODY FLAP							3601
54.00	15.556	LOS BLOCKED BY BODY FLAP							3601
54.00	20.000	LOS BLOCKED BY BODY FLAP							3601
54.00	24.444	LOS BLOCKED BY BODY FLAP							3601
54.00	28.889	LINE OF SIGHT MISSED THE GAS. DX= 3.583-01CM; DY= -2.383-01CM; DZ= 4.318-01CM							0.
54.00	33.333	LINE OF SIGHT MISSED THE GAS. DX= 3.583-01CM; DY= -2.710-01CM; DZ= 4.120-01CM							0.
54.00	37.778	LINE OF SIGHT MISSED THE GAS. DX= 3.583-01CM; DY= -3.021-01CM; DZ= 3.898-01CM							0.
58.00	2.222	LOS BLOCKED BY BODY FLAP							3601
58.00	6.667	LOS BLOCKED BY BODY FLAP							3601
58.00	11.111	LOS BLOCKED BY BODY FLAP							3601
58.00	15.556	LOS BLOCKED BY BODY FLAP							3601
58.00	20.000	LOS BLOCKED BY BODY FLAP							3601
58.00	24.444	LOS BLOCKED BY BODY FLAP							3601
58.00	28.889	LINE OF SIGHT MISSED THE GAS. DX= 3.230-01CM; DY= -2.498-01CM; DZ= 4.526-01CM							0.
58.00	33.333	LINE OF SIGHT MISSED THE GAS. DX= 3.230-01CM; DY= -2.841-01CM; DZ= 4.319-01CM							0.
58.00	37.778	LINE OF SIGHT MISSED THE GAS. DX= 3.230-01CM; DY= -3.167-01CM; DZ= 4.086-01CM							0.
62.00	2.222	LOS BLOCKED BY BODY FLAP							3601
62.00	6.667	LOS BLOCKED BY BODY FLAP							3601
62.00	11.111	LOS BLOCKED BY BODY FLAP							3601
62.00	15.556	LOS BLOCKED BY BODY FLAP							3601
62.00	20.000	LOS BLOCKED BY BODY FLAP							3601
62.00	24.444	LOS BLOCKED BY BODY FLAP							3601
62.00	28.889	LOS BLOCKED BY BODY FLAP							3601
62.00	33.333	LINE OF SIGHT MISSED THE GAS. DX= 2.862-01CM; DY= -2.958-01CM; DZ= 4.497-01CM							0.
62.00	37.778	LINE OF SIGHT MISSED THE GAS. DX= 2.862-01CM; DY= -3.297-01CM; DZ= 4.254-01CM							0.
66.00	2.000	LOS BLOCKED BY BODY FLAP							3601
66.00	6.000	LOS BLOCKED BY BODY FLAP							3601
66.00	10.000	LOS BLOCKED BY BODY FLAP							3601
66.00	14.000	LOS BLOCKED BY BODY FLAP							3601
66.00	18.000	LOS BLOCKED BY BODY FLAP							3601
66.00	22.000	LOS BLOCKED BY BODY FLAP							3601
66.00	26.000	LOS BLOCKED BY BODY FLAP							3601
66.00	30.000	LOS BLOCKED BY BODY FLAP							3601
66.00	34.000	LINE OF SIGHT MISSED THE GAS. DX= 2.479-01CM; DY= -3.114-01CM; DZ= 4.617-01CM							0.
66.00	38.000	LINE OF SIGHT MISSED THE GAS. DX= 2.479-01CM; DY= -3.429-01CM; DZ= 4.388-01CM							0.

A49

RTR 014-9

THETA DEGREES	PHI	SHAPE FACTOR	FLUX=WATTS/SQ-CM DELTA	SUM	RAD=WATTS/SQ-CM-SR LOS	AVG	COMB OPT PATH CM-ATM(STP)	LPLOCK	SZERO	SMIN
70.00	2.000	LOS BLOCKED BY ORBITER LOWER FUSELAGE						1200	0.	0.
70.00	6.000	LOS BLOCKED BY ORBITER LOWER FUSELAGE						1200	0.	0.
70.00	10.000	LOS BLOCKED BY ORBITER LOWER FUSELAGE						1200	0.	0.
70.00	14.000	LOS BLOCKED BY ORBITER LOWER FUSELAGE						1200	0.	0.
70.00	18.000	LOS BLOCKED BY BODY FLAP						3601	0.	0.
70.00	22.000	LOS BLOCKED BY BODY FLAP						3601	0.	0.
70.00	26.000	LOS BLOCKED BY BODY FLAP						3601	0.	0.
70.00	30.000	LOS BLOCKED BY BODY FLAP						3601	0.	0.
70.00	34.000	LINE OF SIGHT MISSED THE GAS: DX= 2.085-01CM, DY= -3.203-01CM, DZ= 4.749-01CM							0.	0.
70.00	38.000	LINE OF SIGHT MISSED THE GAS: DX= 2.085-01CM, DY= -3.527-01CM, DZ= 4.514-01CM							0.	0.

NUMERICAL PLUME SHAPE FACTOR= .03550 PLUME RADIANCE = 2.2771+00 WATTS/SQ-CM-STER
 NUMERICAL TOTAL SHAPE FACTOR= .09843 OVERALL RADIANCE= 8.2119-01 WATTS/SQ-CM-STER
 EXACT TOTAL SHAPE FACTOR = .10052 TOTAL FLUX = 2.5393-01 WATTS/SQ-CM

CALCULATION TIME 11 SECONDS

ADZ

```

1. @ASG,TJ GASRAD,U9S,17020
2. @REWIND GASRAD
3. @FREE TPF$:
4. @ASG,T TPF$,F/1/POS/5
5. @ASG,T 3,F///2500
6. @ASG,T 4,F///2500
7. @ASG,T 8,F///500
8. @ASG,T 10.,F///2500
9. @COPIE GASRAD
10. @FREE GASRAD
11. @XQT GASRAD
12. SAMPLE PROBLEM 2. ANALYSIS OF BAND MODEL PARAMETERS ON A SINGLE LOS.
13. -1 12 5 12 11 0 1 0 0 0 0
14. 40. 50. 10.
15. 170. 190. 20.
16. 2000. 4000. 25.
17. 0. 600. 3. 50.
18. H2O1(G) C102(G) C101(G) N2(G) O2(G)
19. @ADD TITAN
20. 0 63. 0. 0. 0. 0.
21. 0 31.5 0. 0. 0. 0.
22. 0 -31.5 0. 0. 0. 0.
23. -1
24. -1
25. 110 120 131 141 151 132 142 152 133 143 153
26. @ADD H2OCMB } H2O, CO2, and CO BAND MODEL PARAMETER
27. @ADD CO2CMB } CARD IMAGE DATA ELEMENTS FROM INPUT TAPE
28. @ADD COGDC }
29.
30. } 3 BLANK CARDS FOR BAND MODEL INPUT
31. }
32. ← ONE BLANK CARD TO TERMINATE RUN
33. @XQT PLOT ← EXECUTE PLOT PROGRAM
34. @FIN

```

SAME AS SAMPLE PROBLEM 1

3 BLANK CARDS FOR BAND MODEL INPUT

ONE BLANK CARD TO TERMINATE RUN

EXECUTE PLOT PROGRAM

LBM (TITAN FIRST STAGE) 20K LEVEL PLUME (8/30/79).

BETA H2O/CO2/N2/O2

ISYMSC= 0

HANG=

.00

CTCD=

.00

AP=

ICASE=

1

5.000+01

BP=

3.000-01

NOCON= 5 H2O1(G)

C101(G)

C102(G)

N2(G)

O2(G)

.00	1			
5.00	1	30	1	
10.00	1	30	1	
15.00	1	30	1	
20.00	1	30	1	
25.00	1	30	1	
30.00	1	30	1	
35.00	1	30	1	
40.00	1	30	1	
45.00	1	30	1	
50.00	1	30	1	
55.00	1	30	1	
60.00	1	30	1	
70.00	1	30	1	
80.00	1	30	15	
90.00	1	30	13	
100.00	1	30	14	
110.00	1	30	12	
120.00	1	30	10	
130.00	1	30	5	
130.10	1	30	2	
140.00	1	30	3	
150.00	1	30	1	
160.00	1	30	10	
170.00	1	29	13	
180.00	1	30	17	
	.00	26	1	

PARTIAL ECHO PRINT OF FLOWFIELD INPUT
IN SUBROUTINE FFPREP

ORIGINAL PAGE #
OF FOUR QUALITY

SAMPLE PROBLEM 2

A53

RTR 014-9

190.00	1		
	.00	29	1
200.00	1		
	.00	29	1
220.00	1		
	.00	30	1
240.00	1		
	.00	30	1
260.00	1		
	.00	30	1
280.00	1		
	.00	30	14
300.00	1		
	.00	30	12
320.00	1		
	.00	30	11
340.00	1		
	.00	30	3
340.10	1		
	.00	30	3
343.75	1		
	.00	30	4
360.00	1		
	.00	30	8
380.00	1		
	.00	27	1
398.30	1		
	.00	26	1
420.00	1		
	.00	22	1
440.00	1		
	.00	23	1
460.00	1		
	.00	24	1
482.00	1		
	.00	21	1
502.80	1		
	.00	21	1
520.70	1		
	.00	21	1
541.60	1		
	.00	22	1
562.50	1		
	.00	22	1
580.30	1		
	.00	22	1
600.50	1		
	.00	21	1
621.40	1		
	.00	21	1
641.70	1		
	.00	20	1
662.40	1		
	.00	20	1
682.60	1		
	.00	21	1

AS4

RTR 014-9

700.50

.00

1
-00
0

21

1

A55

RTR 014-9

SAMPLE PROBLEM 2

2 AXISYMMETRIC PLUMES USING CASE 1 WITH EXIT CTRLINE LOCATIONS AND DIRECTIONS INDICATED RUN DATE 050180

RADIATION PROBLEM IDENTIFICATION - SAMPLE PROBLEM 2. ANALYSIS OF BAND MODEL PARAMETERS ON A SINGLE LOS.

FLOW FIELD IDENTIFICATION - - - - LBM (TITAN FIRST STAGE) 20K LEVEL PLUME (8/30/79).

GAS IDENTIFICATION = H2O/CO/CO2/N2/O2

ENG. NO.	LOCATION OF EXIT CENTER			DIRECTION COSINES OF AXIS		
	X	Y	Z	X	Y	Z
1	31.50	.00	.00	.00000	.00000	1.00000
2	-31.50	.00	.00	.00000	.00000	1.00000

FLOW FIELD CONICAL LIMITS - INTERCEPT= 5.000+01 SLOPE= 3.000-01

ENGLISH UNITS - LENGTH IN INCHES - TEMPERATURE IN DEGREES RANKINE - PRESSURE IN PSFA

LIMITS OF INTEGRATION	VARIABLES	INITIAL VALUE	FINAL VALUE	INCREMENT
	Z-INDEX	1	LAST	
	THETA	40.00	50.00	10.0000
	PHI	170.00	190.00	20.0000
	NU	2000.	4000.	25.
	S	.00	600.00	3.0000
	TEMP STEP SIZE			50.0000

SET TO GIVE A SINGLE LINE-OF-SIGHT AT 45,180

POINT LOCATION	X	Y	Z
	63.00	.00	.00
COSINES OF U	1.00000	.00000	.00000
V	.00000	1.00000	.00000
W	.00000	.00000	1.00000

CONSTITUENTS H2O1(G) C102(G) C101(G) N2(G) O2(G) ← NO PARTICULAR ORDER REQUIRED

COORDINATE DATA INPUT FOR THE POINT OF INTEREST AND PLUMES

	ICS NO.	X	Y	Z	CHI	PSI	OMEGA
POINT OF INTEREST	0	63.00	.00	.00	.00	.00	.00
PLUME NO. 1	0	31.50	.00	.00	.00	.00	.00
PLUME NO. 2	0	-31.50	.00	.00	.00	.00	.00

NO FLOW FIELD SCALE FACTORS WERE USED.

F2	F3	F4	F5	F6
0001	.0000	.7898	.2099	
0620	.0640	.3430	.0000	
0001	.0000	.7895	.2097	
0640	.0630	.3450	.0000	
0003	.0000	.7890	.2094	
0650	.0620	.3450	.0000	
0000	.0000	.7900	.2100	
0660	.0610	.3460	.0000	
0000	.0000	.7900	.2100	
0700	.0580	.3490	.0000	
0000	.0000	.7900	.2100	
0740	.0540	.3520	.0000	
0000	.0000	.7900	.2100	
0750	.0530	.3530	.0000	
0001	.0000	.7898	.2099	
0750	.0530	.3530	.0000	
0001	.0000	.7898	.2097	
0760	.0520	.3540	.0000	
0000	.0000	.7900	.2100	
0790	.0500	.3550	.0000	
0000	.0000	.7900	.2100	
0820	.0480	.3470	.0000	
0000	.0000	.7900	.2100	
0870	.0440	.3590	.0000	
0000	.0000	.7899	.2099	
0870	.0440	.3590	.0000	
0001	.0000	.7897	.2098	
0570	.0670	.3390	.0000	
0001	.0000	.7897	.2098	
0580	.0670	.3390	.0000	
0001	.0000	.7897	.2098	
0580	.0670	.3390	.0000	
0000	.0000	.7900	.2100	
0580	.0670	.3390	.0000	
0000	.0000	.7900	.2100	
0600	.0650	.3400	.0000	
0000	.0000	.7900	.2100	
0600	.0650	.3400	.0000	
0000	.0000	.7900	.2100	
0600	.0650	.3400	.0000	

F2	F3	F4	F5	F6
.0000	.0000	.7899	.2100	
.0610	.0640	.3410	.0000	
.0000	.0000	.7899	.2099	
.0955	.0356	.3597	.0000	
.0001	.0000	.7898	.2099	
.0955	.0356	.3598	.0000	
.0001	.0000	.7896	.2098	
.0955	.0356	.3598	.0000	
.0002	.0000	.7894	.2096	
.0955	.0355	.3601	.0000	
.0000	.0000	.7900	.2100	
.0956	.0351	.3616	.0001	
.0000	.0000	.7900	.2100	
.0959	.0338	.3656	.0002	
.0000	.0000	.7900	.2100	
.0964	.0306	.3762	.0010	
.0000	.0000	.7900	.2100	
.0961	.0226	.4084	.0066	
.0000	.0000	.7900	.2100	
.0950	.0190	.4259	.0111	
.0000	.0000	.7899	.2100	
.0932	.0158	.4440	.0169	
.0000	.0000	.7899	.2100	
.0909	.0132	.4611	.0231	
.0000	.0000	.7899	.2099	
.0896	.0118	.4705	.0267	
.0001	.0000	.7898	.2099	

RANGE OF COEFFICIENT TABLES

E 5.00000 SECONDS

64	65	66
.05	.05	.01

00.
38-02
74-02
10-02
36-03
44-03
97-03
15-03
23-03
40-03
22-03

500. 3000.

287-02 2.748-02
152-02 2.803-02
129-02 2.730-02
109-02 2.639-02
276-02 2.475-02
145-02 2.411-02
759-02 2.193-02
106-02 2.020-02
512-02 1.893-02
591-02 1.829-02
559-02 1.911-02
591-02 1.938-02
581-02 1.820-02
107-02 1.365-02
343-02 1.028-02
168-02 9.828-03
256-02 9.919-03
223-02 1.110-02
387-02 1.238-02
583-02 1.401-02
824-02 1.611-02
097-02 1.793-02
206-02 1.902-02
206-02 1.884-02
097-02 1.729-02
835-02 1.465-02

500. 3000.

810+00 2.440+01
130+00 2.330+01
010+01 2.610+01
150+01 2.810+01
240+01 3.480+01
100+01 3.580+01
680+01 6.540+01
440+01 8.980+01
900+01 1.170+02
090+01 1.250+02
300+01 1.330+02
540+01 1.410+02
790+01 1.510+02
080+01 1.610+02

0. 3000.
0*01 1.710+02
0*01 1.820+02
0*01 1.940+02
0*01 2.070+02
0*01 2.210+02
0*01 2.350+02
0*01 2.510+02
0*01 2.670+02
0*01 2.840+02
0*01 2.600+02
0*01 2.370+02
0*01 2.170+02
0*01 1.980+02
0*01 1.810+02
0*01 1.650+02
0*01 1.510+02
0*01 1.370+02
0*01 1.250+02
0*01 1.150+02
0*01 1.050+02
0*01 9.600+01
0*01 8.760+01
0*01 8.000+01
0*01 7.300+01
0*01 6.670+01
0*01 6.090+01
0*01 5.560+01
0*01 5.080+01
0*01 4.640+01
0*01 4.240+01
0*01 3.870+01
0*01 3.530+01
0*01 3.230+01
0*01 2.950+01
0*01 2.690+01
0*01 2.460+01
0*01 2.660+01
1*00 2.290+01
1*00 1.730+01
1*00 1.700+01
1*00 1.370+01
1*00 1.360+01
1*00 1.240+01
1*00 1.070+01
1*00 9.580+00

000 3000
15-03 3.185-03
131-03 2.839-03
01-03 2.639-03
137-03 2.502-03
63-03 2.430-03
132-03 2.357-03
88-03 2.293-03
181-03 2.284-03
84-03 2.266-03
198-03 2.248-03
113-03 2.257-03
104-03 2.266-03
60-03 2.284-03
138-03 2.302-03
60-03 2.348-03
155-03 2.393-03
111-03 2.457-03
228-03 2.548-03
123-03 2.684-03
306-03 2.894-03
221-03 3.121-03
342-03 3.440-03
764-03 3.795-03
373-03 4.177-03
707-03 4.550-03
925-03 5.005-03
788-03 5.478-03
853-03 6.051-03
869-03 6.688-03
273-03 7.289-03
539-03 8.053-03
708-03 8.827-03
190-02 9.646-03
190-02 1.065-02
452-02 1.174-02
551-02 1.292-02
835-02 1.410-02
933-02 1.547-02
020-02 1.702-02
250-02 1.838-02
490-02 2.002-02
774-02 2.193-02
872-02 2.384-02
090-02 2.548-02
221-02 2.666-02

10. 3000.
10+00 1.010+01
50+00 1.030+01
70+00 1.320+01
70+00 1.590+01
70+00 1.850+01
70+00 1.400+01
70+00 9.410+00
70+00 1.000+01
70+00 8.770+00
70+00 1.290+01
70+01 4.470+01
70+00 2.010+01
70+00 1.580+01
70+01 2.450+01
70+00 1.360+01
70+00 1.260+01
70+00 1.160+01
70+00 8.890+00
70+00 9.300+00
70+00 1.080+01
70+00 9.940+00
70+00 1.160+01

10. 3000.
19-02 6.626-02
16-02 9.765-02
18-02 1.529-01
17-01 2.324-01
18-01 3.336-01
11-01 4.707-01
14-01 6.430-01
11-01 7.964-01
12+00 9.772-01
18+00 1.089+00
12+00 1.212+00
14+00 1.127+00
13+00 1.089+00
19+00 8.634-01
19+00 6.591-01
14-01 2.486-01
19-01 3.213-02
10 0.000

RTR 014-9

400.	3000.
.000	0.000
.000	0.000
.000	0.000
.000	0.000
.000	0.000
.000	0.000
.000	0.000
.000	0.000
.234+02	6.234+02
.234+02	6.234+02
.234+02	6.234+02
.234+02	6.234+02
.117+02	1.344+03
.350+03	2.239+03
.312+03	2.129+03
.119+03	1.580+03
.321+03	2.118+03
.470+03	2.408+03
.706+03	2.800+03
.140+03	3.545+03
.122+03	5.244+03
.213+03	8.924+03
.730+03	9.753+03
.579+03	8.863+03
.161+03	8.624+03
.245+03	5.226+03
.252+03	2.011+03
.571+02	8.472+02
.121+02	4.564+02
.116+02	2.998+02
.642+02	2.367+02
.094+02	3.230+02
.757+02	1.122+03
.530+03	2.595+03
.419+03	4.118+03
.263+03	3.942+03
.318+03	2.188+03
.939+02	1.275+03
.077+02	3.123+02
.606+01	5.372+01

C101(G) WAVE NO. (1/CM)	ABSORPTION COEFFICIENTS TEMPERATURES (DEG K)						
	300.	600.	1200.	1800.	2400.	3000.	5000.
2000.	6.077-04	2.445-02	8.392-02	8.912-02	7.476-02	5.896-02	2.793-02
2025.	8.000-03	1.000-02	5.000-02	1.188-01	8.643-02	6.259-02	2.749-02
2050.	9.801-02	2.645-01	2.209-01	1.407-01	9.026-02	6.102-02	2.589-02
2075.	1.000-01	5.000-01	2.400-01	1.427-01	8.294-02	5.419-02	2.486-02
2100.	1.871+00	8.408-01	2.621-01	1.197-01	6.617-02	4.528-02	2.542-02
2125.	2.198+00	5.000-01	1.587-01	7.665-02	5.228-02	4.225-02	2.850-02
2150.	1.099+00	2.866-01	1.112-01	8.114-02	6.624-02	5.617-02	3.569-02
2175.	3.261+00	1.103+00	3.372-01	1.788-01	1.185-01	8.767-02	4.457-02
2200.	1.340+00	1.001+00	4.204-01	2.286-01	1.476-01	1.057-01	5.005-02
2225.	1.270-01	3.963-01	3.251-01	2.093-01	1.432-01	1.045-01	4.924-02
2250.	2.128-03	6.365-02	1.567-01	1.388-01	1.086-01	8.478-02	4.299-02
2275.	3.451-06	3.156-03	4.209-02	6.256-02	6.162-02	5.445-02	3.220-02
2300.	1.623-10	2.708-05	4.832-03	1.636-02	2.347-02	2.544-02	1.936-02
2325.	0.000	9.423-09	1.202-04	1.656-03	4.563-03	6.939-03	9.364-03
2350.	0.000	0.000	1.725-08	7.456-06	1.153-04	4.958-04	2.958-03

NOTE THAT FINE STRUCTURE PARAMETERS (1/d)
WERE NOT INPUT FOR CO. THIS IS THE ONLY
CONSTITUENT FOR WHICH THIS CAN OCCUR WITH
THE PRESENT CODING.

A67

RTR 014-9

THETA	PHI	SHAPE	FLUX-WATTS/SQ-CM	RAD-WATTS/SQ-CM-SR	AVG	COMB OPT PATH	LBLOCK	SZERO	SMIN
DEGREES		FACTOR	DELTA SUM	LOS AVG	TRANS	CM-ATM(STP)			
45.00	180.000	9.696-03	5.86-02 5.86-02	1.922+00 1.922+00	.514	1.601+01	0	0.	294.

NUMERICAL PLUME SHAPE FACTOR=	.00970	PLUME RADIANCE =	1.9223+00 WATTS/SQ-CM-STER
NUMERICAL TOTAL SHAPE FACTOR=	.00970	OVERALL RADIANCE=	1.9223+00 WATTS/SQ-CM-STER
EXACT TOTAL SHAPE FACTOR =	.00965	TOTAL FLUX =	5.8557-02 WATTS/SQ-CM

CALCULATION TIME 4 SECONDS

AF

RTR 014-9

XC/X* XD/X* AVE FINE STRUCTURE
PARAMETERS
AC AD

.353	.047	4.772-02	1.380-02
1.000	.999	9.131+00	3.341+00
.231	.044	6.996-03	4.423-03
.386	.057	4.703-02	1.299-02
.999	1.000	7.184+00	2.780+00
.226	.042	7.243-03	4.548-03
.437	.075	5.085-02	1.419-02
.996	.999	6.895+00	2.743+00
.166	.024	6.791-03	4.447-03
.506	.104	5.790-02	1.635-02
.995	.999	7.006+00	2.796+00
.161	.023	6.760-03	4.464-03
.534	.119	5.465-02	1.562-02
.994	.999	6.948+00	2.795+00
.161	.023	6.653-03	4.396-03
.555	.132	5.308-02	1.539-02
.987	.995	6.784+00	2.767+00
.202	.036	6.678-03	4.418-03
.689	.237	7.968-02	2.348-02
.967	.965	6.199+00	2.599+00
.220	.042	6.843-03	4.591-03
.690	.238	6.303-02	1.870-02
.920	.834	5.392+00	2.329+00
.138	.018	6.714-03	4.563-03
.743	.304	7.565-02	2.270-02
.828	.571	4.511+00	2.004+00
.124	.015	6.724-03	4.691-03
.788	.375	8.311-02	2.512-02
.669	.303	3.209+00	1.457+00
.137	.019	6.796-03	4.828-03
.847	.498	9.261-02	2.805-02
.495	.150	2.152+00	9.952-01
.181	.031	6.926-03	4.952-03
.867	.559	1.006-01	3.084-02
.380	.088	1.608+00	7.575-01
.288	.073	7.114-03	5.073-03

LONG FORM OF
SPECTRAL OUTPUT

RTR 014-9

WAVE NUMBER 1/CM	WAVE LENGTH MICRON	IRRADIANCE WATTS/ CM -STER	G	OPTICAL DEPTH	CONSTITUENT IDENTIFICA- TION	X*	X/X*	XC/X*	XD/X*	AVE FINE STRUCTURE PARAMETERS AC	AD
2300.	4.348	1.140-03	.0000	1.462+01							
				1.001-01	H201(G)	1.116-01	.898	.893	.646	1.183-01	3.402-02
				1.448+01	C102(G)	4.728+01	.306	.302	.056	1.188+00	5.614-01
				3.975-02	C101(G)	7.048-02	.564	.542	.256	7.329-03	5.196-03
2325.	4.301	8.912-04	.0000	1.182+01							
				8.453-02	H201(G)	9.180-02	.921	.917	.738	1.213-01	3.772-02
				1.173+01	C102(G)	5.430+01	.216	.214	.030	6.530-01	3.096-01
				6.021-03	C101(G)	6.461-03	.932	.907	.899	7.507-03	5.309-03
2350.	4.255	9.333-04	.0002	8.317+00							
				7.173-02	H201(G)	7.638-02	.939	.935	.815	1.335-01	4.180-02
				8.246+00	C102(G)	5.512+01	.150	.149	.015	3.125-01	1.455-01
				2.975-05	C101(G)	2.975-05	1.000	1.000	1.000	7.720-03	5.453-03
2375.	4.211	1.208-03	.0349	3.356+00							
				5.801-02	H201(G)	6.068-02	.956	.952	.886	1.470-01	4.627-02
				3.298+00	C102(G)	3.910+01	.084	.084	.005	6.982-02	3.128-02
2400.	4.167	7.948-04	.5900	5.276-01							
				5.237-02	H201(G)	5.430-02	.964	.960	.918	1.606-01	5.099-02
				4.752-01	C102(G)	4.866+00	.098	.097	.007	1.166-02	5.741-03
2425.	4.124	9.797-05	.9575	4.342-02							
				4.342-02	H201(G)	4.458-02	.974	.969	.951	1.740-01	5.578-02
2450.	4.082	8.496-05	.9637	3.696-02							
				3.696-02	H201(G)	3.766-02	.982	.976	.970	1.924-01	6.193-02
2475.	4.040	7.326-05	.9691	3.142-02							
				3.142-02	H201(G)	3.183-02	.987	.982	.982	2.100-01	6.821-02
2500.	4.000	6.740-05	.9715	2.896-02							
				2.896-02	H201(G)	2.926-02	.990	.984	.987	2.253-01	7.433-02
2525.	3.960	6.647-05	.9719	2.853-02							
				2.853-02	H201(G)	2.878-02	.992	.986	.989	2.446-01	8.153-02
2550.	3.922	6.644-05	.9720	2.837-02							
				2.837-02	H201(G)	2.858-02	.993	.987	.991	2.655-01	8.940-02
2575.	3.883	6.779-05	.9716	2.877-02							
				2.877-02	H201(G)	2.900-02	.992	.986	.990	2.535-01	8.615-02
2600.	3.846	6.931-05	.9711	2.931-02							
				2.931-02	H201(G)	2.956-02	.991	.985	.989	2.432-01	8.336-02
2625.	3.810	7.782-05	.9678	3.268-02							
				3.268-02	H201(G)	3.304-02	.989	.983	.986	2.356-01	8.116-02
2650.	3.774	8.203-05	.9662	3.443-02							
				3.443-02	H201(G)	3.487-02	.987	.981	.983	2.220-01	7.751-02
2675.	3.738	9.916-05	.9591	4.174-02							
				4.174-02	H201(G)	4.250-02	.982	.976	.974	2.120-01	7.476-02
2700.	3.704	1.184-04	.9508	5.044-02							
				5.044-02	H201(G)	5.172-02	.975	.969	.959	1.999-01	7.147-02
2725.	3.670	1.484-04	.9381	6.386-02							
				6.386-02	H201(G)	6.620-02	.965	.959	.930	1.881-01	6.822-02
2750.	3.636	1.695-04	.9298	7.284-02							
				7.284-02	H201(G)	7.612-02	.957	.951	.907	1.803-01	6.590-02
2775.	3.604	1.878-04	.9220	8.120-02							
				8.120-02	H201(G)	8.561-02	.949	.943	.880	1.710-01	6.315-02

A71

WAVE NUMBER 1/CM	WAVE LENGTH MICRON	IRRADIANCE WATTS/ CM -STER	G	OPTICAL DEPTH	CONSTITUENT IDENTIFICA- TION	X*	X/X*	XC/X*	XD/X*	AVE FINE STRUCTURE PARAMETERS	
										AC	AD
2800.	3.571	2.279-04	.9048	1.000-01							
				1.000-01	H201(G)	1.073-01	.932	.926	.823	1.617-01	6.052-02
2825.	3.540	2.495-04	.8963	1.094-01							
				1.094-01	H201(G)	1.187-01	.922	.916	.788	1.545-01	5.829-02
2850.	3.509	2.758-04	.8866	1.203-01							
				1.203-01	H201(G)	1.286-01	.936	.929	.843	2.036-01	7.907-02
2875.	3.478	3.188-04	.8682	1.413-01							
				1.413-01	H201(G)	1.535-01	.920	.913	.790	1.933-01	7.601-02
2900.	3.448	3.441-04	.8577	1.535-01							
				1.535-01	H201(G)	1.753-01	.876	.869	.639	1.349-01	5.232-02
2925.	3.419	3.666-04	.8477	1.652-01							
				1.652-01	H201(G)	1.921-01	.860	.852	.595	1.275-01	4.994-02
2950.	3.390	4.071-04	.8311	1.851-01							
				1.851-01	H201(G)	2.208-01	.838	.830	.539	1.221-01	4.817-02
2975.	3.361	4.369-04	.8178	2.011-01							
				2.011-01	H201(G)	2.461-01	.817	.808	.492	1.160-01	4.616-02
3000.	3.333	4.855-04	.7984	2.251-01							
				2.251-01	H201(G)	2.847-01	.791	.781	.439	1.115-01	4.463-02
3025.	3.306	5.180-04	.7849	2.422-01							
				2.422-01	H201(G)	3.152-01	.768	.758	.400	1.067-01	4.294-02
3050.	3.279	6.056-04	.7505	2.870-01							
				2.870-01	H201(G)	3.965-01	.724	.713	.333	1.027-01	4.172-02
3075.	3.252	5.992-04	.7531	2.835-01							
				2.835-01	H201(G)	3.958-01	.716	.706	.325	9.822-02	4.014-02
3100.	3.226	7.095-04	.7077	3.457-01							
				3.452-01	H201(G)	5.261-01	.656	.645	.256	9.393-02	3.873-02
				5.117-04	C102(G)	5.117-04	1.000	1.000	.971	2.884+00	1.693+00
3125.	3.200	7.867-04	.6746	3.936-01							
				3.921-01	H201(G)	6.461-01	.607	.597	.211	8.924-02	3.715-02
				1.516-03	C102(G)	1.516-03	1.000	1.000	.998	4.634+00	2.756+00
3150.	3.175	8.502-04	.6520	4.277-01							
				4.249-01	H201(G)	7.414-01	.573	.563	.185	8.614-02	3.616-02
				2.825-03	C102(G)	2.825-03	1.000	1.000	.995	4.494+00	2.708+00
3175.	3.150	9.019-04	.6288	4.640-01							
				4.618-01	H201(G)	8.665-01	.533	.524	.158	8.191-02	3.468-02
				2.187-03	C102(G)	2.187-03	1.000	1.000	.980	4.571+00	2.761+00
3200.	3.125	9.661-04	.6026	5.065-01							
				5.027-01	H201(G)	1.029+00	.489	.480	.132	7.717-02	3.303-02
				3.748-03	C102(G)	3.748-03	1.000	1.000	.991	4.844+00	2.942+00
3225.	3.101	1.105-03	.5340	6.274-01							
				6.215-01	H201(G)	1.193+00	.521	.512	.156	1.057-01	4.690-02
				5.839-03	C102(G)	5.839-03	1.000	1.000	.999	5.280+00	3.225+00
3250.	3.077	1.081-03	.5488	6.000-01							
				5.924-01	H201(G)	1.488+00	.398	.392	.088	6.755-02	2.974-02
				7.665-03	C102(G)	7.665-03	1.000	1.000	.998	6.194+00	3.781+00
3275.	3.053	1.162-03	.5115	6.704-01							
				6.557-01	H201(G)	1.820+00	.360	.355	.073	6.571-02	2.925-02
				1.474-02	C102(G)	1.474-02	1.000	1.000	.999	7.170+00	4.444+00

RTR 014-9

SAMPLE PROBLEM 2

(* XC/X* XD/X* AVE FINE STRUCTURE
PARAMETERS
AC AD

36	.331	.064	6.421-02	2.877-02
00	1.000	1.000	9.058+00	5.675+00
61	.355	.076	8.754-02	4.068-02
00	1.000	1.000	1.254+01	7.922+00
23	.319	.062	8.074-02	3.782-02
00	.999	1.000	1.420+01	9.131+00
14	.310	.059	8.481-02	4.014-02
00	.999	1.000	1.523+01	9.969+00
85	.281	.049	7.734-02	3.685-02
00	.999	1.000	1.447+01	9.540+00
75	.272	.047	7.908-02	3.798-02
00	.996	1.000	8.420+00	5.686+00
47	.245	.038	6.855-02	3.313-02
99	.990	.999	4.160+00	2.888+00
37	.235	.036	6.549-02	3.180-02
94	.977	.994	2.280+00	1.619+00
32	.230	.034	6.417-02	3.116-02
80	.956	.977	1.420+00	1.020+00
34	.232	.035	6.796-02	3.313-02
58	.932	.946	1.003+00	7.241-01
37	.235	.036	6.741-02	3.297-02
34	.908	.904	7.668-01	5.525-01
43	.240	.037	6.484-02	3.143-02
28	.902	.891	7.507-01	5.376-01
44	.242	.037	5.754-02	2.762-02
65	.939	.956	1.505+00	1.072+00
227	.225	.032	5.215-02	2.476-02
87	.966	.986	2.851+00	2.032+00
245	.243	.038	5.849-02	2.875-02
94	.976	.993	4.884+00	3.534+00
243	.241	.038	6.446-02	3.204-02
90	.968	.989	4.291+00	3.145+00

EACH SYMBOL REPRESENTS A RADIATION STEP OF .192231 WATTS/SQ-CM.
THE TA SCALE GOES TO 90.000 DEGREES

(0 DEG)

(270 DEG) *

* (90 DEG)

9 ← SINGLE LINE-OF-SIGHT

(180 DEG)

FINISH
NORMAL EXIT. CPU TIME: 24712 TOTAL SUPS: 57141 (MILLISECONDS)

AXOT PLOT

BEGINNING OF PLOT SECTION

} PLOT PROGRAM OUTPUT

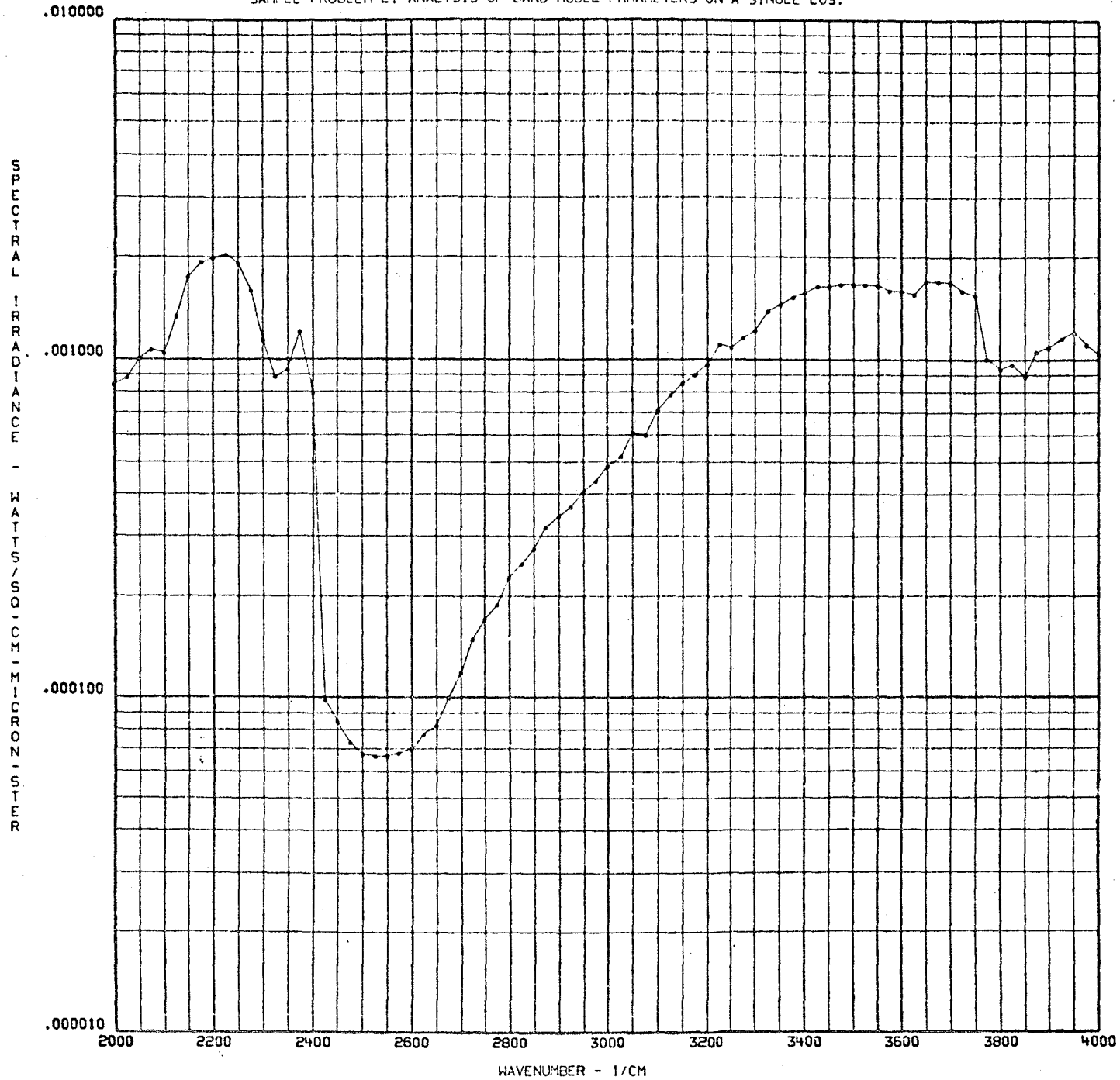
END OF PLOT SECTION. PLOT TIME 8.00000 SECONDS

A75 NORMAL EXIT. CPU TIME: 4715 TOTAL SUPS: 9780 (MILLISECONDS)

BFIN

RTR 014-9

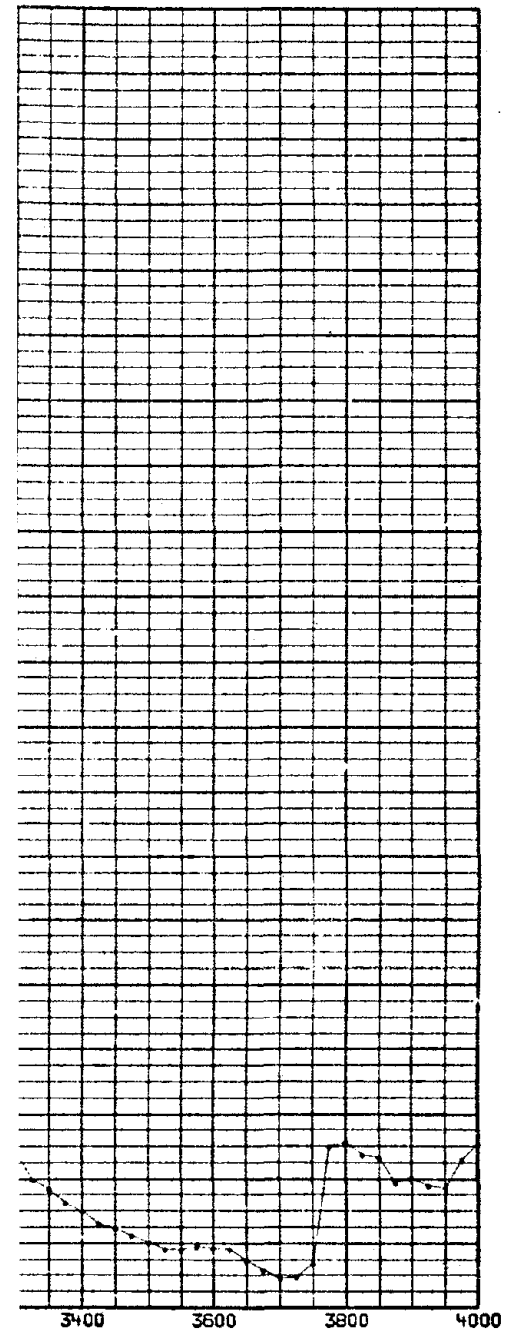
SAMPLE PROBLEM 2. ANALYSIS OF BAND MODEL PARAMETERS ON A SINGLE LOS.



A76

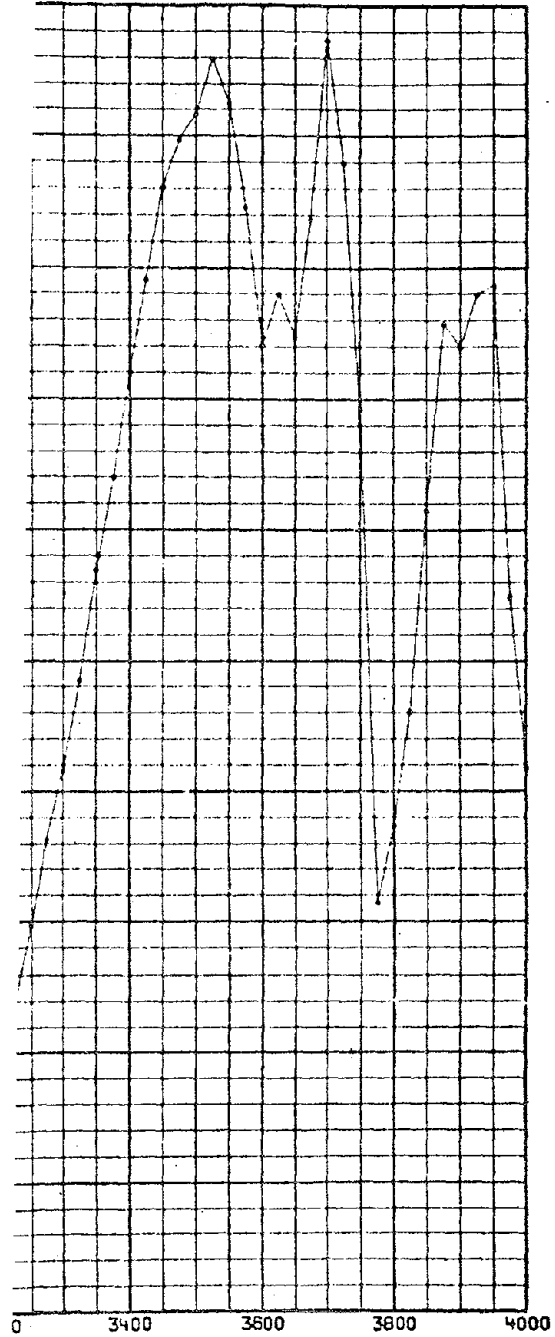
ORIGINAL PAGE IS
OF POOR QUALITY

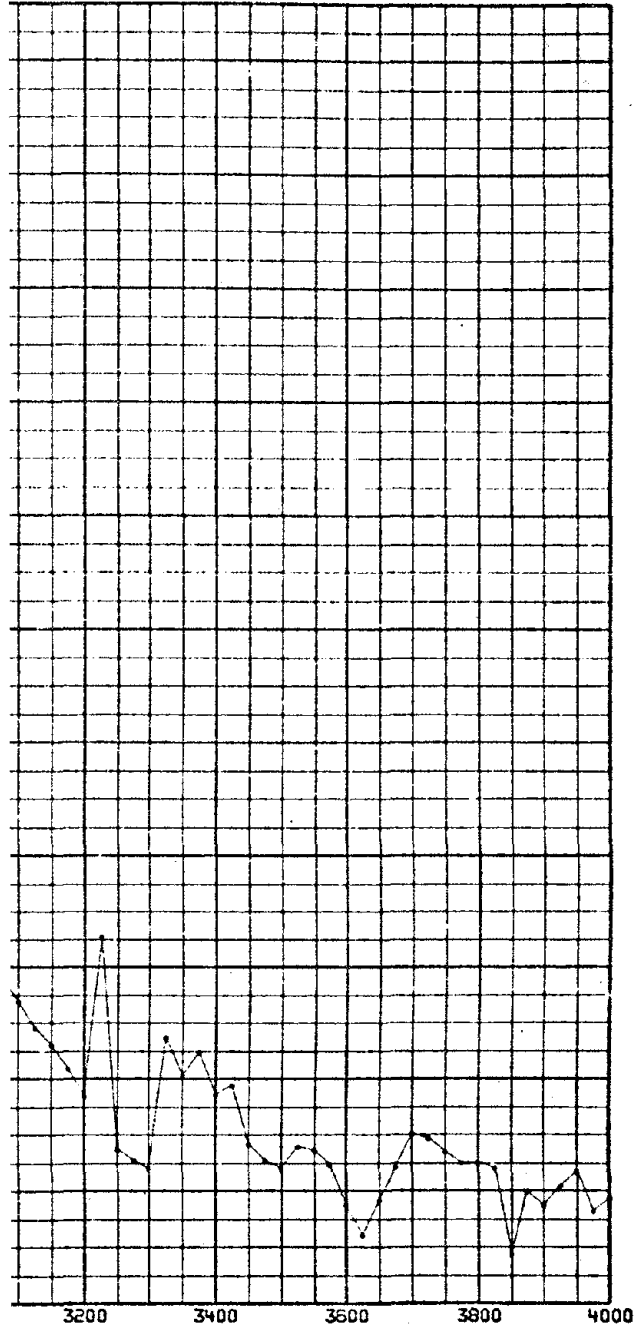
RTR 014-9



RTR 014-9

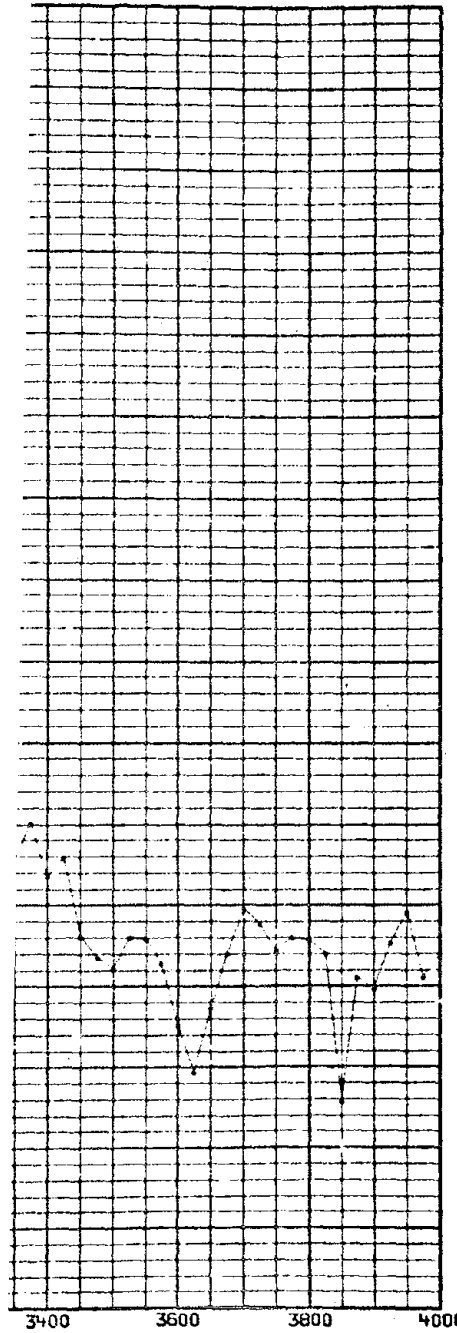
N A SINGLE LOS.



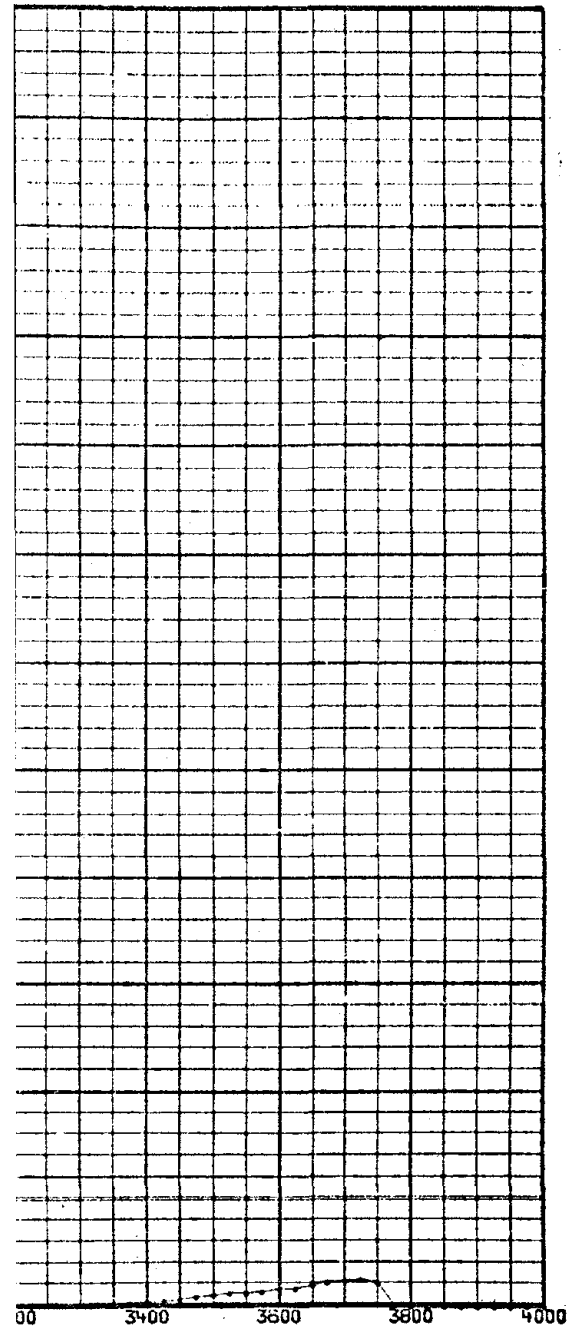


CH

FILE LOS.

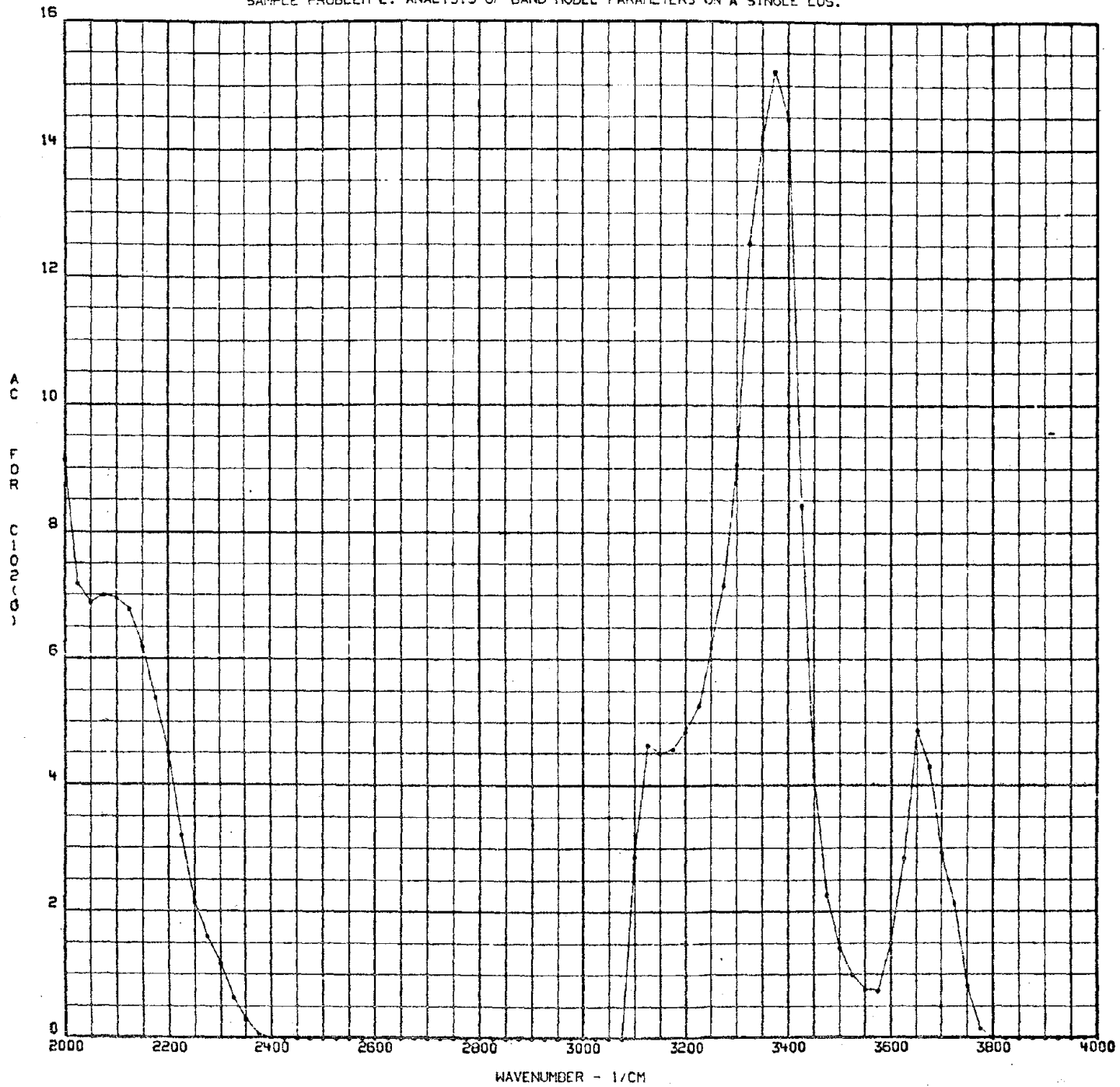


S ON A SINGLE LOS.

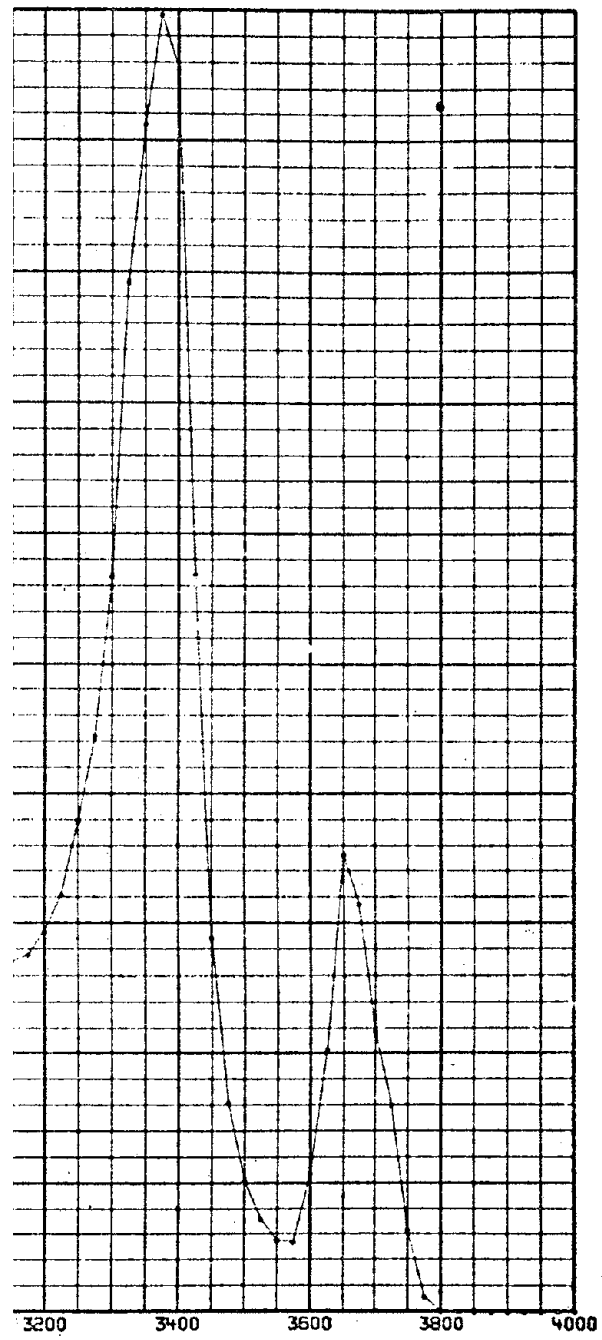


RTR 014-9

SAMPLE PROBLEM 2. ANALYSIS OF BAND MODEL PARAMETERS ON A SINGLE LOS.

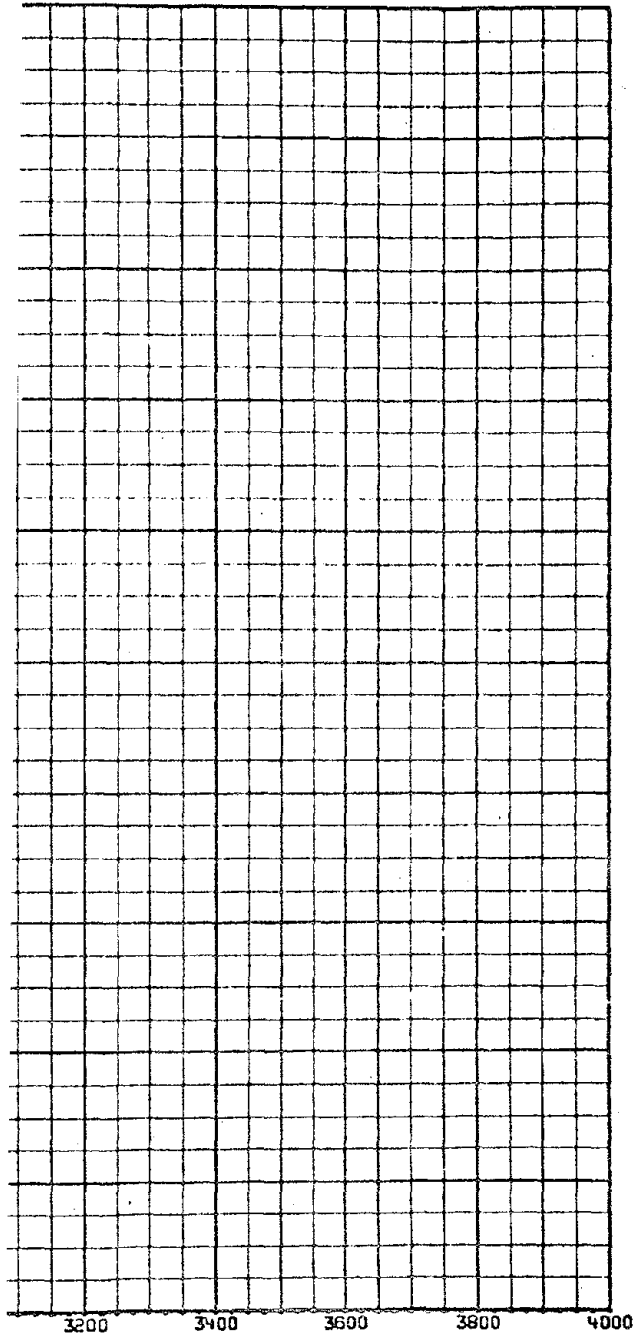


TERS ON A SINGLE LOS.



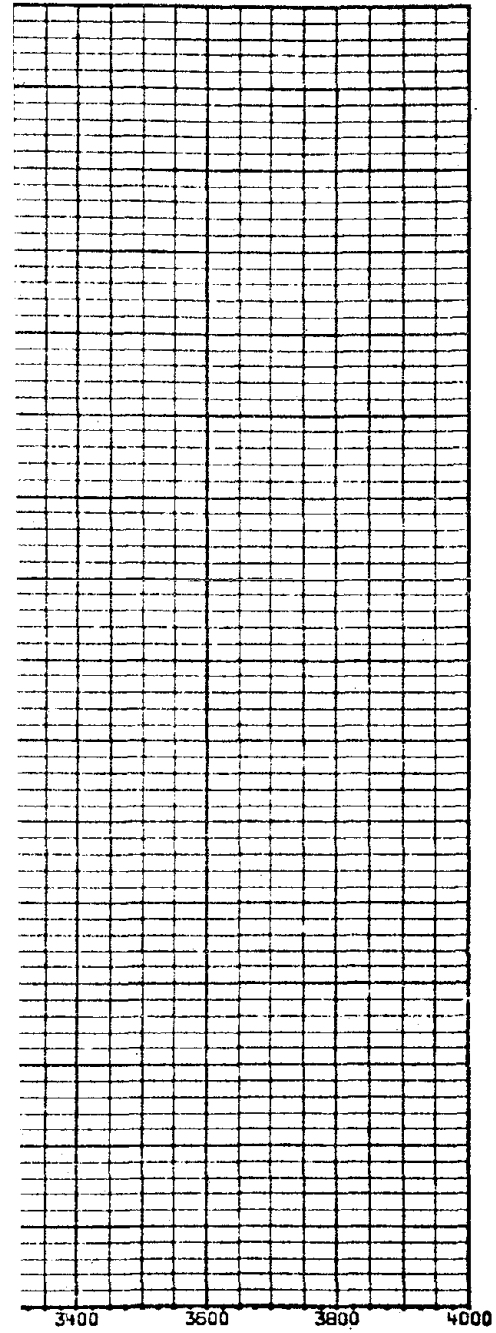
RTR 014-9

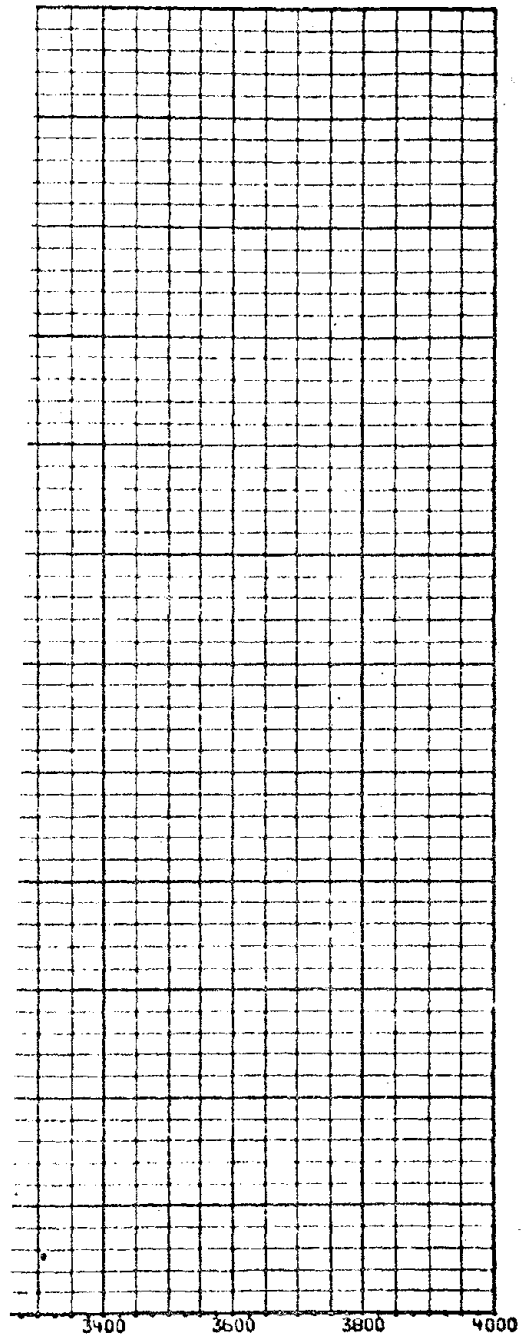
METERS ON A SINGLE LOS.



CM

RTR 014-9





A4 PROGRAM ELEMENTS

<u>SUBROUTINE OR FUNCTION NAME</u>	<u>DECK NAME</u>
ACDATA	ACDATA
BLOCKM	BLOCKM
BLOKIN	BLOKIN
FFPREP	FFPREP
FLOUT	FLOUT
FLOW	FLOW
FLOWAX	FLOWAX
FLOWIN	FLOWIN
FLOW3D	FLOW3D
MAIN	MAIN
NOGO	NOGO
PLANCK	PLANCK
PLUMPT	PLUMPT
RAD	RAD
SKIP	SKIP
SLG	SLGMLT
	YNGH20
SLIMIT	SLIMIT
SPCOUT	SPCOUT
VIEW	VIEW
YAPPRX	YAPPRX
YF	YF

SUBROUTINE NAME: ACDATA

DESCRIPTION

ACDATA reads the band model parameter input (absorption coefficients, \bar{k} , and line densities, $1/\bar{d}$). The data are scaled if specified by input and averaged over the spectral integration interval (DENU) if the spectral interval of the data (IDNU(I)) is smaller than the integration interval (IDNU(I) < DENU). The band model data to be used in the problem is printed in either a short form (initial and final values in each table) or long form (the complete table).

CALLING SEQUENCE

CALL ACDATA

COMMON BLOCKS AND EXTERNAL REFERENCES

COMMON/CONTROL/	COMMON/ABCOEF/
COMMON/CONID/	COMMON/RADSUB/
COMMON/FLOSCL/	EXP
COMMON/GOMTRY/	SQRT
COMMON/BLOCKO/	

METHOD OF SOLUTION

Band model parameters are read in the format specified for cards 17 through 19 (Appendix A1), and they are placed in the table COEF (J,K) where the J index represents temperature and the K index represents wavenumber. The wavenumber interval for each constituent is specified by the initial and final values (NUL(I) and NUU(I)) and the spacing between entries is IDNU(I). The

subroutine assigns the index (K) for the initial values of absorption coefficient (ICOEF(I)) and the line density (IFIN(I)) to enable later location of the parameters while maintaining a minimum size sequential table.

If scale factors are used (Card 2, ISCALA=1) the band model parameters are multiplied by the nonzero scale factors input on Card 15.

If the input spectral integration increment (DENU) is larger than the input interval in the band model parameter table (IDNU (I)), the parameters are averaged as indicated in Eqs. 19 and 20 (Section 3.3).

Note that there must be an integral number of IDNU(I) intervals in DENU.

Selection of the format for printed output is made based on NABS (Card 2).

SUBROUTINE NAME: BLOCKM

DESCRIPTION

BLOCKM tests a line-of-sight vector for intersection with specified blocking (or shading) surfaces. If intersections occur, the upper limit of the vector (corresponding to the upper limit of integration) is adjusted to correspond to the closest surface intersection.

CALLING SEQUENCE

CALL BLOCKM

COMMON BLOCKS AND EXTERNAL REFERENCES

COMMON/CONTRL/	COMMON/FLOWS/
COMMON/CONID/	COMMON/SLIMTC/
COMMON/FLOSCL/	NOGO
COMMON/GOMTRY/	SQRT
COMMON/BLOCKO/	COS
COMMON/BLOKOP/	

METHOD OF SOLUTION

The upper limit of each line-of-sight (LOS) is the value SMIN which is initially assigned equal to the input value SMAX. This initial value may be reduced in subroutine SLIMIT and BLOCKM.

The subroutine operates on surfaces in the order of input starting with surface sequence number IBLOCK and proceeding to NBLOCK. Surfaces with sequence

index below IBLOCK are either the point-of-interest (1) or the plumes (2 to 1+NEUG). The dimensionless vector length (DELTA) is computed for each surface using Eq. 39. The minimum value of DELTA is maintained in DCOMP. After all surfaces have been tested, the value of SMIN is redefined as

$$SMIN = DCOMP * SMIN$$

SUBROUTINE NAME: BLOKIN

DESCRIPTION

BLOKIN reads all surface geometry input and prepares the necessary transformation vectors and matrices for later use in other subroutines. The surface input includes the point-of-interest, plume origins and blocking surfaces. The sequence of the surfaces is defined as follows:

1	Point-of-interest
2 to 1+NENG	Plumes
IBLOCK to NBLOCK	Blocking surfaces

The parameter NENG is defined from the input for IFLOW (Card 2), and IBLOCK=2+NENG. The upper index, NBLOCK, is set by the program when surface input is terminated.

CALLING SEQUENCE

CALL BLOKIN

COMMON BLOCKS AND EXTERNAL REFERENCES

COMMON/CONTROL/	COMMON/SLIMTC/
COMMON/CONID/	COMMON/CHIPOF/
COMMON/FLOSCL/	ATAN
COMMON/GOMTRY/	SIN
COMMON/BLOCKO/	COS
COMMON/BLOKOP/	TAN
COMMON/FLOWS/	

METHOD OF SOLUTION

The transformation matrices $(T(J,K,I))$ and vector components $(R1(I), R2(I), R3(I))$ are computed for each surface as described in Section 4.1 (Eqs. 30 and 31). Values of conical parameters for the approximate plume boundaries are computed and surface coefficients A, B, C (Eq. 38) and CC (Eq. 39) are defined for the plumes and blocking surfaces.

SUBROUTINE NAME: FFPREP

DESCRIPTION

FFPREP prepares a binary file of flowfield gas properties on Unit 8 using either card input or binary input on Unit 11. The input can be scaled if desired to convert dimensional units or change flowfield scale. A limited amount of output is provided to assist in diagnostics if the program encounters an error.

CALLING SEQUENCE

CALL FFPREP

COMMON BLOCKS AND EXTERNAL REFERENCES

COMMON/CONTRL/	COMMON/BLOCKO/
COMMON/CONID/	COMMON/BLOKUP/
COMMON/FLOSCL/	COMMON/FLOWS/
COMMON/GOMTRY/	COMMON/SLIMTC/

METHOD OF SOLUTION

Gas property input is read, scaled if necessary and output to Unit 8.

SUBROUTINE NAME: FLOUT

DESCRIPTION

FLOUT reads the files on problem description from Unit 10 and prepares printed output of the problem description. Following the output, all dimensioned parameters are converted to metric units and radius.

CALLING SEQUENCE

CALL FLOUT

COMMON BLOCKS AND EXTERNAL REFERENCES

COMMON/CONTRL/	COMMON/FLOWS/
COMMON/CONID/	COMMON/SLIMTC/
COMMON/FLOSCL/	COMMON/CHIPOF/
COMMON/COMTRY/	SCLOCK
COMMON/BLOCKO/	SKIP
COMMON/BLOKOP/	COS

METHOD OR SOLUTION

Data on the problem description is read from Unit 10 and printed. If the case is being run from a Unit 10 generated on a previous run, tests are made to assure compatibility and diagnostics are generated if inconsistencies are noted.

SUBROUTINE NAME: FLOW

DESCRIPTION

FLOW controls sequencing of the set of overlay subroutines involved in generating line-of-sight property data on Unit 10.

CALLING SEQUENCE

CALL FLOW

COMMON BLOCKS AND EXTERNAL REFERENCES

COMMON/CONTRL/	COMMON/SLIMTC/
COMMON/CONID/	COMMON/CUIPOF/
COMMON/FLOSCL/	FLOWIN
COMMON/GOMTRY/	FLOUT
COMMON/BLOCKO/	FLOW3D
COMMON/BLOKOP/	FLOWAX
COMMON/FLOWS/	

METHOD OF SOLUTION

Calling of Subroutines FLOWIN, FLOUT, FLOW3D and FLOWAX are controlled by the input parameter IFLOW (Card 2).

SUBROUTINE NAME: FLOWAX

DESCRIPTION

FLOWAX uses axisymmetric flowfield gas property data input on Unit 8 to prepare line-of-sight gas property output on Unit 10.

CALLING SEQUENCE

CALL FLOWAX

COMMON BLOCKS AND EXTERNAL REFERENCES

COMMON/CONTRL/	COMMON/SLIMTC/
COMMON/CONID/	PLUMPT
COMMON/FLOSCL/	CPUTIM
COMMON/GOMTRY/	BLOCKM
COMMON/BLOCKO/	SLIMIT
COMMON/BLOKOP/	SIN
COMMON/FLWS/	COS

METHOD OF SOLUTION

Gas property data input from Unit 8 describes properties in an axisymmetric format with arbitrary radial positions (R) specified at selected axial positions (Z). Linear interpolations are made in the flowfield gas property data (as described in Section 4.3) to provide gas property data at each position on a line-of-sight defined by the input problem geometry. As each line-of-sight is processed, the integration limits in s are redefined if necessary by subroutines SLIMIT and BLOCKM.

After each line-of-sight is processed, it is checked for negative property values, temperatures outside the usual range of the band model parameter table, and zero temperatures. If all temperatures are zero or if the adjusted integration limits indicate the line-of-sight does not intersect the plume flowfield, the line-of-sight sequence number, LSET, is set negative to indicate the line-of-sight missed the gas.

SUBROUTINE NAME: FLOWIN

DESCRIPTION

FLOWIN reads or controls other subroutines (FFPREP and BLOKIN) which read flowfield and geometry input. The data, along with that read in MAIN, are output as the initial records on Unit 10.

CALLING SEQUENCE

CALL FLOWIN

COMMON BLOCKS AND EXTERNAL REFERENCES

COMMON/CONTRL/	COMMON/FLOWS/
COMMON/CONID/	COMMON/SLIMTC/
COMMON/FLOSCL/	COMMON/CHIPOF/
COMMON/GOMTRY/	SCLOCK
COMMON/BLOCKO/	FFPREP
COMMON/BLOKOP/	BLOKIN

METHOD OF SOLUTION

Problem description and integration limits and intervals are read in this subroutine. If the flowfield properties are input on cards, Subroutine FFPREP is called to prepare the property data on Unit 8. Subroutine BLOKIN is called to read all surface geometry input.

SUBROUTINE NAME: FLOW3D

DESCRIPTION

FLOW3D uses 3-dimensional flowfield gas property data input on Unit 8 to prepare line-of-sight gas property output on Unit 10.

CALLING SEQUENCE

CALL FLOW3D

COMMON BLOCKS AND EXTERNAL REFERENCES

COMMON/CONTRL/	PLUMPT
COMMON/CONID/	CPUTIM
COMMON/FLOSCL/	BLOCKM
COMMON/GOMTRY	SLIMIT
COMMON/BLOCKO/	SIN
COMMON/BLOKOP/	COS
COMMON/FLOWS/	ATAN2
COMMON/SLIMTC	SQRT

METHOD OF SOLUTION

Gas property data input from Unit 8 describe properties in a cylindrical coordinate system with arbitrary radial positions (R) specified at selected axial (Z) and angular (η) positions. Linear interpolations are made in the flowfield gas property data (as described in Section 4.3) to provide gas property data at each position on the lines-of-sight defined by the input problem geometry. As each line-of-sight is processed, the integration limits in s are redefined if necessary by Subroutines SLIMIT and BLOCKM.

After each line-of-sight is processed, it is checked for negative property values, temperatures outside the usual range of the band model parameter table, and zero temperatures. If all temperatures are zero or if the adjusted integration limits indicate the line-of-sight does not intersect the plume, the line-of-sight sequence number, LSET, is set negative to indicate the line-of-sight missed the gas.

SUBROUTINE NAME: MAIN

DESCRIPTION

MAIN reads the problem title, control parameters, and integration limits, but the primary function is to control overlay for the upper level program segments.

CALLING SEQUENCE

NONE

COMMON BLOCKS AND EXTERNAL REFERENCES

COMMON/CONTRL/	EXIT
COMMON/CONID/	FLOW
COMMON/FLOSCL/	RAD
COMMON/COMTRY/	VIEW
COMMON/BLOCKO/	

METHOD OF SOLUTION

Reads the first 6 input cards and checks to see if the program limits for number of constituents or spectral intervals will be exceeded. Calls are made to the three segments FLOW, RAD, and VIEW, then the next case is read. When the next case title is blank, the system routine EXIT is called.

SUBROUTINE NAME: NOGO

DESCRIPTION

NOGO is an integer function which determines if an intersection between a line-of-sight and a blocking surface is within the portion of the surface described by the γ limits defined in Fig. 4.3.

CALLING SEQUENCE

FUNCTION = NOGO (X,Y,A,B)

where X,Y are two coordinates of the point of intersection in the surface coordinate system, and A and B are the γ limits, GMIN(I) and GMAX(I).

COMMON BLOCKS AND EXTERNAL REFERENCES

COMMON None

ATAN2

METHOD OF SOLUTION

The angle of the intersection in a plane normal to the Z-axis is determined in degrees, and it is converted to a positive angle if it was in the 3rd or 4th quadrant. The value is then checked against the γ -limits for the surface to determine if the intersection is within the limits (NOGO=1) or outside the limits (NOGO=-1).

SUBROUTINE NAME: PLANCK

DESCRIPTION

PLANCK provides integrated values of the Planck function using a tabulated function.

CALLING SEQUENCE

CALL PLANCK (PNU1, PNU2, T, PLA)

where PNU1=PNU(1)=Lower wavenumber limit (cm⁻¹)

PNU2=PNU(2)=Upper wavenumber limit (cm⁻¹)

T = Temperature (K)

PLA = Integrated value of the Planck function (watts/cm²-sr)

COMMON BLOCKS AND EXTERNAL REFERENCES

COMMON None

EXP

METHOD OF SOLUTION

The value of the spectral integral of the function

$$PL(I) = \pi \int_0^{PNU(I)} N_{\omega}^{\circ} d_{\omega} / \sigma T^4$$

is determined for the lower (I=1) and upper (I=2) limits of wavenumber. In this function N_{ω}° is the Planck function, ω is the wavenumber and σ is the Stefan-Boltzman constant. The integrated value of the Planck function is then

$$PLA = \frac{\sigma}{\pi} T^4 (PL(2)-PL(1))$$

For the range $0.05 \leq PL(I)/T \leq 1$, a table of values (Ref. 10) for the integrals are linearly interpolated, while outside this range, integrals are based on limiting approximations of the Planck function. For $PNU(I)/T < 0.05$

$$N_{\omega}^{\circ} \approx \frac{1}{\pi} \frac{3.7405 \times 10^{-12} \omega^3}{1.43879 \omega/T}$$

and the integral is

$$\pi \int_0^{\omega} N_{\omega}^{\circ} d_{\omega} / \sigma T^4 = 0.15284 (\omega/T)^3.$$

For $PNU(I)/T > 10$,

$$N_{\omega}^{\circ} \approx \frac{1}{\pi} \frac{3.7405 \times 10^{-12} \omega^3}{\exp(1.43879 \omega/T)}$$

and the integral is

$$\pi \int_0^{\omega} N_{\omega}^{\circ} d_{\omega} / \sigma T^4 = 1.0 - 0.4585 \exp(-1.4388 \omega/T) [((\omega/T + 2.0851)\omega/T + 2.8984)\omega/T + 2.0145]$$

SUBROUTINE NAME: PLUMPTDESCRIPTION

PLUMPT determines the location in the plume coordinate system of a point location specified in the central coordinate system. If there are multiple axisymmetric plumes, the plume system chosen is the one in which the point is closest to the plume axis.

CALLING SEQUENCE

CALL PLUMPT (X,Y,Z,XW,YW,ZW,RW,N1,N2,NP)

where X,Y, Z = coordinates of the point in the central coordinate system,
 XW, YW, ZW = coordinates returned by the subroutine in the plume system,
 RW = distance of the point from the plume Z-axis,
 N1,N2 = lower and upper limits of the surface sequence index,
 corresponding to the plumes (usually 2, 1+NENG), and
 NP = surface sequence index of the plume the point is located in.

COMMON BLOCKS AND EXTERNAL REFERENCES

COMMON/CONTROL/

COMMON/BLOKOP/

COMMON/CONID/

COMMON/FLOWS/

COMMON/FLOSCL/

COMMON/SLIMTC/

COMMON/COMTRY/

COMMON/CHIPOF/

COMMON/BLOCKO/

SQRT

METHOD OF SOLUTION

Initialize $RW=10^{20}$ and $NP=0$, then enter a loop for $N=N1,N2$ and compute the location in the plume XN,YN,ZN and radius RN for each plume. If the ZN value is outside the range of Z currently stored for the flowfield, proceed to the next N , but if is not, test the radial position. If $RN \leq RW$ assign this point and plume as the solution

$$RW=RN,$$
$$XW=XN,$$
$$YW=YN,$$
$$ZW=ZN,$$

and

$$NP=N,$$

and continue the loop through the plumes in search of another solution with $RN < RW$. When the loop is complete, the solution for the plume closest to the point is returned.

SUBROUTINE NAME: RAD

DESCRIPTION

RAD controls sequencing of the set of overlay subroutines involved in radiation calculations.

CALLING SEQUENCE

CALL RAD

COMMON BLOCKS AND EXTERNAL REFERENCES

COMMON/CONTRL/	COMMON/ABCOEF/
COMMON/CONID/	COMMON/RADSUB/
COMMON/FLOSCL/	ACDATA
COMMON/CONTRY/	SLG
COMMON/BLOCKO/	SPCOUT

METHOD OF SOLUTION

Subroutine ACDATA is called unconditionally. Since all input cards may have been read at this point, control is returned to MAIN if an error is detected so that the next case may be attempted. If IERROR=0, Subroutine SLG is called for the radiation prediction, and if spectral output is called for (NSPEK > 0), Subroutine SPCOUT is called. Note that there are two decks with the subroutine name SLG, so the subroutine used will depend on the deck name used in the mapping process (refer to Section A1.1).

SUBROUTINE NAME: SKIP

DESCRIPTION

SKIP renews the page for output and returns the line counter to zero.

CALLING SEQUENCE

CALL SKIP

COMMON BLOCKS AND EXTERNAL REFERENCES

COMMON/CONTRL/

COMMON/GOMTRY/

COMMON/CONID/

COMMON/BLOCKO/

COMMON/FLOSCL/

METHOD OF SOLUTION

Not applicable.

SUBROUTINE NAME: SLG (DECK SLGMLT)

DESCRIPTION

SLG(SLGMLT) reads line-of-sight property data from Unit 10, predicts the transmissivity using an exponential line strength distribution (Eqs. 10 and 12) with the Curtis-Godson approximation (Eq. 15) for inhomogeneous gas effects. Radiation is predicted using Eq. 14. See also SLG(YNGH20).

CALLING SEQUENCE

CALL SLG

COMMON BLOCKS AND EXTERNAL REFERENCES

COMMON/CONTRL/	CPUTIM
COMMON/CONID/	PLANCK
COMMON/FLOSCL/	SQRT
COMMON/GOMTRY/	EXP
COMMON/BLOCKO/	ALOG
COMMON/ABCOEF/	SIN
COMMON/RADSUB/	

METHOD OF SOLUTION

Integration of Eq. 14 is performed using the numerical form

$$\dot{q}/A = \sum_{\theta_1}^{\theta_f} \sum_{\phi_1}^{\phi_f} \sum_{\omega_1}^{\omega_f} \sum_{i=1}^J \Delta N^\circ(\omega, i) [\tau(\omega, i-1) - \tau(\omega, i)] \sin\theta \cos\theta \Delta\phi \Delta\theta$$

where $\tau(\omega, 0) = 1$ and $\Delta N^\circ(\omega, i)$ is used in preference to $N^\circ(\omega, i)\Delta\omega$ to more accurately represent the Planck function when large wavenumber intervals are used. In addition, $\Delta\tau$ is used as equivalent to $(d\tau/ds)ds$. Actual values of the line-of-sight increments indicated by i may be determined

by either the input Δs value (DS) or a multiple of Δs (DSS) set by the temperature step criteria TDIFF (described in Section 3.4).

Values of the transmissivity are determined using Eqs. 10 and 12 with Curtis-Godson approximations of the band model parameters indicated by Eqs. 15. The pressure (p), mole fractions (c), and temperature (T) are obtained from the line-of-sight property values read from Unit 10. The line half-widths are computed using Eqs. 8 and 9, and the absorption coefficient (\bar{k}) and line density ($1/\bar{d}$) are determined from tables prepared by Subroutine ACDATA. The tables are prepared to correspond to the exact values of the wavenumbers to be used in the integration to represent the center of the intervals. Linear interpolation is performed between temperature entries in the tables to obtain values at the gas temperature.

SUBROUTINE NAME: SLG (DECK YNGH20)

DESCRIPTION

SLG(YNGH20) reads line-of-sight property data from Unit 10, predicts the transmissivity and radiance using an exponentially-tailed-inverse line strength distribution with the Intuitive Derivative Method for inhomogeneity (Eq. 17). This method is for water vapor only and does not include Doppler broadening. See also SLG(SLGMLT).

CALLING SEQUENCE

COMMON/CONTRL/	CPUTIM
COMMON/CONID/	YAPPRX
COMMON/FLOSCL/	SQRT
COMMON/GOMTRY/	EXP
COMMON/BLOCKO/	SIU
COMMON/ABCOEF/	ALOG
COMMON/RADSUB/	

METHOD OF SOLUTION

The method of solution uses Eq. 14 in the form

$$\dot{q}/A = \sum_{\theta_j}^{\theta_f} \sum_{\phi_j}^{\phi_f} \sum_{\omega_j}^{\omega_f} \sum_{s_{zero}}^{s_{min}} N^o(\omega, s) \left[\sum_{s-\Delta s}^s \frac{d\tau(\omega, s')}{ds'} ds' \right] \Delta\omega \sin\theta \cos\phi \Delta\phi \Delta\theta$$

where the terms in the inner [] brackets are defined in Eq. 17. Property values for the integration are based on the input Δs increment (DS) which may be lengthened to a multiple of Δs (DSS) by the temperature step size parameter TDIFF (described in Section 3.4). These incremental lengths are usually too large for accurate integration of Eq. 17 in regions of moderate to strong absorption, so the inner bracketed

term is integrated using a smaller step size determined by the input parameter IRAD and the strength of absorption represented by the initial value of the parameter DFO ($=\bar{k} c p \Delta s$).

The pressure (p), mole fraction (c), and temperature (T) used in Eq. 17 are obtained from line-of-sight property data on Unit 10. The line half-width (γ_c) is computed from Eq. 8, and the absorption coefficient (\bar{k}) and line density ($1/\bar{d}$) are determined from tables for water vapor prepared by Subroutine ACDATA. The tables are prepared to correspond to the exact values of the wavenumbers representing the centers of the integration intervals. Linear interpolation is performed between entries in the tables to obtain values at the gas temperatures.

SUBROUTINE NAME: SLIMIT

DESCRIPTION

SLIMIT adjusts the integration limits on each line-of-sight to correspond to the portion of the line within the conical surfaces approximating the plume boundaries.

CALLING SEQUENCE

CALL SLIMIT

COMMON BLOCKS AND EXTERNAL REFERENCES

COMMON/CONTRL/	COMMON/BLOKOP/
COMMON/CONID/	COMMON/FLOWS/
COMMON/FLOSCL/	COMMON/SLIMTC/
COMMON/GOMTRY/	COMMON/CHIPOF/
COMMON/BLOCKO/	SQRT

METHOD OF SOLUTION

Solutions for the intersection of the line-of-sight with the limiting cone for each plume are obtained from Eq. 39. If no solutions exist, both limits (SZERO and SMIN) are set at zero. If solutions exist for a plume, the solutions are assigned as the upper and lower limits based on tests on: (1) the direction of the line relative to the plume axis, (2) whether the origin of the line is inside or outside of the cone, (3) the position of the line-of-sight origin relative to the cone apex, and (4) the relative values of the solutions. After all plumes are processed, solutions are compared to select the smallest for SZERO and the largest for SMIN.

In the process of obtaining solutions, the range of the cone is limited to the Z-range of the plume by β limits (Fig. 4.3-surface Type 5) which are set in the flowfield subroutine FLOWAX or FLOW3D.

SUBROUTINE NAME: SPCOUT

DESCRIPTION

SPCOUT provides printed output for spectral radiation data. The spectral radiation is the only parameter output for the integrated problem. All other parameters are for the final line-of-sight only. The subroutine also prepares a binary file on Unit 4 for use by the plot program PLOTIT.

CALLING SEQUENCE

CALL SPCOUT

COMMON BLOCKS AND EXTERNAL REFERENCES

COMMON/CONTRL/	COMMON/ABCOEF/
COMMON/CONID/	COMMON/RADSUB/
COMMON/FLOSCL/	CPUTIM
COMMON/GOMTRY/	ALOG
COMMON/BLOCKO/	SQRT

METHOD OF SOLUTION

Spectral parameters produced in Subroutine SLG are used for spectral output and to compute desired spectral parameters. The equations used are those for the Curtis-Godson approximation with an exponential line strength distribution which were used in Deck SLGMLT, so the parameters printed in the "long form" output (Card 2 Col. 27 = 2 or 4) are not correct for use with Deck YNGH20 or any other band model. Because of this, the code in SPCOUT will disable the long form output if the parameter IRAD used by Deck YNGH20 is greater than zero.

SUBROUTINE NAME: VIEW

DESCRIPTION

VIEW prepares a polar plot on the printer depicting line-of-sight radiance as a function of elevation angle θ and azimuth angle ϕ . This is a visualization tool to assist in judging the correctness of the point and plume orientations and give an approximate indication of the areas of intense radiation.

CALLING SEQUENCE

CALL VIEW

COMMON BLOCKS AND EXTERNAL REFERENCES

COMMON/CONTRL/

COMMON/BLOCKO/

COMMON/CONID/

SIN

COMMON/FLOSCL/

COS

COMMON/GOMTRY/

METHOD OF SOLUTION

A table IFIELD(51,83) is used to represent 51 lines with 83 symbols per line. Symbols are assigned based on the results on each line-of-sight read from Unit 10. An averaging method is used to approximate a result when several lines-of-sight must be represented by a single symbol. But no interpolation is performed, so widely spaced lines-of-sight result in widely spaced symbols.

With the maximum radiance on any line-of-sight as RADMAX (watts/cm²-sr) the symbols used have the following meanings with the line-of-sight radiance noted as N.

<u>Symbol Index</u>	<u>Symbol</u>	<u>Meaning</u>
1	1	0.1 RADMAX < N < 0.2 RADMAX
2	2	0.2 < < < 0.3
3	3	0.3 < < < 0.4
4	4	0.4 < < < 0.5
5	5	0.5 < < < 0.6
6	6	0.6 < < < 0.7
7	7	0.7 < < < 0.8
8	8	0.8 < < < 0.9
9	9	0.9 < < < 1.0
9	10	0.9 < < < 1.0
blank	11	Missed the gas
B	12	Blocked
0	13	0 < N ≤ 0.1 RADMAX
*	14	Polar grid marks

SUBROUTINE NAME: YAPPRX

DESCRIPTION

YAPPRX evaluates an approximation for $y(x,r,q)$ described in Eq. 17i.

CALLING SEQUENCE

CALL YAPPRX(X,R,Q,Y)

where $X = \pi x_e(\omega,s)$ (defined by Eqs. 17b and 17d)

$R = r(\omega,s)$ (defined by Eqs. 17c and 17f)

$Q = q(\omega,s)$ (defined by Eqs. 17e and 17g)

$Y = y(x,r,q)$ (defined by Eq. 17i)

COMMON BLOCKS AND EXTERNAL REFERENCES

COMMON None

SQRT

YF

METHOD OF SOLUTION

The method of approximating $y(x,r,q)$ is that described by Dr. Stephen Young in Ref. 7.

FUNCTION NAME: YF

DESCRIPTION

YF is the value of $y(x,r,1)$ used in the approximation (Subroutine YAPPRX) of $y(x,r,q)$

CALLING SEQUENCE

FUNCTION = YF(X,R)

where $X = \pi x_e(\omega,s)$ (defined by Eqs. 17b and 17d)

$R = r(\omega,s)$ (defined by Eqs. 17c and 17f)

COMMON BLOCKS AND EXTERNAL REFERENCES

COMMON None

SQRT

METHOD OF ANALYSIS

The equation for $y(x,r,1)$ (Ref. 17) is

$$YF(X,R) = y(x,r,1) = [2r(1+x) + (1+r^2)(1+x^2)^{\frac{1}{2}}] / [(1+x^2)^{\frac{1}{2}}(r+(1+x^2)^{\frac{1}{2}})^2]$$

A5 PLOT PROGRAM

The plot program is the single module PLOTIT along with all the external references for plotting subroutines supplied by the MSFC Library. The only input required is the binary file on Unit 4 prepared as output in Subroutine SPCOUT (described in Appendix A2, Table A2.2). Description of the plot parameters (Card 16) is read in Subroutine ACDATA and passed to PLOTIT by the binary file.

Output consists of the plots, diagnostic messages described in Section A2.2, and messages identifying the beginning and the end of the program to verify execution.